

**UNIVERSIDADE FEDERAL DE SANTA MARIA
CENTRO DE CIÊNCIAS NATURAIS E EXATAS
PROGRAMA DE PÓS-GRADUAÇÃO EM BIODIVERSIDADE ANIMAL**

Dilson Vargas Peixoto

**MORFOLOGIA PÓS-CRANIANA DE UM NOVO ESPÉCIME DE
LESTODON ARMATUS GERVAIS, 1855 (XENARTHRA,
MYLODONTIDAE) DO QUATERNÁRIO DO SUL DO BRASIL**

Santa Maria, RS
2019

Dilson Vargas Peixoto

**MORFOLOGIA PÓS-CRANIANA DE UM NOVO ESPÉCIME DE
LESTODON ARMATUS GERVAIS, 1855 (XENARTHRA,
MYLODONTIDAE) DO QUATERNÁRIO DO SUL DO BRASIL**

Dissertação apresentada ao Curso de Pós-Graduação em Biodiversidade Animal, da Universidade Federal de Santa Maria (UFSM, RS), como requisito parcial para a obtenção do título de **Mestre em Biodiversidade Animal**.

Orientador: Prof. Dr. Leonardo Kerber

Santa Maria, RS
2019

Vargas Peixoto, Dilson

MORFOLOGIA PÓS-CRANIANA DE UM NOVO ESPÉCIME DE *Lestodon armatus* GERVAIS, 1855 (XENARTHRA, MYLODONTIDAE) DO QUATERNÁRIO DO SUL DO BRASIL / Dilson Vargas Peixoto.- 2019.

90 f.; 30 cm

Orientador: Leonardo Kerber

Coorientador: Átila Augusto Stock Da Rosa
Dissertação (mestrado) - Universidade Federal de Santa Maria, Centro de Ciências Naturais e Exatas, Programa de Pós-Graduação em Biodiversidade Animal, RS, 2019

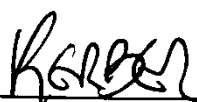
1. Megafauna 2. Anatomia pós-craniana 3. Pleistoceno
4. Xenarthra 5. Vale do Seival I. Kerber, Leonardo II.
Stock Da Rosa, Átila Augusto III. Título.

Dilson Vargas Peixoto

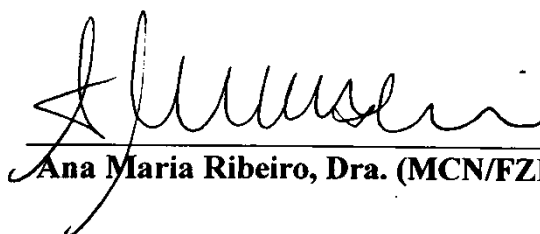
**MORFOLOGIA PÓS-CRANIANA DE UM NOVO ESPÉCIME DE
LESTODON ARMATUS GERVAIS, 1855 (XENARTHRA,
MYLODONTIDAE) DO QUATERNÁRIO DO SUL DO BRASIL**

Dissertação apresentada ao Curso de Pós-Graduação em Biodiversidade Animal, da Universidade Federal de Santa Maria (UFSM, RS), como requisito parcial para a obtenção do título de **Mestre em Biodiversidade Animal**.

Aprovado em 26 de fevereiro de 2019:



Leonardo Kerber, Dr. (UFSM)
(Presidente/Orientador)



Ana Maria Ribeiro, Dra. (MCN/FZBRS)



Átila Augusto Stock da Rosa, Dr. (UFSM)

Santa Maria, RS
2019

DEDICATÓRIA

Dedico à toda Natureza da América do Sul, para que seja mais valorizada e conhecida. Também dedico ao meu Ego, para que sossegue; à ansiedade, que me acompanhou durante esses dois anos; ao desânimo, que andou de mãos dadas comigo nos últimos momentos da pesquisa.

AGRADECIMENTOS

Primeiramente agradeço à Coordenação de Aperfeiçoamento de Pessoal de Nível Superior (CAPES), projeto nº 001, pelo financiamento da pesquisa.

Por meu orientador Leonardo Kerber e coorientador Átila A. S. da Rosa pela dedicação e grande apoio que me deram (agradeço do fundo do coração), bem como pela parceria e amizade.

Pelos meus colegas e amigas do PPG em Biodiversidade Animal pelos perrengues que enfrentamos juntos, desabafos, “ombro amigo” e, principalmente, pelas parcerias inesquecíveis. Apesar de serem vários, agradeço especialmente à Amanda Brum, Felipe Cerezer, Gianfrancis Ugalde, Tiane Macedo de Oliveira e Tuane Carvalho, pessoas que me identifiquei mais e que tive mais contato. Claro que não posso esquecer de Conrado Mário da Rosa e Jonathan Della Flora, meus amigos que me convidaram para participar de seus campos no Caverá, momentos esses de estudo prático, parceria e tranquilidade. Muito bom conviver com vocês.

Agradeço aos colegas e às colegas do Centro de Apoio à Pesquisa Paleontológica e do Laboratório de Estratigrafia e Paleobiologia pela companhia, incentivo e ajuda.

Agradeço a Andrés Rinderknecht, Ana Maria Ribeiro e Jamil Pereira, curadores e curadora das coleções científicas que tão bem me receberam e me ajudaram.

Agradeço a Leopoldo Witeck Neto por ter encontrado o material que estudei e por todas as pessoas que nos acompanharam naquele campo em 2010.

Também, agradeço ao “objeto” de minha pesquisa, ao animal que viveu há muito tempo atrás e que hoje nos dá testemunho de sua magnificência. Além disso, agradeço às condições que possibilitaram sua preservação até chegar às minhas mãos.

Por fim, agradeço ao universo pela oportunidade dessa jornada de dois anos nos Mestrado e ter me ajudado a identificar o rumo da minha vida.

Ha’evete pavẽ

RESUMO

MORFOLOGIA PÓS-CRANIANA DE UM NOVO ESPÉCIME DE *LESTODON ARMATUS* GERVAIS, 1855 (XENARTHRA, MYLODONTIDAE) DO QUATERNÁRIO DO SUL DO BRASIL

AUTOR: Dilson Vargas Peixoto

ORIENTADOR: Leonardo Kerber

COORIENTADOR: Átila Augusto Stock Da-Rosa

Durante o Cenozoico da América do Sul, as preguiças-terricolas (Folivora) apresentaram grande irradiação adaptativa que culminou em uma grande diversidade de formas durante o Pleistoceno. Com exceção de algumas espécies arborícolas, a maioria das preguiças foram extintas ao fim desse período. Dentre os Pilosa, Mylodontidae foi um dos clados mais representativos por conta da grande quantidade de espécies. A maior espécie desse foi *Lestodon armatus*, cuja distribuição ocupava grande parte do continente. Neste trabalho, reportamos um novo espécime (UFSM 11535) atribuído a *L. armatus*, o qual foi encontrado em bom estado de preservação em um novo sítio fossilífero chamado Arroio do Lestodon, no Vale do Seival, Caçapava do Sul, Rio Grande do Sul, Brasil. Além de vértebras, costelas, dentes e outros fragmentos, o que mais se destaca é a preservação de um dos membros posteriores em posição de articulação, evidenciando quase todos os ossos. Foi feita uma descrição detalhada dos ossos do pós-crânio do espécime, assim como comparação com outros espécimes. A atribuição a *L. armatus* se dá principalmente pela presença dos seguintes caracteres: I) separação das facetas ectal e sustentacular no astrágalo; II) função do ectocuneiforme como metatarsal II pela fusão dos dois ossos; III) pelo processo odontoide do astrágalo em forma de polia com cerca de 90° em relação à faceta discoide; IV) separação por uma crista das facetas astragalianas na tíbia, e V) côndilo medial do fêmur maior que o côndilo lateral. Entre os aportes sobre a variação da morfologia pós-craniana, registramos pela primeira vez o fusionamento entre fíbula e tíbia em *L. armatus* e a presença de dois sesamoides no metatarsal III. Como futuras perspectivas, análises mais abrangentes da morfologia pós-craniana dos Mylodontidae, bem como de outros pilosos, são necessárias para verificar a presença de variações anatômicas individuais, bem como testar a relevância filogenética dos caracteres presentes nesta região do esqueleto.

Palavras-chave: Megafauna, anatomia pós-craniana, Pleistoceno, Mammalia, Xenarthra, Vale do Seival.

ABSTRACT

POST-CRANIAL MORPHOLOGY OF A NEW SPECIMEN OF *LESTODON ARMATUS* GERVAIS, 1855 (XENARTHRA, MYLODONTIDAE) FROM SOUTHERN BRAZIL

AUTHOR: Dilson Vargas Peixoto

ADVISOR: Leonardo Kerber

CO-ADVISOR: Átila Augusto Stock Da-Rosa

During the Cenozoic of South America, the terrestrial sloths (Folivora) had wide adaptive irradiation that culminated in a great diversity of forms during the Pleistocene. Except for some arboreal species, most sloths were extinguished at the end of this period. Among the clades included in Pilosa, Mylodontidae was one of the most representative, showing a large number of species. The largest species of this clade was *Lestodon armatus*, whose distribution occupied a large portion of the continent. In this work, a new and well-preserved specimen (UFSM 11535) assigned to *L. armatus* is reported. The specimen was found in a new fossiliferous locality designated Arroio do Lestodon in the Seival Valley, Caçapava do Sul, Rio Grande do Sul, Brazil. UFSM 11535 includes vertebrae, ribs, teeth, and an articulated hindlimb that include almost all bones. A detailed description of these post-cranial bones was provided as well as a comparison with other specimens. The taxonomic assignment of UFSM 11535 to *L. armatus* is based on the presence of the following characters: I) separation of the ectal and sustentacular facets in the astragalus; II) the function of the ectocuneiform as metatarsal II by the fusion of the two bones; III) odontoid process of the astragalus in the form of a pulley with about 90° in relation to the discoid facet; IV) separation by a crest of the astragali facets in the tibia, and V) the medial condyle of the femur larger than the lateral condyle. Among the contributions to the knowledge on the variation of post-cranial morphology, the fusion between fibula and tibia and the presence of two sesamoids in the metatarsal III was recorded for the first time in *L. armatus*. As future perspectives, more comprehensive analyzes of the post-cranial morphology of Mylodontidae and other sloths are necessary to verify the presence of individual anatomical variations, as well as to test the phylogenetic relevance of the characters present in this region of the skeleton.

Keywords: Megafauna, post-cranial anatomy, Pleistocene, Mammalia, Xenarthra, Vale do Seival.

Sumário

APRESENTAÇÃO DA ESTRUTURA DA DISSERTAÇÃO	5
1 INTRODUÇÃO	6
1.1 O clado Mylodontidae	6
1.2 Os mamíferos e a extinção do Pleistoceno/Holoceno	9
1.3 Principais localidades fossilíferas do Pleistoceno do Rio Grande do Sul	11
1.3 Objetivos	112
1.3.1 Objetivo geral.....	12
1.3.2 Objetivos específicos.....	12
2 ARTIGO	13
A new record of <i>Lestodon armatus</i> Gervais, 1855 (Xenarthra, Mylodontidae) from the Quaternary of southern Brazil and remarks on the postcranial anatomy	13
3 CONCLUSÕES	83
4 REFERÊNCIAS	84

APRESENTAÇÃO DA ESTRUTURA DA DISSERTAÇÃO

A presente dissertação de mestrado tem o objetivo de reportar uma nova localidade fossilífera e de descrever um novo espécime de uma preguiça-terrícola do clado Mylodontidae do Quaternário do Rio Grande do Sul, detalhando sua anatomia pós-craniana. O espécime foi coletado no sítio Arroio do Lestodon, descrito no manuscrito aqui apresentado. A dissertação foi elaborada em forma de artigo científico já submetido ao periódico *Historical Biology* e sua estrutura está organizada de acordo com as normas do Manual de Dissertações e Teses da UFSM (MDT). Este documento integra os requisitos necessários para a obtenção do título de Mestre em Ciências Biológicas – área Biodiversidade Animal, pelo Programa de Pós-Graduação em Biodiversidade Animal da Universidade Federal de Santa Maria.

No **Capítulo 1**, apresentamos uma breve caracterização sobre as preguiças-terrícolas, extinção de grandes mamíferos durante o Pleistoceno/Holoceno e sobre as principais localidades fossilíferas deste intervalo presentes no Rio Grande do Sul.

O **Capítulo 2** inclui o corpo principal deste documento, representado pelo manuscrito produzido durante o desenvolvimento do mestrado. O artigo é intitulado de "A new record of *Lestodon armatus* Gervais, 1855 (Xenarthra, Mylodontidae) from the Quaternary of southern Brazil and remarks on the postcranial anatomy". Visando a produção de um documento sucinto, detalhes sobre os materiais e métodos, que incluem coleções, área de estudo e demais informações, estão incluídos diretamente no artigo científico.

No **Capítulo 3** estão as principais conclusões deste estudo.

1 INTRODUÇÃO

1.1 O clado Mylodontidae

Entre cerca de 45 a 12 milhões de anos a América do Sul esteve quase isolada dos outros continentes (WOODBURN, 2010). Esse aspecto possibilitou a origem e diversificação de linhagens endêmicas de mamíferos. Dentre tais linhagens, ressalta-se o clado Xenarthra (Figura 1).

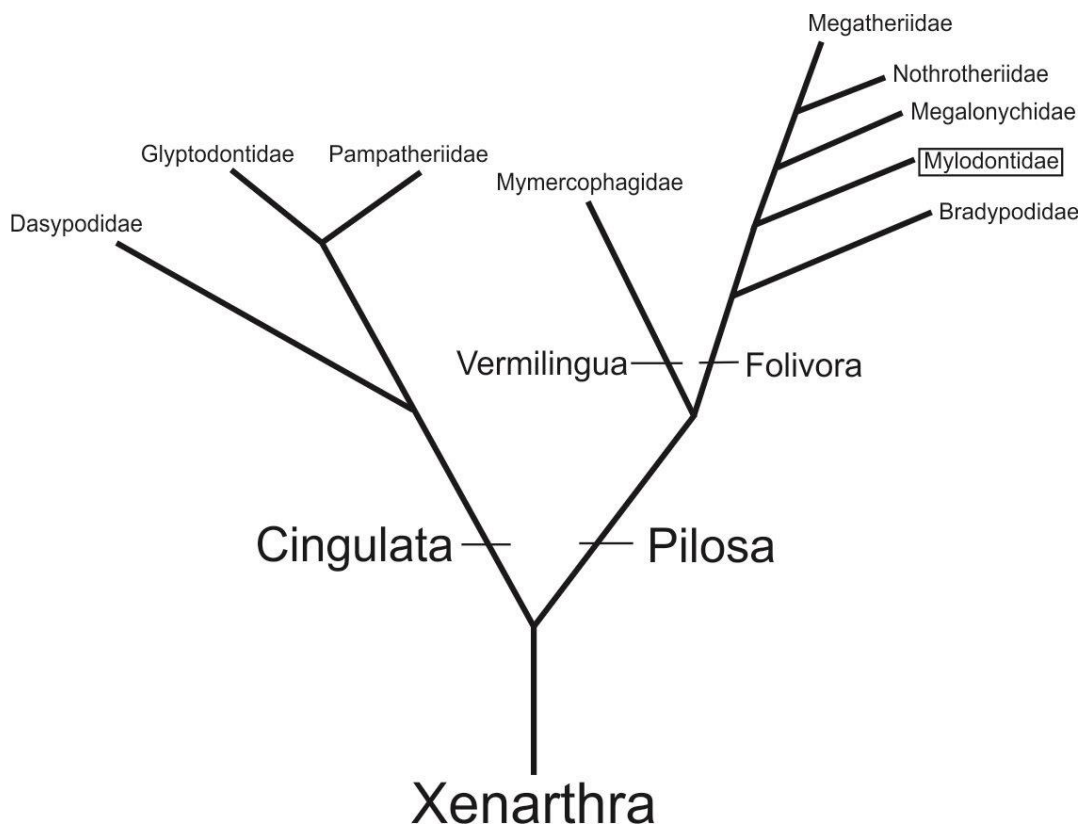


Figura 1. Cladograma simplificado ilustrando as relações filogenéticas de Xenarthra. Fonte: Adaptação de Gaudin (2004).

Os Xenarthra correspondem a animais de dentição reduzida ou ausente, ausência de esmalte dentário e articulação extra nas vértebras lombares (PAULA COUTO, 1979; GAUDIN, 1995; GAUDIN, 2004). São subdivididos em dois clados menos inclusivos (Figura 1): Cingulata, onde estão inseridos os gliptodontes, pampaterídeos e tatus, e Pilosa (DELSUC et al., 2004). Pilosa, por sua vez, divide-se em Vermilingua, grupo ao qual estão os tamanduás e tamanduás, e Tardigrada ou Folivora, em que estão os animais conhecidos popularmente como

preguiças (Figura 1) (DELSUC et al., 2004; GAUDIN, 2004) onde a herbivoria foi um fato determinante nos processos evolutivos que levaram a diversidade morfológica do clado (PUJOS et al., 2012). Atualmente os Xenarthra são menos diversos (Figura 2).

Os representantes mais antigos de Folivora são do gênero *Pseudoglyptodon* Engelmann, 1987 do final do Eoceno (MCKEEENA et al., 2006). Apesar das formas mais basais serem animais pequenos e possivelmente semiarborícolas, a diversificação ocorrida ao longo do Cenozoico propiciou o surgimento de espécies de grande tamanho, como por exemplo *Megatherium americanum* Cuvier, 1796, a maior preguiça terrestre conhecida.

No tocante as relações filogenéticas dentro de Folivora, destacam-se os clados Bradypodidae, clado monogenérico com representantes atuais do gênero *Bradypus* Linnaeus, 1758 (Figura 2); Megatheroidea, formado por Megalonychidae, Megatheriidae e Nothrotheriidae; e Mylodontidae (GAUDIN, 2004). Os Megatheroidea incluem animais plantígrados, ou seja, que apoiam toda a planta do pé no chão, bem como espécies com pedolateralismo, onde o pé apoiava-se lateralmente (MCDONALD, 2012). Outra peculiaridade nesse grupo foi a diversidade de modos de locomoção, já que haviam espécies semiarborícolas como *Hapalops* Ameghino, 1887 e suspensívoras como *Choloepus* dentre os Megalonychidae; e aquáticas do gênero *Thalassocnus* De Muizon e McDonald, 1995 em Nothrotheriidae (PUJOS et al., 2012).



Figura 2. Representantes atuais de Xenarthra. Cingulata do gênero *Euphractus* Wagler, 1930 (1), Vermilingua do gênero *Myrmecophaga* Linnaeus, 1798 (2), Folivora dos gêneros *Choloepus* Linnaeus, 1758 (Megalonychidae) (3) e *Bradypus* Linnaeus, 1758 (Bradypodidae) (4). Fonte: autor

Em relação ao clado Mylodontidae, de maior interesse aqui, este caracteriza-se pelo compartilhamento de dentes circulares e/ou bilobados e redução do processo zigomático do esquamosal, entre outras características (GAUDIN, 2004; MCDONALD E DE IULIIS, 2008). Diferentemente dos megateroideos, todos os Mylodontidae possuíam pedolateralismo (PUJOS et al., 2012).

Os Mylodontidae tiveram uma ampla distribuição e diversificação em relação às outras famílias de pilosos, com espécies habitando o sul da América do Sul à América do Norte, sendo um dos primeiros grupos a participarem do Grande Intercâmbio Biótico Americano, já no Mioceno (MARSHALL, 1988; WOODBURN, 2010; CIONE et al., 2015). Segundo as revisões mais recentes (e.g. GAUDIN, 1995, 2004; CARTELLE et al., 2009; MIÑO-BOILINI, 2012; MIÑO-BOILINI et al., 2014), o clado divide-se em três subfamílias: Lestodontinae, Mylodontinae e Scelidotheriinae. Em Scelidotheriinae estão inclusos os gêneros *Catonyx* Ameghino, 1891, “*Scelidodon*” Ameghino, 1881, *Scelidotherium* Owen, 1839, e *Valgipes* Gervais, 1873; e Mylodontinae é composto por *Mylodon* Owen, 1840, *Mylodonopsis* Cartelle, 1991, *Glossotherium* Owen, 1840, *Octodontotherium* Hoffstetter, 1956, *Paramylodon* Brown, 1903, *Pseudopreprotherium* Hirschfeld, 1985; já em Lestodontinae estão *Lestodon* Gervais, 1855 e a preguiça do Mioceno *Thinobadistes* Webb, 1989, embora Webb (1989) a classifique como uma tribo Lestodontini dentro de Mylodontinae.

O gênero *Lestodon* possui três espécies, sendo *L. urumaquensis* Linares, 2004 e *L. codorensis* Linares, 2004 do final do Mioceno/início do Plioceno (LINARES, 2004), e *L. armatus* do Pleistoceno (PAULA COUTO, 1979; CZERWONOGORA E FARIÑA, 2012). Espécimes de *L. armatus* têm sido encontrados na Argentina (BARGO et al., 1986; DESCHAMPS E BORROMEI, 1992; DESCHAMPS, 2005), Bolívia (MARSHALL E SEMPERE, 1991; COLTORTI et al., 2007), Brasil (PAULA COUTO, 1944; 1973; CARVALHO, 1952; OLIVEIRA, 1996; LOPES et al., 2001; GHILARDI et al., 2011), Uruguai (UBILLA, 2004; MARTÍNEZ & UBILLA, 2004; UBILLA et al., 2004; FARIÑA et al., 2013) e, possivelmente, no Paraguai (HOFFSTETTER, 1978).

Apesar dos achados atribuídos a *L. armatus* terem sido recuperados da Argentina à Amazônia, a espécie poderia ser mais abundante na região sudeste da América do Sul durante o Pleistoceno, ou seja, nos arredores do estuário do rio da Prata, variando pouco sua distribuição nos períodos glaciais e interglaciais (GALLO et al., 2013; VARELA E FARIÑA, 2016). Segundo Czerwonogora et al. (2011), a espécie era consumidora preferivelmente de plantas C3, estando associada a ambientes abertos, secos e frios, como o existente nessa região. Sendo

assim, ela provavelmente era simpátrica com outros milodontídeos, como *G. robustum* e *M. darwini* (VARELA E FARIÑA, 2016).

Muitas das descrições anatômicas de fósseis de Folivora tratam de elementos cranianos e dentários. Sendo assim, as relações filogenéticas são baseadas majoritariamente em caracteres cranianos. Entretanto, descrições minuciosas de elementos pós-cranianos, como membros, tarsais, carpais e falanges são mais raros. Destacam-se os estudos sobre pós-crânio de Amson et al. (2015a, 2015b) sobre *Thalassocnus*; McAfee (2016) para *Mylodon*, e Stock (1914) para *Paramylodon*, além das descrições do século XIX, como os trabalhos de Owen (1842, 1861) para *Glossotherium* e *Megatherium*, e Gervais (1873) para *Lestodon*.

Como o achado de espécimes com os ossos em posição de articulação é algo não tão usual, a identificação de ossos isolados do pós-crânio a nível de espécie e/ou gênero às vezes torna-se dificultosa. Dentre os milodontídeos, por exemplo, apenas o fêmur e o astrágalo são os elementos mais confiáveis para a identificação, visto que cada gênero dentro desse grupo possui características conspícuas em tais ossos. A variação mais característica do astrágalo entre milodontídeos se dá principalmente pelo ângulo do processo odontoide em relação à faceta discoide e a junção ou não das facetas ectal e sustentacular. Nos gêneros *Glossotherium*, *Mylodon* e *Paramylodon* estas duas facetas são contíguas, enquanto que em *Lestodon* elas são separadas por um sulco (OWEN, 1842; STOCK, 1917; STOCK, 1925; KRAGLIEVICH, 1928; KRAGLIEVICH, 1934; PITANA, 2011; PÜSCHEL et al., 2017). Por esse motivo alguns pesquisadores sugeriram atribuir *Lestodon* a uma nova família, Lestodontidae (WEBB, 1989) embora trabalhos mais recentes o incluam em Mylodontidae (GAUDIN, 2004).

Dessa forma, destaca-se a relevância de descrições anatômica de ossos pós-cranianos uma vez que estas podem contribuir com as diagnoses das espécies e para com o conhecimento sobre as relações filogenéticas dos táxons em questão.

1.3 Principais localidades fossilíferas do Pleistoceno do Rio Grande do Sul

Entre as latitudes 25°S e 40° S, nas quais o RS está incluído, existem diversas localidades fossilíferas, onde vertebrados pleistocênicos têm sido coletados (Figura 3). A partir dos fósseis encontrados nessas localidades, é possível estudar a biodiversidade pretérita dessa região. As datações absolutas disponíveis indicam que a maioria do sedimento foi depositado durante o Pleistoceno tardio. Na região Oeste, destacam-se o Arroio Touro Passo, município de Uruguaiana (HSIOU, 2007; KERBER E OLIVEIRA 2008a, b; GASPARINI et al., 2009; PITANA, 2011; KERBER et al. 2014), Rio Quarai, no município de Quarai (RIBEIRO et al.,

2008; PITANA, 2011), e localidade Sanga da Cruz, no município de Alegrete (KERBER E OLIVEIRA, 2008c; PITANA, 2011).

Outras localidades com abundante material fossilífero do Pleistoceno tardio situam-se no leste do Rio Grande do Sul. Uma delas é a Planície Costeira, onde há numerosos fósseis submersos que são trazidos pelas ondas do mar e redepositados na linha de costa, e os depósitos de origem fluvial do Arroio Chuí (SCHERER et al, 2009; PITANA, 2011; KERBER et al, 2011; MOTHÉ, 2012).

Menos conhecidas, e não tão abundantes em material fóssil, são as localidades do centro do estado do Rio Grande do Sul. Por exemplo, a localidade de Marco Português, município de São Gabriel, e também sítios nos municípios de Bagé, Dom Pedrito, Nova Palma, Rosário do Sul, São Pedro do Sul e Toropi. Entre as localidades do centro do estado que mais se destacam pela quantidade e qualidade de fósseis são a Sanga dos Borba, em Pantano Grande, e o Vale do Seival, em Caçapava do Sul. Nessa última região mencionada, o Vale do Seival possui fósseis de *Eremotherium laurilardi* Lund, 1842 e *Megatherium americanum* coletados (OLIVEIRA et al., 2002), e é onde se insere o novo sitio paleontológico que reportamos neste trabalho.

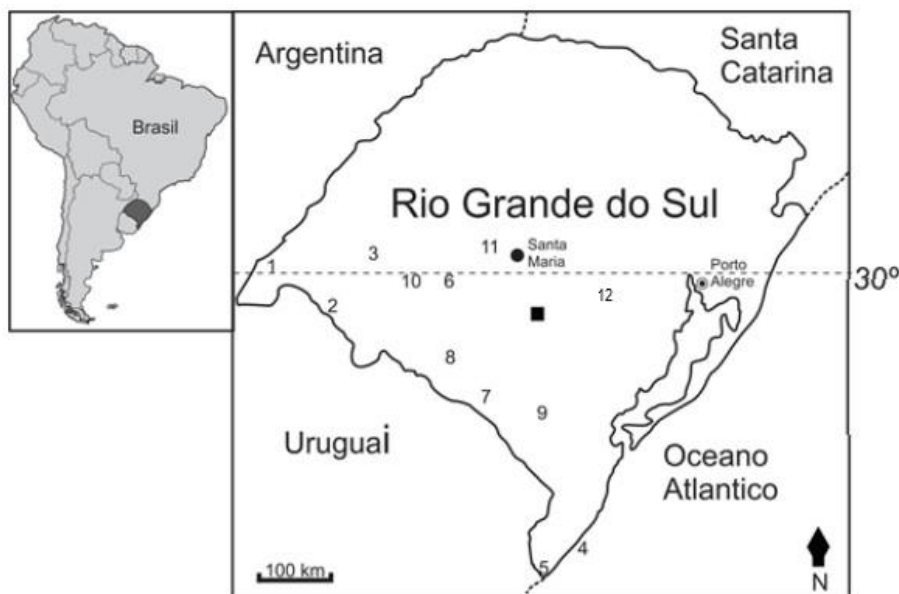


Figura 3. Mapa do Rio Grande do Sul com principais localidades fossilíferas atribuídas ao Pleistoceno tardio. 1) Uruguaiana, 2) Quaraí, 3) Alegrete, 4) Planície Costeira, 5) Arroio Chuí, 6) São Gabriel, 7) Bagé, 8) Dom Pedrito, 9) Pinheiro Machado, 10) Rosário do Sul, 11) São Pedro do Sul/Toropi, 12) Pantano Grande. Localidades de onde foi coletado o material para estudo: Caçapava do Sul (quadrado).
Fonte: Autor

1.2 Os mamíferos e a extinção do Pleistoceno/Holoceno

A radiação adaptativa dos mamíferos já presentes no continente, bem como a chegada de linhagens oriundas de outros continentes através do Grande Intercâmbio Biótico Americano – GABI (WOODBURNE, 2010), culminou na existência de uma fauna caracterizada por formas de grande porte, conhecida como megafauna pleistocênica. Além de linhagens pouco diversificadas durante o Cenozoico (Meridiolestida e Gondwanatheria), de linhagens autóctones do continente sul-americano (Xenarthra, Meridiungulata, e Metatheria) e de linhagens que chegaram à América do Sul durante o Eoceno (Caviomorpha e Plathyrrini) oriundas da África (GOIN et al. 2012), a mastofauna pleistocênica também se compunha por grupos holárticos, que se fizeram presentes a partir do Mioceno e Plioceno, principalmente após a formação do istmo do Panamá (~2.8 milhões de anos atrás) (WEBB, 1985; WOODBURNE, 2010; CIONE et al. 2015). Dentre estes estavam os Carnivora, Proboscidea, Cetartiodactyla, Perissodactyla, Cricetidae e Soricidae (CIONE et al. 2015), constituindo muitas das espécies atualmente existentes no continente.

Ao final do Pleistoceno/início do Holoceno registra-se uma extinção de nível continental, cujas causas são ainda discutidas, onde os principais grupos afetados foram os grandes mamíferos e grandes quelônios terrestres (menos conhecidos do que os grandes mamíferos). Sobreviveram apenas algumas das espécies de médio porte, como a onça (*Panthera onca* Linnaeus, 1758), o cervo-do-pantanal (*Blastocerus dichotomus* Illiger, 1815), a capivara (*Hydrochoerus hydrochaeris* Linnaeus, 1766), o guanaco (*Lama guanicoe* Müller, 1776), entre outros (CIONE et al., 2003). Entre os grupos mais afetados, destacam-se os xenatros (de interesse neste trabalho), cujas formas de grande porte (gliptodontes, pampatérios e preguiças-terrácolas) foram todas extintas.

Como ressaltado acima, as causas desta extinção ainda são discutidas. Diversas hipóteses têm sido propostas e, entre as principais, destacam-se: atribuição às mudanças climáticas ocorridas na transição entre o Pleistoceno/Holoceno, onde houve um aumento da precipitação pluviométrica e da temperatura, modificando o clima em relação as condições áridas e frias que ocorreram durante o Último Máximo Glacial (vide QUATTROCCHIO et al., 2008); a chegada dos humanos e sua excessiva caça à megafauna, o que foi chamado de Efeito *Blitzkrieg* (vide BROOK E BOWMAN, 2004); e a falta de imunidade da fauna nativa sul-americana com a introdução de patógenos pelas espécies holárticas (FERIGOLO, 1999).

Cione et al. (2003) propuseram uma hipótese que, de certa forma, unifica as versões supracitadas, além de mostrar diversos aspectos não abordados anteriormente – a hipótese do

Broken Zig-Zag. Segundo estes autores, durante o Pleistoceno havia uma alternância entre períodos glaciais e interglaciais. Durante os períodos glaciais, o continente era dominado por ambientes abertos, enquanto que, em interglaciais havia um aumento das áreas florestais, culminando na fragmentação das paisagens campestres. Logo, durante as glaciações, os animais de grande porte ampliavam suas áreas de distribuição e, conseqüentemente, ampliavam sua diversidade genética. Em contrapartida, nas interglaciações, dado a fragmentação dos ambientes, as populações de grandes mamíferos reduziam suas áreas de distribuição e também a diversidade genética. Sendo assim, durante pelo menos cerca de 2.5 milhões de anos, houve um “zig-zag” entre períodos de grande número de indivíduos e aumento de variabilidade genética, e períodos de redução no número de indivíduos e baixa variabilidade genética. Sendo assim, devido à redução de variabilidade genética, os períodos interglaciais seriam mais propícios a riscos de extinção.

1.3 Objetivos

1.3.1 Objetivo geral

- Reportar o achado de Mylodontidae (UFSM 11535) em uma nova localidade fossilífera no Vale do Seival, Quaternário do sul do Brasil;

1.3.2 Objetivos específicos

- i) Apresentar uma nova localidade fossilífera do Quaternário no Vale do Seival, Rio Grande do Sul;
- ii) Realizar identificação taxonômica de UFSM 11535;
- iii) Descrever em detalhe a morfologia pós-craniana de UFSM 11535 em comparação com outros táxons e verificar a presença de variações anatômicas.

2 ARTIGO CIENTÍFICO

A new record of *Lestodon armatus* Gervais, 1855 (Xenarthra, Mylodontidae) from the Quaternary of southern Brazil and remarks on its postcranial anatomy

Dilson Vargas-Peixoto^{a*}, Cícero Schneider Colusso^a, Átila Augusto Stock Da-Rosa^b and Leonardo Kerber^c

^aPrograma de Pós-Graduação em Biodiversidade Animal, Universidade Federal de Santa Maria, Santa Maria, Brazil; ^bDepartamento de Geociências, Universidade Federal de Santa Maria, Santa Maria, Brazil, ^cCentro de Apoio à Pesquisa Paleontológica, Universidade Federal de Santa Maria, São João do Polêsine, Brazil.

*corresponding author: Avenue Roraima, nº 1000, Camobi, Santa Maria, Rio Grande do Sul, Brazil, 97105-900, e-mail: iiuni_kantal@hotmail.com

Short biographical: The authors are researchers of vertebrate paleontology of South America. This work was supported by the Coordenação de Aperfeiçoamento de Pessoal de Nível Superior under Grant nº 001.

A new record of *Lestodon armatus* Gervais, 1855 (Xenarthra, Mylodontidae) from the Quaternary of southern Brazil and remarks on its postcranial anatomy

Mylodontidae (Xenarthra: Folivora) includes ground sloths of medium and large size, with the largest representative of the group being *Lestodon armatus*. Fossils of this species have been found in Pleistocene fossiliferous deposits of South America, with most of its records at the southern portion of the continent. Here, we reported the discovery of a mylodontid assigned to *L. armatus* recovered from a Quaternary deposit in Caçapava do Sul, southern Brazil. The specimen is composed of cranial fragments, vertebrae, articulated hind limb, and pes, as well as other post-cranial elements. We described the post-cranial elements of this specimen, including some elements not yet described for this species, such as the ossified meniscus, cyamo-fabella, and the fusion of the tibia and fibula. The new record contributes to the knowledge on the anatomy of this species as well as to the study of the diversity of the extinct mammalian fauna from southern Brazil.

Keywords: Morphology, Mylodontidae, Megafauna, Xenarthra, Quaternary, Pleistocene.

Introduction

Xenarthra is an American clade of Eutherian mammals and is one of the four main lineages of living placental mammals (Xenarthra, Afrotheria, Laurasiateria, and Euarchontoglires) (Murphy et al. 2001a,b; Asher et al. 2009; O’Leary et al. 2013). In South America, during the Pleistocene, this clade was very conspicuous in the mammalian fauna, as it had a high diversity compared to the present. Xenarthra includes Cingulata: armadillos (Dasypodidae) and glyptodonts (Glyptodontidae); and Pilosa: anteaters (Vermilingua), arboreal, and terrestrial sloths (Folivora) (also called Tardigrada or Phyllophaga) (Gaudin 2004; Gaudin and McDonald 2008; Pujos et al. 2012).

The Pleistocene terrestrial sloths are classified into four families: Megalonychidae, Megatheriidae, Nothrotheriidae, and Mylodontidae (Gaudin 2004; Pujos et al. 2012). Mylodontidae is composed of Scelidotheriinae and Mylodontinae, and the tribe Lestodontini within the Mylodontinae subfamily (Gaudin 2004). This family had a wide geographic range and a high number of species in comparison to other Pilosa clades. They were distributed from southern South America to North America. Mylodontid sloths were among the first mammals that participated in the Great American

Biotic Interchange, migrating from South America to North America during the late Miocene (Marshall 1988; Woodburne 2010; Cione et al. 2015).

The mylodontid genus *Lestodon* Gervais, 1855 includes three species in South America: *L. urumaquensis* Linares, 2004 and *L. codorensis* Linares, 2004, that lived during the late Miocene/Early Pliocene of the northern part of the continent (Linares 2004), and *L. armatus* from the Pleistocene (Paula Couto 1979; Czerwonogora and Fariña 2012). Fossils assigned to *L. armatus* have been found in Argentina (Bargo et al. 1986; Deschamps and Borromei 1992; Deschamps 2005), Bolivia (Marshall and Sempere 1991; Coltorti et al. 2007), Brazil (Paula Couto 1944, 1973; Carvalho 1952; Oliveira 1996; Lopes et al. 2001; Ghilardi et al. 2011), Uruguay (Ubilla 2004; Martínez and Ubilla 2004; Ubilla et al. 2004; Fariña et al. 2013), and possibly in Paraguay (Hoffstetter 1978). Although specimens assigned to *L. armatus* have been found from Argentina to the Brazilian Amazonia (Gallo et al. 2013), they are more abundant in the southern and southeast portion of the continent (Varela and Fariña 2016). This mylodontid was the largest species of the family, and according to Czerwonogora et al. (2011), *L. armatus* had a diet mainly composed of C3 plants from cold and dry grasslands. Therefore, it was possibly sympatric with *Glossotherium robustum* Owen, 1842 and *Myiodon darwini* Owen, 1839 in the southern Uruguay and Buenos Aires province, Argentina (Varela and Fariña 2016).

Here, we report a new finding that includes a fragment of the skull, teeth, and postcranial remains collected in a new fossiliferous locality “Arroio do *Lestodon*”, which is located in a small river at Caçapava do Sul, Rio Grande do Sul state (Fig. 1). The material represents a single individual because some elements were found in articulation. As most of the fossil records of *L. armatus* are represented by craniodental elements, and in some cases by the astragalus, here we describe some previously undescribed postcranial bones, contributing to the knowledge on the anatomy of this taxon.

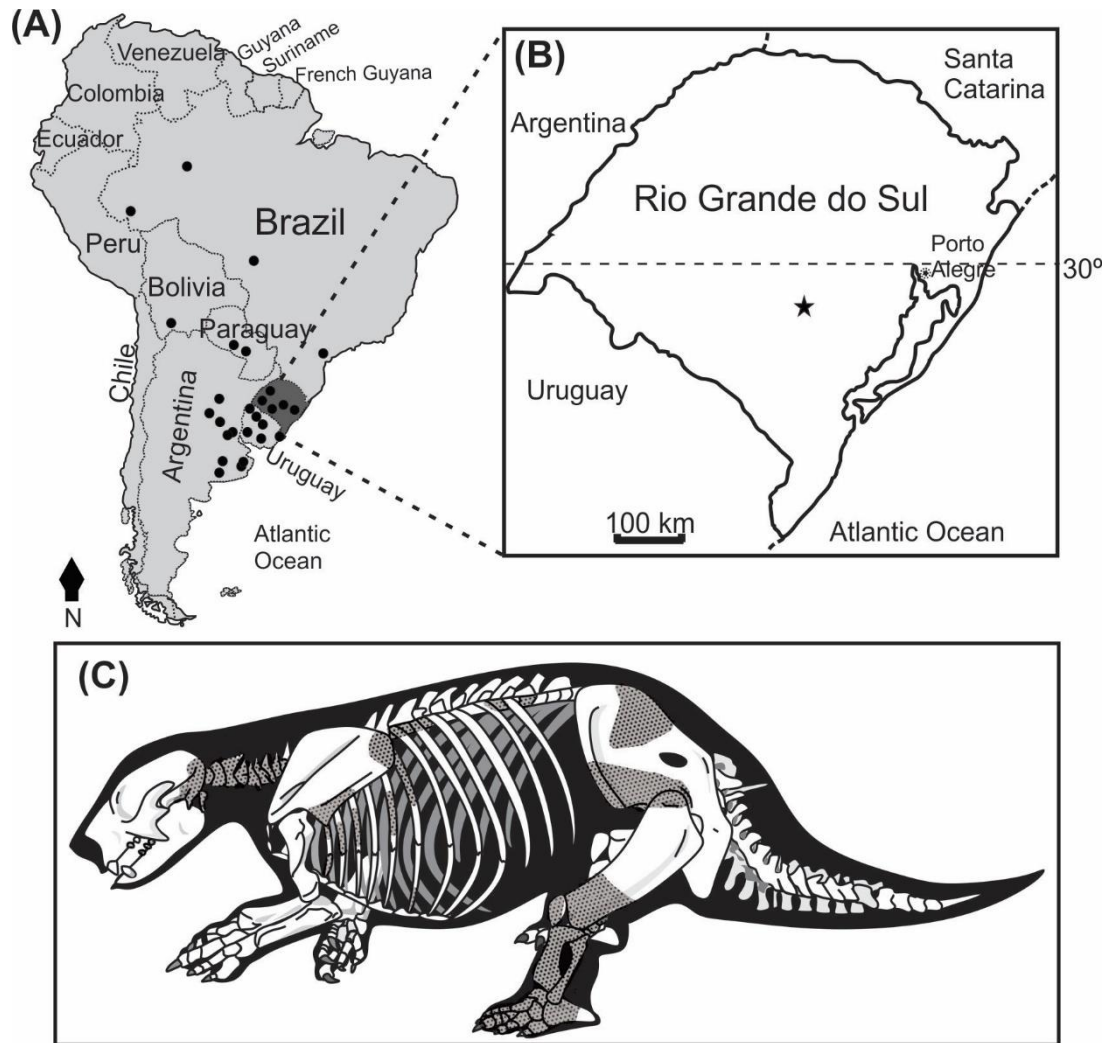


Figure 1. (A) Fossil record of *Lestodon armatus* in South America, based on Gallo et al. (2013); (B) State of Rio Grande do Sul (B) and location of fossiliferous site “Arroio do Lestodon”, were where UFSM 11535 was found (star); (C) preserved portions of the bones of UFSM 11535. The skeleton is based on Fariña et al. (2013).

Material and methods

Methodology

The specimen UFSM 11535 is housed in the Laboratório de Estratigrafia e Paleobiologia of the Universidade Federal de Santa Maria. The fossils here studied were found in a watercourse informally called “Arroio do *Lestodon*”, a tributary of a larger river in that region, the Arroio Seival, located at Caçapava do Sul municipality, State of Rio Grande do Sul, Brazil, in 2010. The specimen was found buried in the mud, together with vertebrae, ribs, teeth fragments and other non-identified fossils.

The material was measured with a digital caliper. UFSM 11535 was compared with

other specimens assigned to *Lestodon* from the paleontological collections of Fundação Zoobotânica of Rio Grande do Sul, Museu Coronel Tancredo Fernandes de Mello in Santa Vitória do Palmar, Rio Grande do Sul, and Museo Nacional de Historia Natural of Uruguay. The specimen was also compared with anatomical descriptions of ground sloths in the literature: De Iuliis (1994, 1996) for *Eremotherium* and *Megatherium*; Kraglievich (1928, 1934) and McAfee (2016) for *Myiodon*; Owen (1842), Pitana (2011) and Püschel et al. (2017) for *Glossotherium*; Stock (1917, 1925) for *Paramyiodon*; Miño-Boilini et al. (2014) for *Scelidotherium*; Webb (1989) for *Thinobadistes*; Gervais (1873) and Tambusso et al. (2015) for *Lestodon*; Brandoni et al. (2004), Linares (2004), Salas et al. (2005), Pérez et al. (2010) and McDonald (2012) for general features from families and subfamilies of sloths.

The anatomic nomenclature follows Bargo et al. (2006) for the teeth, Amson et al. (2014) for the hind limbs and pes, and Schaller (2007) for the remaining structures. The orientation of the bones follows Schaller (2007).

Institutional abbreviations

EPM-PV – Paleovertebrate collection of Emigdio Pinto Martino, Santa Vitória do Palmar, Brazil; **FMNH** – Field Museum of Natural History, United State of America; **MCN-PV** – Paleovertebrate collection of Museu de Ciências Naturais, Fundação Zoobotânica do Rio Grande do Sul, Brazil; **MCTFM** – Museu Coronel Tancredo Fernandes de Mello, Santa Vitória do Palmar, Brazil; **MNHN** – Museo Nacional de Historia Natural de Uruguay
SGO – Paleontology Area of Museu Nacional de História Natural of Chile; **UFSM** – Universidade Federal de Santa Maria, Santa Maria, Brazil.

Geographic and geological remarks

The Arroio Seival is located between the cities of Caçapava do Sul, and Lavras do Sul, Rio Grande do Sul state, Brazil. In this region, there are exposures of fluvial deposits with a conglomeratic base and sandstone on the top, deposited during the Quaternary (Ribeiro and Scherer 2009). Fossils found there include *Epieuryceros* sp., *Glyptodon* sp., *Toxodon* sp., *Morenelaphus* sp., Megatheriidae, and Mylodontidae (Oliveira 1996; Oliveira et al. 2002).

UFSM 11535 was found near this locality in an outcrop informally designated as “Arroio do *Lestodon*” (30°46'55.09"S 53°42'43.00"W) (Fig. S1). It is a stream approximately 1.5 m wide composed of sand and pebble. “Arroio do *Lestodon*” is a tributary of the Carajá stream, which is a drain of the Hilário stream. These small watercourses are part of the hydrographic basin of the Camaquã River.

The outcrops exposed in the region of the Arroio Seival and “Arroio do *Lestodon*” are still without absolute ages. Oliveira et al. (2002) correlated Arroio Seival with the Arroio Pessegueiro (Passo do Megatério), another fossiliferous outcrop in the Seival region and suggested a middle Pleistocene age for those fossiliferous strata. This interpretation was based on the fossil record from the Pampean region of Argentina, having the *Epieuryceros* as a biostratigraphic element (Oliveira et al. 2002), because this genus is present in outcrops of Ensenadan (Cione and Tonni 1995) and Bonaerian (Cione and Tonni 2005; Cione et al. 2015). In the Bonaerian beds, there are the earliest records of *Megatherium americanum* Cuvier, 1796 that extended until the late Pleistocene (Oliveira et al. 2002; Tonni et al. 2009, Cione et al. 2015). Therefore, these two outcrops of Caçapava do Sul would be in the lapse of coexistence of *Epieuryceros* and *M. americanum* (Oliveira et al. 2002; Ribeiro and Scherer 2009). However, the material assigned to *Epieuryceros* requires a comparative review to confirm its identification, because the material is a portion of the antler, which is a quite variable structure. Besides, the taxon was not found in any other outcrops from southern Brazil.

Although Oliveira et al.’s (2002) suggestion that the fossiliferous deposits of the studied region were deposited during the middle Pleistocene, evidence on the age of these layers is still very scarce for such an assertion, because neither fossils nor sediments have been dated, and thus depend on further studies in order to clarify such questions. Due to the scarcity of data for the deposition these beds, we herein assigned a Quaternary age for the fossils found there.

Results

Systematic paleontology

XENARTHRA Cope, 1889

FOLIVORA Delsuc, Catzeflis, Stanhope, Douzery, 2001

MYLODONTOIDEA Gill, 1872

MYLODONTIDAE Gill, 1872

LESTODON Gervais, 1855

Type species. Lestodon armatus Gervais, 1855

Lestodon armatus Gervais, 1855

(Figs. 2-8, S2-S19; Tables S1-S5)

Referred material. UFSM 11535 is composed of teeth (right ML2, right ml2, ml3, and ml4), right stylohyal, cervical vertebrae, lumbar vertebrae, thoracic vertebrae, fragment of scapula, ribs, sacrum, pelvic girdle, left humerus, cymano-fabella, left tibia, left fibula, left astragalus, left navicular, left cuboideus, left calcaneus, left ectocuneiform, left digits II, III, IV and V.

Geographic provenance. “Arroio do *Lestodon*” (30°46'55.09"S 53°42'43.00"W), Seival locality, near Caçapava do Sul and Lavras do Sul cities, Rio Grande do Sul, Brazil.

Description

Cranial fragments. UFSM 11535 preserves fragments of occipital bone, both occipital condyles, the petrosal region of temporal bone and, possibly parts of the basisphenoid. The petrosal region is much irregular having depressions with a thin wall of the inner region of the skull. On the external region, the surface is smooth.

Teeth. From the right upper teeth of UFSM 11535, only the upper molariform (ML) 2 is preserved. The right lower series conserves the lower molariforms (ml) 2, 3 and 4 (Fig. S2). All the molariforms are mesiodistally longer than labiolingually.

The ML2 is lingually curved and relatively flat on the lingual surface. The ml2 is slightly distally curved, and its outline is oval when observed in occlusal view. The ml3 is lingually more curved and ellipsoidal than ML2 and ml2. The ml4 is bilobated, with oblique eight outline. The mesial lobe is larger than the distal, which is lingually projected in relation to the larger lobe. The vasodentin is not preserved in this tooth, nor in the ML2.

Stylohyal. The stylohyal shows the proximal end wider than the distal extremity. The articulation facet to the basicranium is small and located cranially in relation to the axis of this bone (Fig. 2A, B, D). The proximal region of the stylohyal is compressed lateromedially, having a tubercle for insertion of the *m. occiptohyoideus* and with the origin of the *m. stylohyoideus* on the ventrocaudal part (Pérez et al. 2010; Tambusso et al. 2015) (Fig. 2A, D, E). This tubercle is perpendicular in relation to the distal axis of the stylohyal. The medial view there is a triangular fossa for insertion of *m. occiptohyoideus* between the tubercle and the articular surface to the basicranium (Fig. 2A, D), and it is not present on the juvenile specimen (Tambusso et al. 2015). Other insertion surfaces for this muscle can be seen ventrodistally as a shallow fossa, and on the lateral face, where a third fossa is limited by the proximal edge, as well as on the articular surface to the basicranium.

Distally, the stylohyal is elongated and has a triangular outline. It curves abruptly in the craniolateral direction to gently return to the medioventral direction in the same axis of the bone. This curve is flattened mediolaterally, and distally it has a crest on the lateral surface. The crest may indicate the attachment of the *m. hyoglossus*. The depression of the medial surface of the distal end might indicate the *m. styloglossus* attachment (Pérez et al. 2010) (Fig. 2C, E, F). The epihyal facet is slightly convex, rounded and oriented medially (Fig. 2C-F).

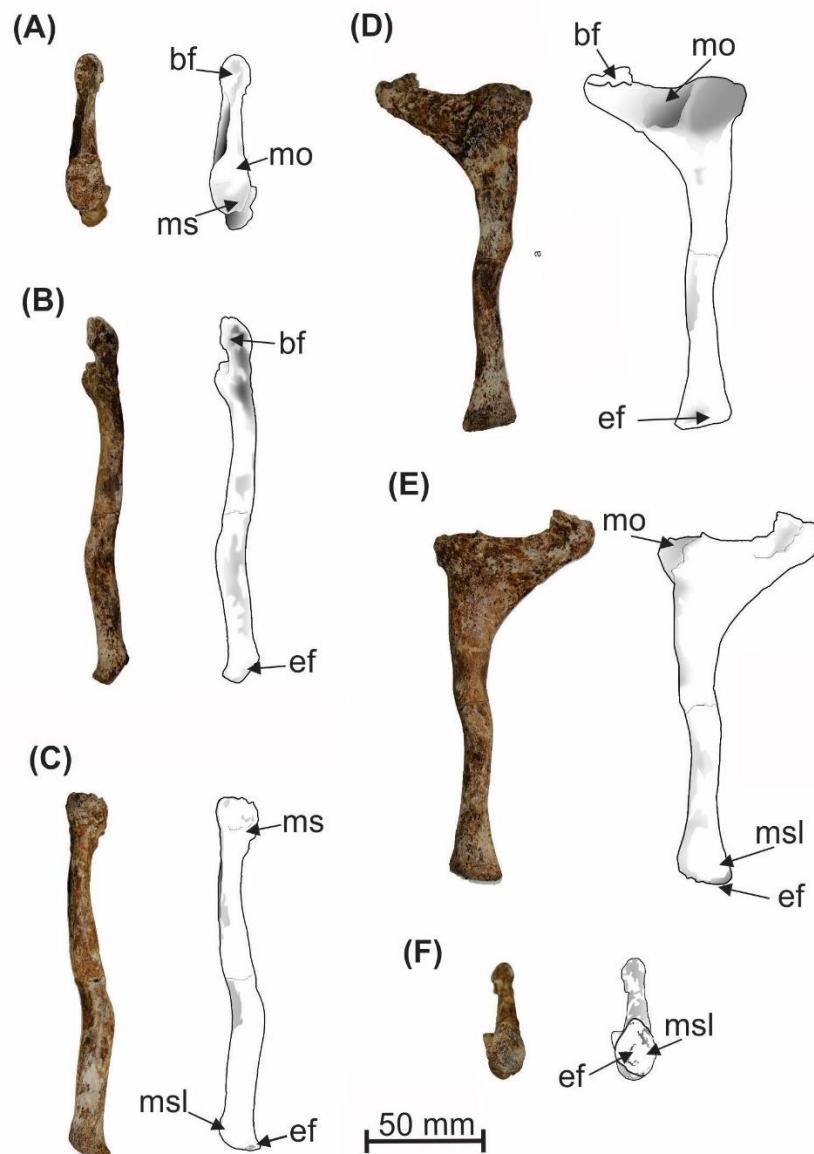


Figure 2. Right stylohyal of *Lestodon armatus* (UFSM 11535). (A) proximal, (B) dorsal, (C) ventral, (D) medial, (E) lateral and (F) distal views. Abbreviations: bf, basicranium facet; ef, epihyal facet; mo, insertion of *m. occipitohyoideus*; ms, origin of *m. stylohyoideus*; msl, attachment of *m. styloglossus*. Scale: 50 mm.

Atlas. The occipital condyle facets are concave, oval and have the ventral part smaller than the dorsal region (Fig. 3A). Their medial edges are straight. The lateral edges of these facets are dorsolaterally projected cranially.

The two occipital condyle facets are separated by the arches of the atlas. The dorsal arch is relatively flat in the ventral face and has the cranial edge situated caudally to dorsal edges of the facets (Fig. 3A-C). Caudodorsally to the condyle facets is located the foramen for the first spinal nerve (Fig. 3B-D), which crosses the arch, reaching the medullary canal (Paula Couto 1979). In the cranial view, the cranial edge of the dorsal arch and the dorsal edge of the occipital condyle facet are rectilinear.

The articular facets to the axis (Fig. 3C) are directed caudomedially and situated caudodorsally in relation to the occipital condyle facet. They are oval, with the dorsal edge larger than the ventral edge and less concave than the occipital condyle facets.

The dorsal edge of the axis facet is prominent, and cranially to this edge, there is a sulcus for a vertebral artery that delimits the facet. This sulcus connects to the nerve-spinal canal, situated laterally to these facets (Fig. 3C). The nerve-spinal canal connects to the transverse foramen cranially in the other side of the atlas wing.

The caudal edge of the dorsal arch is extended lateroventrally, forming a bridge over the canal located laterodorsal to the axis facets (Fig. 3C). The caudal edge of the atlas wing is enlarged near the axis facets, presenting a tuberosity lateroventrally to these facets. Dorsolateral to this tuberosity, there is a rough and narrow depression. In the dorsal edge of this depression, there is a crest that is extended to the lateral margin of the atlas wing.

The atlas wing is prominent (Fig. 3A-E), forming a plateau in the lateral edge. Cranially to the bridge that forms the caudal edge of arches, there is a depression that limits a perpendicular process in the lateral edge of the wing. Other depressions are located cranially to this process. Cranioventrally, the wing shows the transverse foramen located close to the base of the occipital condyle facet.

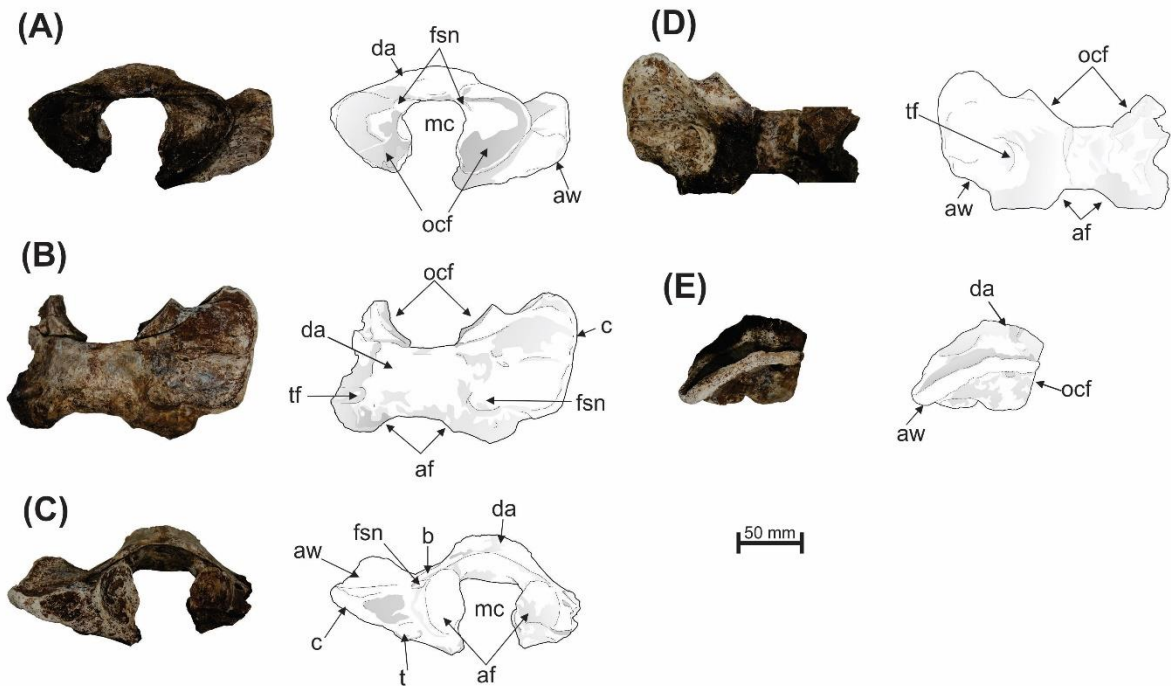


Figure 3. Atlas of *Lestodon armatus* (UFSM 11535). (A) cranial, (B) dorsal, (C) caudal, (D) ventral and (E) lateral views. Abbreviations: af, axis facet; aw, atlas wing; b, bridge; c, crest; dr, dorsal region; fsn, foramen for spinal nerve; mc, medular canal; ocf, occipital condyle facet; t, tuberosity. Scale: 50 mm.

Axis. The articular facets to the atlas are rounded, slightly convex, and located cranio-laterally (Fig. S3A-C, E, F). Cranially, between the two facets, is the odontoid process (Fig. S3A-F). This process is rounded and shows a flat ventral surface. The transverse foramen is caudal to the atlas facet and extends caudolaterally (Fig. S3C, D).

On the ventral face of the axis, there is an extended “arrow-shaped” crest, with a larger, rounded caudal end that forms a tubercle (Fig. S3E). The caudal face of the axis body is ovate, showing the dorsal edge slightly concave. The ventral edge is triangular. The caudal articular facet for the third cervical is convex.

The spinous process of the axis is incomplete (Fig. S3A-D, F). Nevertheless, it is possible to observe that it is caudodorsally extended on the axis. The caudal edge is thicker than the cranial. Caudal to the spinous process, there is a depression on both sides, with the left one slightly deeper than the right one. The base of the caudal area of the spinous process is roughened. This region is oriented caudally and has five small foveae. The caudal zygapophysis is trapezoidal.

Third to seventh cervical vertebrae. The third to seventh cervical vertebrae show the vertebral centrum dorsoventrally flattened. Their cranial face is oval with the ventral edge lower than the

dorsal edge because the latter is cranially projected (Fig. S4B, C, F). The cranial and caudal edges are larger in comparison to the vertebral center, with the caudal one larger than the cranial one.

On the dorsal surface of the vertebral centrum, there is a depression surrounded cranially and caudally by small tuberosities. On the ventral face, the ventral crest is connected to the ventral edge of the cranial and the caudal surfaces of the vertebral centrum (Fig. S4E). This crest separates two depressions and connects the transverse process, where the transverse foramen is located.

The spinous process is “cross-shaped” (one central axis with two small lateral projections) and dorsocaudally oriented (Fig. S4A-F). A crest originates in the cranial region of the craniodorsal surface of the spinous process. This crest is directed to the location where the spine edge branches off. In the caudal face, another crest originates at the union of two other crests in the caudal articular process bases, extending to the highest edge of the spinous process (Fig. S4D).

The cranial zygapophysis is robust, forming a triangular tubercle (Fig. S4A-C, F). The articular facet to the corresponding cranial zygapophysis of the caudally sequential vertebrae is flat and concave (Fig. S4B-D, F). In the cranial view, the outline of the cranial zygapophysis edge and the spinous process base are “W-shaped” (Fig. S4A). Between the cranial and caudal zygapophysis, there is a depression in the lateral and medial faces.

The caudal zygapophysis is directed caudolaterally. The articular facet to the cranial zygapophysis of the adjacent vertebrae is divided into two continuous parts. Most of it is wide and lateroventrally directed. The small part is narrow and laterally directed. On the caudal view, the caudal zygapophysis and the neural arch have the shape of an “inverted Y” (Fig. S4D).

The outline of the vertebral foramen has the shape of a dome. The ventral face of the neural arch (dorsal region of the canal) shows a tubercle on each base of the cranial zygapophysis.

Thoracic vertebrae. In UFSM 11535, only the centrum of the first five thoracic vertebrae are preserved. The centrum is oval-shaped in the cranial and caudal views, with the dorsal portion larger than the ventral. It is compressed lateroventrally, and the ventral crest is located in the middle of the ventral face. This crest passes along the centrum in the craniocaudal direction and laterally presents oval foramina. The dorsal face of the vertebral centrum is flat.

Lumbar vertebrae. UFSM 11535 preserves two lumbar vertebrae. The centrum is more circular when compared to the other vertebrae and laterally compressed. It is cranially projected in the dorsal portion of the cranial surface and caudally projected in the ventral portion of the caudal surface. Thus, the lumbar vertebral centrum has shape of an inverted trapezium in lateral view.

On the ventral surface, there is a crest that passes along the vertebral centrum in the craniocaudal axis like all the other vertebrae. Laterally to this crest, the bone is perforated by foramina. Its dorsal surface is slightly concave.

Sacrum. Only two fused vertebral centra are preserved in UFSM 11535, possibly the fifth and sixth sacral vertebrae, which are fragmented in the cranial portion. The vertebrae are robust and laterally have dorsoventrally directed depressions.

In the sixth vertebrae, there is a sacral ventral foramen passing dorsoventrally through the vertebral body. Small foramina for sacral nerves are present on the dorsal surface of two vertebrae.

Scapulae. UFSM 11535 preserves a fragment of the right scapular blade. It corresponds to the glenoid region, preserving part of the articular facet that is flat and rounded. On the lateral surface, part of the scapular spine and caudal edge are preserved.

Pelvic girdle. A small fragment of the pelvic girdle is preserved, including the left acetabulum and the adjacent part of the ilium.

Femur. The femur is fragmented at the proximal end. The condyles for tibial articulation are connected through the patellar facet, which is concave (Fig. 4A). The caudal edge of the patellar facet is prominent. Caudal to this facet, there is the intercondylar fossa, which is deep in caudodorsal direction. The intercondylar fossa is rough, and within it, there is a transversal crest that begins at the base of the lateral edge of the medial condyle (Fig. 4B, E). Proximal to this fossa, in the caudal view is the popliteal surface (Fig. 4B).

The lateral condyle is extended laterocaudally (Fig. 4A, B, D, E), and is smaller than the medial condyle (Fig. 4A-C, E). Both condyles are caudally extended. They show prominent edges in the limit with the intercondylar fossa, forming a plateau in relation to non-articular regions of the distal end.

Craniolateral, a groove separates the lateral condyle of the lateral epicondyle (Fig. 4A, B, D, E). Distocaudal to the lateral epicondyle, a rough crest extends to the medial edge of the

lateral condyle, and caudally there is a slight depression. Proximal to the lateral condyle, in lateral view, there is a rough and fragmented lateral epicondyle.

The medial surface of the base of the medial condyle is rough and presents foveas. Cranial to the medial condyle there is a process that connects to the patellar facet. Proximomedially and continuous to the medial condyle in caudal view there is a facet to the sesamoid (Fig. 4B). The medial epicondyle is fragmented (Fig. 4C) and appears to be small in relation to the lateral epicondyle.

The diaphysis is craniocaudally flat. The distal end has a depression in the middle region of the cranial surface. Striations originate in the center of this depression and are directed to the fossa, which separates the lateral condyle of the lateral epicondyle. These striations follow an elevation formed in the middle of a depression.

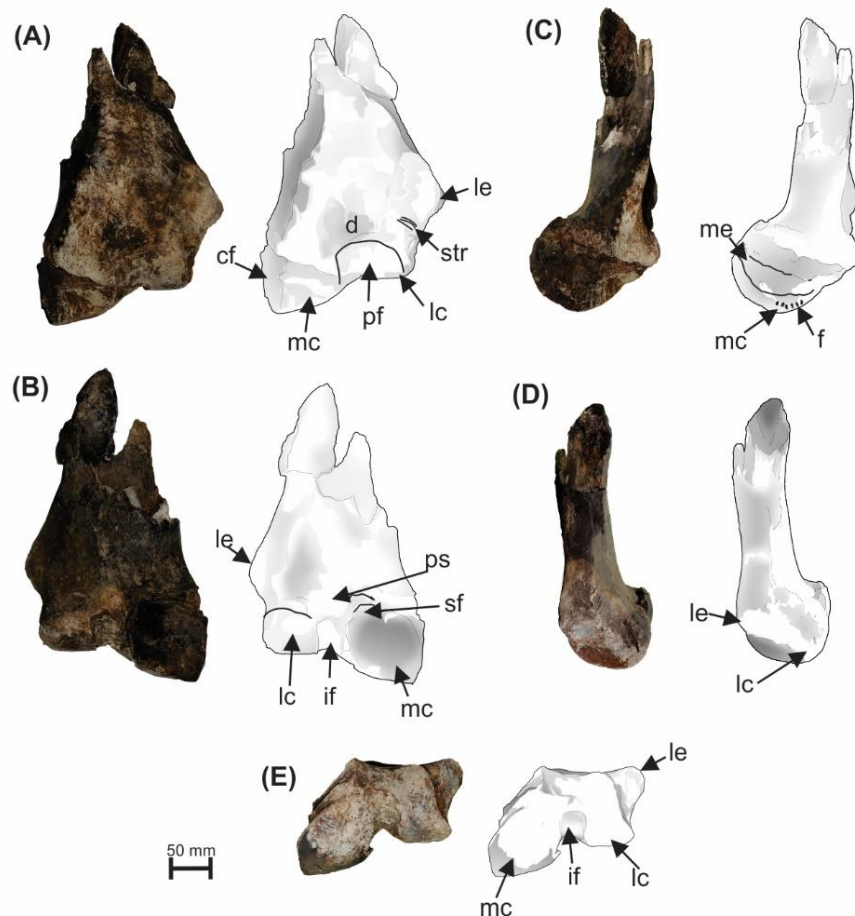


Figure 4. Left femur of *Lestodon armatus* (UFSM 11535). (A) cranial, (B) caudal, (C) medial, (D) lateral and (E) distal views. Abbreviations: d, depression; f, fovea; if, intercondylar fossa; lc, lateral condyle; le, lateral epicondyle; me, medial epicondyle; mc, medial condyle; pf, patellar facet; ps, popliteus surface; sf, sesamoid facet; str, striations. Scale: 50 mm.

Cyamo-fabela. The cyamo-fabela is craniocaudally flat (Fig. S5). On the cranial surface is the tibial facet, which is oval and has prominent edges. The cyamo-fabela is rough and has two crests medially located and separated a sulcus. In the dorsal margin, there is a deep groove. Lateral to this groove, there is a tuberosity, like in the ventral view.

Tibia. The medial tibial condyle is almost circular-shaped, concave and larger than the lateral one (almost three times larger) (Fig. 5A). It shows the craniolateral edge sustained by a rough tuberosity that limits the intercondylar eminence cranially (Fig. 5A, B, D, E).

The lateral tibial condyle is flat and shows a quadrangular outline with the cranial edge curved and craniodistally directed (Fig. 5A). Cranially from the caudolateral edge of the lateral condyle is the cyamo-fabella facet (Fig. 5A).

Cranial to the craniomedial edge of the lateral condyle, there is an ovoid depression. It is the *area intercondylaris cranialis*, which is separated from the intercondylar eminence by a small crest. This crest connects the cranially situated rough tuberosity to the craniomedial edge of the medial condyle (Fig. 5A, C). The intercondylar eminence is rough and convex. It is craniocaudally directed to the bone curvature bordering caudolateral edge of the lateral condyle.

The lateral condyle is elevated like a plateau and connects laterally to the fibula. Cranial to the plateau, the lateral condyle is distally oriented. Craniolateral to the lateral condyle, there is a bridge that connects the tibial tuberosity to the cranial region of the fibula, forming a channel between these two bones (Fig. 5A, B). On this bridge, there are two small crests.

On the cranial face of the proximal region, there is a rough depression, which is separated from the condylar platform by the craniomedial plateau and the tibial tuberosity, both located distally.

The groove that corresponds to *sulcus tuberositatis tibiae* is present medially to the tibial tuberosity and laterally to the craniomedial plateau of the base of the medial condyle (Fig. 5A, B). This sulcus is proximally wider than distally. There is another sulcus parallel to the *sulcus tuberositatis tibiae*, located proximolaterally in the craniomedial plateau.

The tibial diaphysis is craniomedially-caudolaterally flat. It has a tubercle in the craniolateral edge, close to the proximal end, distally to the tibial tuberosity. It has an inconspicuous tuberosity-line obliquely arranged to the tibial axis, which begins at the level of the tuberosity and is directed distomedially.

In craniomedial view, a rough crest is directed proximolateral to distomedial. It separates the tibial body from the rough, high and flat part of the proximal region, forming the

plateau of condyles. Medial to this plateau, there is a rough region that is extended distally to the tibial axis on the medial edge.

In the caudal view, the tibia has a crest following the bone axis in the proximal region. Lateral to this crest, there is a depression that separates from another crest.

The distal end of the tibia is extended to the fibula and shows three articular facets for the astragalus (Fig. 5F). The odontoid facet is concave and circular and is located cranial to the other facets. The discoid facet is extended lateromedially and separate from the odontoid facet by a distal process that is also the edge for astragalar articulation. This crest is concave craniocaudally.

Fibula. The fibula is an elongated bone that is craniocaudally flat. In UFSM 11535, it is partially fused to the tibia at the proximal end (Fig. 5A, B, D). A large process located caudally at the proximal end shows two transversal crests – one located caudomedially, and the other one, semicircular-shaped, positioned caudally (Fig. 5D, E). This latter semicircular crest is about ten times larger than the first crest. Between these crests, there is a sulcus that extends in the distomedial fibular axis until the medial projection for the contact with the tibia (Fig. 5D) and ends close to a triangular groove at the distal end. A small crest transposes this sulcus transversally.

Cranio-lateral to the two crests that limited the sulcus, at the proximal end, there is another sulcus that separates the crests from a largely rounded tuberosity located cranio-laterally (Fig. 5A, B). This rounded tuberosity is flat at the proximal region. Cranially, there is a bridge that connects the fibula to the tibia, near to the tibial tuberosity. Distal to the large tuberosity, there are two crests oriented along the fibular axis. The cranio-medial crest is connected to the distal edge of the bridge.

In the caudomedial face of the proximal end, there is an oval tuberosity located medially to the caudomedial medial crest for tendon anchorage. Distal to this tuberosity, there is another smaller tuberosity.

Distal to the tibial contact, the fibula presents the lateral pyramidal malleolus, in which the articular facet to the astragalus is situated (Fig. 5B-F). This triangular-shaped facet is placed in the same axis of the fibula and is situated around 70° in relation to the articular facet of the tibia with the discoid facet of astragalus (Fig. 5F).

The tubercle of the astragalus facet has a lateral crest directed to the proximal region of the bone axis (Fig. 5F). This crest is rough and directed caudodorsally, making a curve cranioproximally, and then directed caudally, giving a “sigmoid shape” to the crest.

The caudolateral face of the fibular body shows a set of tenuous wavy crests that are oriented along the axis bone (Fig. 5E). Another proximodistal crest in the bone axis is present on the distal portion of the cranio-lateral face.

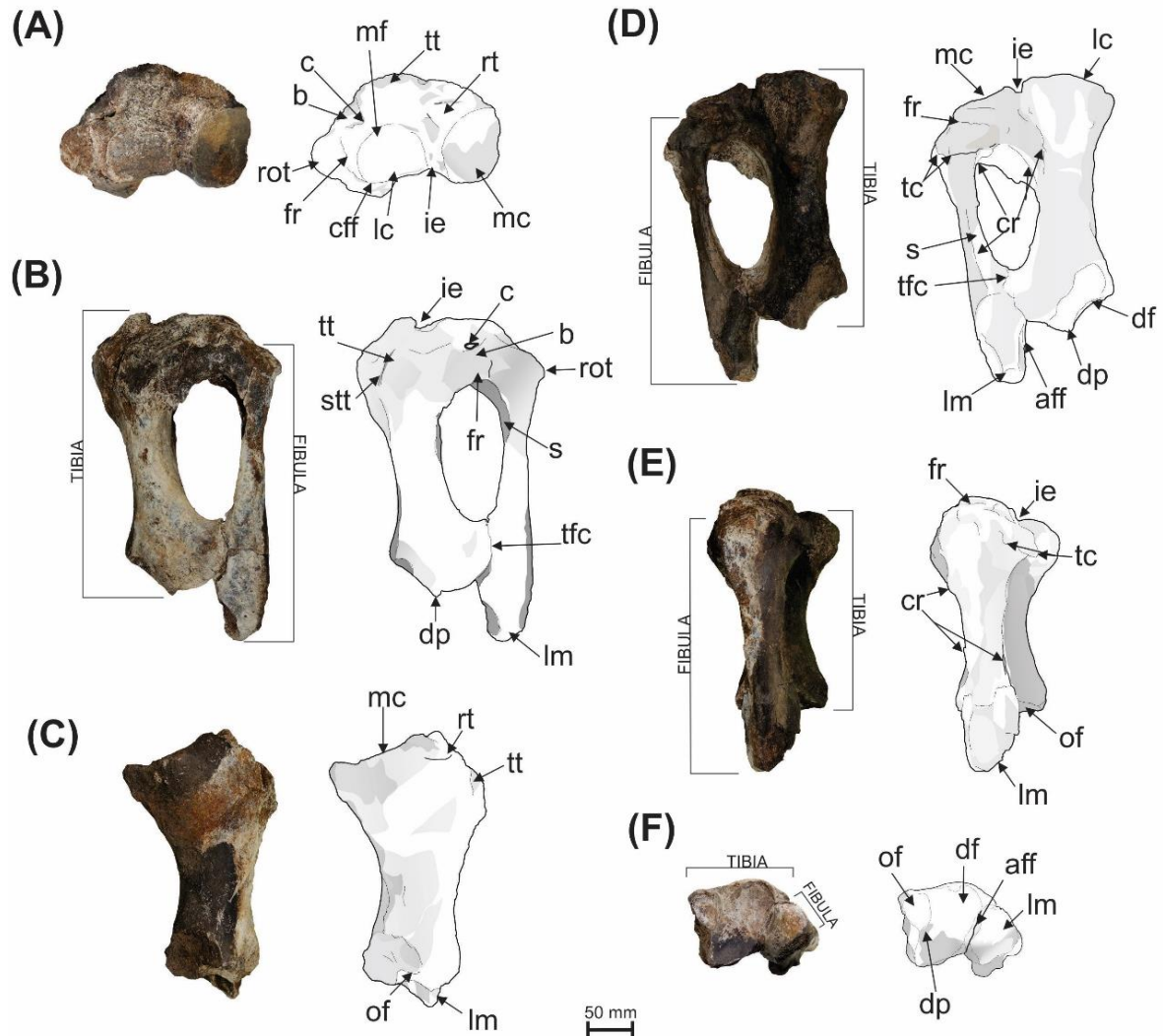


Figure 5. Left tibia and fibula of *Lestodon armatus* (UFSM 11535). (A) proximal view, (B) cranio-lateral view, (C) lateral view of tibia, (D) caudolateral view, (E) medial view of fibula, (F) distal view. Abbreviations: aff, astragalar facet of fibula; b, bridge; c, channel; cff, ciamo-fabella facet; cp, circular-shaped process; cr, crest; dp, distal process; fr, fused region; ie, intercondylar eminence; lc, lateral condyle; lm, lateral malleolus; mc, medial condyle; mf, meniscus facet; of, odontoid facet; rot, rounded tuberosity; rt, rough tuberosity; s, sulcus; stt, sulcus tuberositatis tibiae; tc, transversal crest; tfc, tibiofibular contact; tt, tibial tuberosity. Scale: 50 mm.

Astragalus. The astragalus has two articular facets to the tibia – the odontoid process and the discoid facet (Fig. 6A). The odontoid process is “pulley-shaped” and is positioned at almost 90° to the discoid facet. It then has a bridge that connects to the navicular articular facet (Fig. 6B, C).

The discoid facet is flat and smooth, laterally around over half of the odontoid process and inclined in the direction of this process. It has the same width and length, except in the distal limit, whose width increases around 1/3 following the odontoid process circumference. Distally, the edge of the discoid facet is narrow.

The fibular facet is flat and oval in UFSM 11535 (Fig. 6E). It is located on the lateral face of the astragalus. The fibular facet protrudes from the plantodistal portion like a plateau.

The astragalus has two facets for the calcaneus (Fig. 6C, D). The sustentacular facet is oval, convex and separated from the ectal facet by the *sulcus tali*. The ectal facet is located lateroproximally in plantar view. This face is elongated and concave distoproximally.

The cuboid facet is convex and contiguous with the sustentacular facet. It is located plantarly to the navicular facet and distally to the sustentacular facet.

The *sulcus tali* extends from the medioproximal region until the level of the lateroproximal region of the odontoid process (Fig. 6B-F). A tubercle extends from the lateroproximal edge of the navicular facet to the lateraldistal edge of the base of the discoid facet, crossing the *sulcus tali*. Plantarly to this tubercle, the *sulcus tali* is deeper and narrower in the plantar face of the astragalus, and reasonably long in the proximal face. In this region, the *sulcus tali* is rough and shows some foveas. In the articulation of the astragalus to the calcaneus, the *sulcus tali* is connected to the *sulcus calcanei* forming the *sinus tarsi*.

The navicular facet is contiguous and dorsally placed to the cuboid facet. The navicular facet can be divided into two parts. One part is laterally located, slightly concave, and oval-shaped. The other one is contiguous and located medially to the first, and it is convex and trapezoidal-shaped.

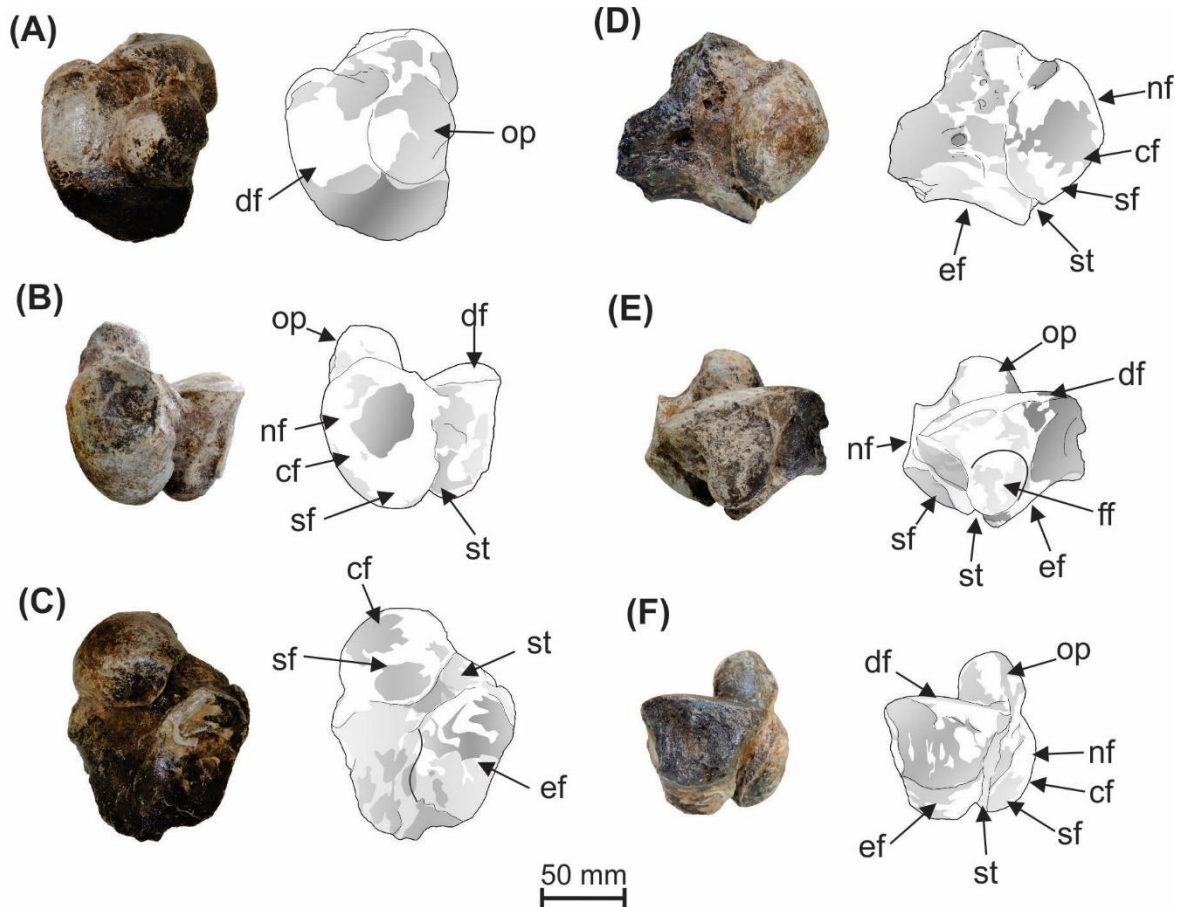


Figure 6. Left astragalus of *Lestodon armatus* (UFSM 11535). (A) proximal, (B) cranial, (C) plantar, (D) medial, (E) lateral and (F) distal views. Abbreviations: df, discoid facet; ef, ectal facet; ff, fibular facet; nf, navicular facet; op, odontoid process; sf, sustentacular facet; st, sulcus tali. Scale: 50 mm.

Calcaneus. The calcaneus of UFSM 11535 is fragmented at its proximal portion. The two astragalar facets are located distally and are divided by the *sulcus calcanei* (Fig. S6 A). The ectal facet is wavy. A tuberosity is situated plantar to this facet, on its proximal edge. The sustentacular facet is elongated and curved. Distally, the cuboid facet is oblique and contiguous with the sustentacular facet (Fig. S6 A, B).

The cuboid facet is concave and distomedially limited by a fossa that ends in a fovea. Plantarly to this fovea, a tubercle is located. Plantarly to this tubercle, a crest is extended parallel to the articulation edge of the cuboid.

On the lateral face, lateral to cuboid and astragalar facets, there is the lateroproximal process, extended almost from the lateral edge of the ectal facet to the base of the cuboid facet. This process is medially limited by a depression. Lateroplantarly to this process, there is a lateroplantarly projected crest (Fig. S6 A-F). The medial region of the calcaneus is characterized by a rough depression (Fig. S6 D).

Cuboid. The lateral region of the cuboid has a rectangular, flat, and rough surface (Fig. S7 D). The astragalar facet is located on the dorsoproximal region (Fig. S7 A, C). It is circular and concave, limited distally by the navicular facet, and which is elongated and contiguous with the ectocuneiform facet (Fig. S7 A-C, E).

The cuboid facet is located on the proximolateral region of the bone (Fig. S7 A, C, D). It is semicircular-shaped, and in its dorsomedial portion, it is elongated and oriented towards the rough tuberosity of the astragalar facet base.

Medially, the cuboid has an irregular transversal fossa, dorsoplantarly directed, and which divides the tuberosity of the astragalar facet from a medioplantarly tuberosity close to the metatarsal V facet and the metatarsal IV edge (Fig. S7 E). This fossa mediolaterally separates the facets for the ectocuneiform and the metatarsal III. Between the tuberosity and the lateral edge of the metatarsal V, there is an oval depression (Fig. S7 D, F). The metatarsal IV facet is located plantarly in relation to the facet for the metatarsal III and is contiguous with the metatarsal V facet (Fig. S7 B, E, F).

The metatarsal III and ectocuneiform facets are located in the dorsal region of the bone (Fig. S7 B-E). The ectocuneiform facet is divided into three parts: two of them are oblique at the dorsal region and contiguous with the navicular facet, and one is contiguous with the metatarsal III facet. At the location of the cuboid articulation with the ectocuneiform and metatarsal III, the transversal fossa forms a sulcus (forming a canal when articulated with the metatarsal III and ectocuneiform) (Fig. S7 B-E).

Navicular. The navicular is “reniform-shaped”. In the proximal view, the astragalar facet is concave, flat in the medial portion and elevated in the lateral portion (Fig. S8 A). The dorsal face has tuberosities in the proximal region (Fig. S8 A, B, D, F). The lateral tuberosity is distally limited by the dorsal depression (Fig. S8 C, E). Distoplantar to this depression it is located the ectocuneiform facet.

The ectocuneiform facet is convex, and lateromedially it shows a fossa separated from the metatarsal II facet (Fig. S8 C-F). The metatarsal II facet is oval and is lateral to the ectocuneiform facet.

In plantar view, the navicular has a tuberosity on the medial edge (Fig. S8 C). The cuboid facet is medially and plantarly contiguous with the metatarsal II facet.

Ectocuneiform. The ectocuneiform has a medioplantar process (Fig. S9 A- B, D-G). The navicular facet is concave and has a triangular shape, located in the dorsoproximal region. In

the distoplantar region is located the metatarsal III facet, which is convex and medially extended (Fig. S9 B-G).

Distoproximally to the navicular facet, there are two cuboid facets (Fig. S9 D-F). The lateral cuboid facet is four times smaller than the navicular facet and is located perpendicular to it. The lateral cuboid facet is semicircular. Plantarly it has a fossa that is separated from the metatarsal III facet (Fig. S9 E, F). The medial cuboid facet is “drop-shaped”. Distolaterally, there is an ellipsoid tubercle.

The lateral face of the ectocuneiform is rough. The medial face is fragmented (Fig. S9 E). The dorsal face is triangular.

The dorsal tubercle is located close to the medial end in the dorsal face (Fig. S9 A-C, G). Laterally it has a small tubercle that connects with the other one, but a fossa separates it. This additional tubercle is the part of the facet edge for metatarsal III.

Metatarsal III. The metatarsal III is “L-shaped” in dorsal and plantar views (Fig. S10 B, C). The proximal region is composed of the ectocuneiform facet, whose dorsomedial portion is more elevated than the plantolateral portion (Fig. S10 A). In the dorsoproximal view, this facet has two levels.

A curved process is extended plantarly in the medial portion of the proximal end (Fig. S10 A-E). Lateral to this medioplantar process, on the plantar face, there is a groove lateroplantarly limited by the medial edge of a cuboid facet (Fig. S10 C). Dorsally to the medioplantar process in the medial face, there is a fossa limited by a dorsomedial tuberosity, located at the higher portion (Fig. S10 B). A circular facet for the metatarsal II is located on this dorsomedial tuberosity. Distal to the tuberosity there is a low crest extended to a dorsomedially limited depression. This crest forms a dorsal edge on the bone, delimiting the medial and dorsal faces.

The dorsal face has a central depression limited dorsoproximally by an irregular crest that forms the base of the ectocuneiform facet edge. This crest is extended laterally in the lateroplantar projection.

The proximal phalanx of the digit I facet is located on the distal end of the bone and has two articular crests. The dorsal is half the size of the plantar and both have sesamoid facet's contiguous in the medial region. Dorsally this facet is limited by a rough depression, proximomedially limited by a tuberosity. An acute crest is extended by the length of the distal face. Medial to the facet, there is an acute process.

The lateroproximal process shows three facets. In the plantar face of this process, the cuboid facet is limited medially by two foveas. In the proximodorsal region, the lateroproximal process has the lowest portion of the ectocuneiform facet. In the distoplantarly region is located the facet for the metatarsal IV (Fig. S10 C, F). The lateral face of this process is rough and shows two foveas in a tenuous depression.

Along the bone axis, there are depressions on the lateral, medial, and dorsal faces, as well as an arris in the plantar face (Fig. S10 C).

The medial face of metatarsal III is dorsally limited by a crest of the dorsal arris, distally by the edge of the flat crest of the phalanx 1 facet, and plantarly by the curvature of the depression of the plantar face and a rough crest (Fig. S10 E). Proximoplantarly, the medial face is limited by the medioplantar process.

Sesamoids. The dorsal sesamoid is elongated dorsoplantarly. Its distal region is convex, and the proximal region on the metatarsal III facet is concave (Fig. 7A-C, E). The metatarsal III facet is divided into two contiguous parts: a dorsal and oval concave facet, and a plantar elongated facet. A tuberosity is located dorsolaterally (Fig. 7A, B, E, F) and laterally to this tuberosity is the proximal phalanx facet (Fig. 7E).

The plantar sesamoid shows a dorsal tuberosity. Proximolateral to this tuberosity it is the proximal phalanx facet, which is limited by a sulcus (Fig. 7K). Proximal it is located the metatarsal III facet (Fig. 7G). The dorsal face is larger than the plantar.

[Figure 7 near here]

Metatarsal IV. The metatarsal IV is located plantarly to the metatarsal III. The proximal face shows trapezoidal shape. On the dorsal portion of this face, the metatarsal III facet is the oval one, and the dorsal edge is a crest with a tuberosity on the dorsolateral region (Fig. 8A, B).

Contiguous and plantarly with the metatarsal III facet, the cuboid facet is the most elevated in relation to any other facet. The cuboid facet is trapezoidal and located in the plantar region of the proximal end. A medial depression separates the metatarsal III facet from the cuboid facet and the medioplantar process (Fig. 8A, B).

Medial to the cuboid facet, there are two tuberosities plantomedially aligned. Between these tuberosities, there is a deep fovea. The most medial tuberosity is rough, and it is the limit of the distally extended medioplantar process.

The metatarsal IV has a semicylindrical body and is distally extended (Fig. 8C). The dorsal edge is smooth, and the plantar region has three crests aligned proximoplantarly to

distodorsally at the proximal portion of the metatarsal IV body. A distal crest is plantodistodorsally directed, forming a triangular tubercle near the distal end (Fig. 8C, D).

Laterally to the triangular tubercle, there is a crest directed to the dorsolateral tubercle (Fig. 8D, E). Lateroproximal to the dorsolateral tubercle there is a crest, and dorsolaterally to this tubercle, the lateral limit of the fossa is extended perpendicular to the bone axis. The proximal phalanx facet limits this fossa distally.

The proximal phalanx facet is lateromedially elongated (Fig. 8F). Plantolaterally to this facet, there is a depression with a fovea that margins a large and rough plantolateral tuberosity. This tuberosity is extended laterally on the plantolateral tubercle (Fig. 8C, F). This tubercle has a lateral edge like a proximodistally-oriented curved crest. A depression is found between the dorsolateral tubercle and the plantolateral tubercle.

On the medial face of the bone, there is a crest oriented proximoplantarly to dorsodistally and located proximodorsally to the proximal crest of the dorsolateral tubercle (Fig. 8D).

On the plantar view, the mediodistal edge of the metatarsal V facet has sigmoidal shape, and medially it shows a conspicuous fossa oriented proximomedially to distolaterally. On the distal edge of this fossa, there are sets of rough tuberosities. Distomedial to these tuberosities located along the bone axis, there are two crests like edges that margin the plantar and medial faces, respectively (Fig. 8B, C). A depression is found between these crests. In the distal region of the plantar face, there is a depression separating the plantolateral tubercle laterally, the proximal phalanx facet distally, and the crest that forms a triangular tubercle dorsomedially.

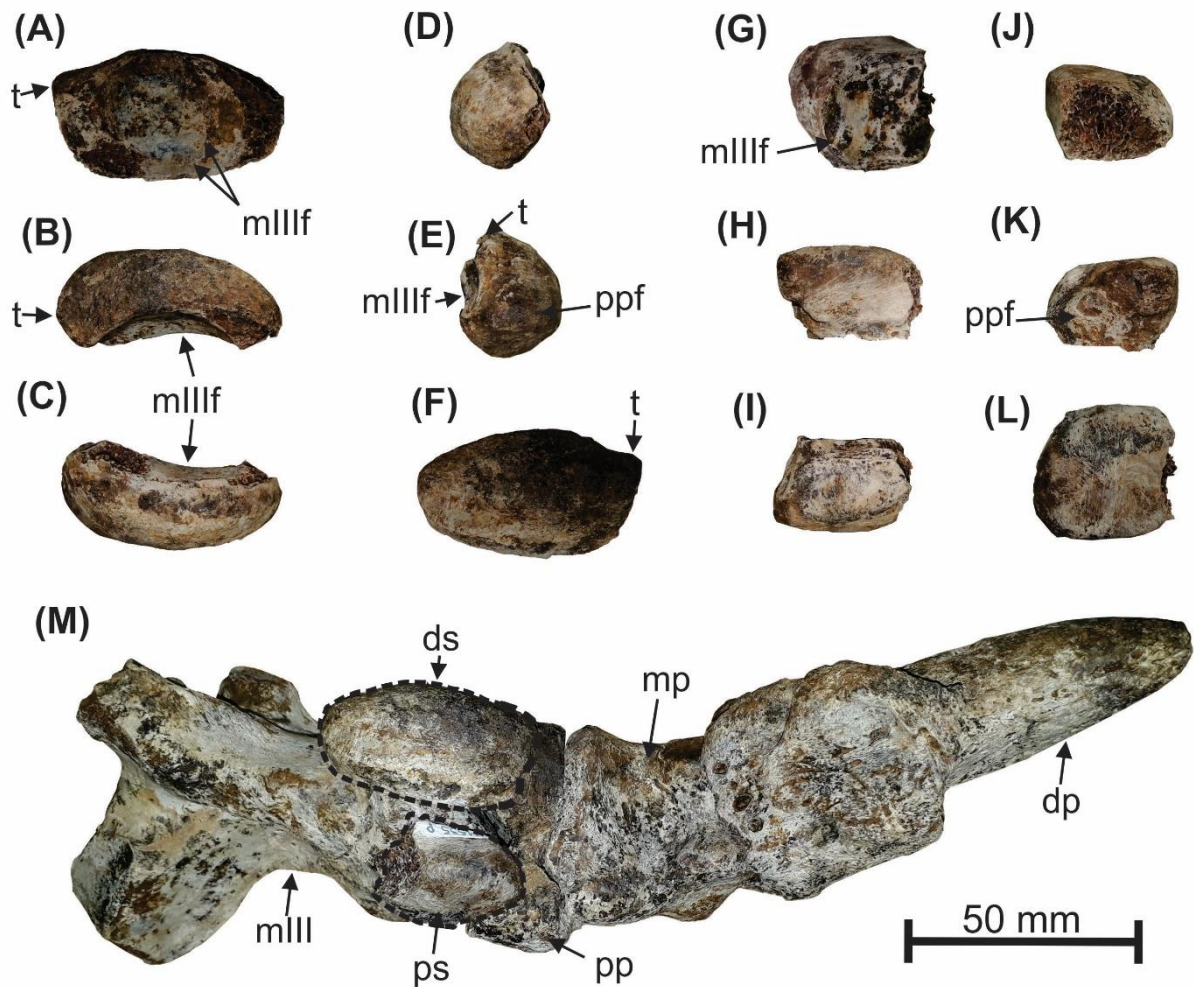


Figure 7. Sesamoids of the metatarsal III of *Lestodon armatus* (UFSM 11535). (A-F) Dorsal sesamoid, (G-L) plantar sesamoid and (M) position of sesamoids in the third digit in (A and G) proximal, (B and H) dorsal, (C and I) plantar, (D and J) medial, (E, K, M) lateral and (F and L) distal views. Abbreviations: dp, distal phalanx; ds, dorsal sesamoid; mp, medial phalanx; ps, plantar sesamoid; mIII, metatarsal III; mIII f, metatarsal III facet; pp, proximal phalanx; ppf, proximal phalanx facet; t, tuberosity. Scale: 50 mm.

Metatarsal IV. The metatarsal IV is located plantarly to the metatarsal III. The proximal face shows trapezoidal shape. On the dorsal portion of this face, the metatarsal III facet is the oval one, and the dorsal edge is a crest with a tuberosity on the dorsolateral region (Fig. 8A, B).

Contiguous and plantarly with the metatarsal III facet, the cuboid facet is the most elevated in relation to any other facet. The cuboid facet is trapezoidal and located in the plantar region of the proximal end. A medial depression separates the metatarsal III facet from the cuboid facet and the medioplantar process (Fig. 8A, B).

Medial to the cuboid facet, there are two tuberosities plantomedially aligned. Between these tuberosities, there is a deep fovea. The most medial tuberosity is rough, and it is the limit of the distally extended medioplantar process.

The metatarsal IV has a semicylindrical body and is distally extended (Fig. 8C). The dorsal edge is smooth, and the plantar region has three crests aligned proximoplantarly to distodorsally at the proximal portion of the metatarsal IV body. A distal crest is plantodistodorsally directed, forming a triangular tubercle near the distal end (Fig. 8C, D).

Laterally to the triangular tubercle, there is a crest directed to the dorsolateral tubercle (Fig. 8D, E). Lateroproximal to the dorsolateral tubercle there is a crest, and dorsolaterally to this tubercle, the lateral limit of the fossa is extended perpendicular to the bone axis. The proximal phalanx facet limits this fossa distally.

The proximal phalanx facet is lateromedially elongated (Fig. 8F). Plantolaterally to this facet, there is a depression with a fovea that margins a large and rough plantolateral tuberosity. This tuberosity is extended laterally on the plantolateral tubercle (Fig. 8C, F). This tubercle has a lateral edge like a proximodistally-oriented curved crest. A depression is found between the dorsolateral tubercle and the plantolateral tubercle.

On the medial face of the bone, there is a crest oriented proximoplantarly to dorsodistally and located proximodorsally to the proximal crest of the dorsolateral tubercle (Fig. 8D).

On the plantar view, the medioidistal edge of the metatarsal V facet has sigmoidal shape, and medially it shows a conspicuous fossa oriented proximomedially to distolaterally. On the distal edge of this fossa, there are sets of rough tuberosities. Distomedial to these tuberosities located along the bone axis, there are two crests like edges that margin the plantar and medial faces, respectively (Fig. 8B, C). A depression is found between these crests. In the distal region of the plantar face, there is a depression separating the plantolateral tubercle laterally, the proximal phalanx facet distally, and the crest that forms a triangular tubercle dorsomedially.

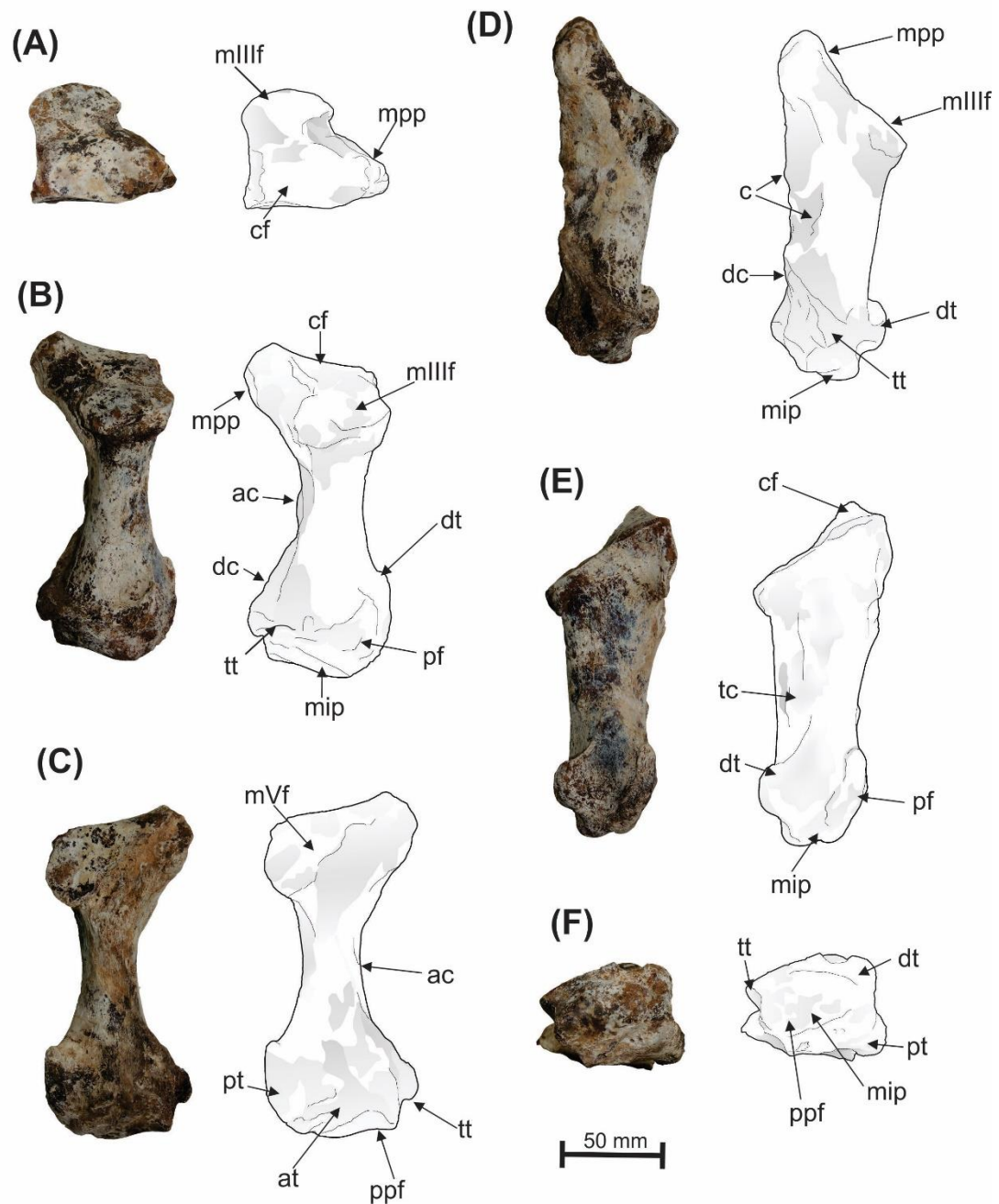


Figure 8. Left metatarsal IV of *Lestodon armatus* (UFSM 11535). (A) proximal, (B) dorsal, (C) plantar, (D) medial, (E) lateral and (F) distal views. Abbreviations: ac, arris crest; at, acute tubercle; c, crest; cf, cuboid facet; d, depression; dc, distal crest; dt, dorsolateral tubercle; mIIIIf, metatarsal III facet; mVf, metatarsal V facet; mip, middle process; mpp, medioplantar process; ppf, proximal phalanx facet; pt, plantolateral tubercle; tt, triangular tubercle. Scale: 50 mm.

Metatarsal V. The metatarsal V is proximodistally elongated and medially curved. The medial face is rough and shows a central depression limited proximoplantarly by a crest oriented dorsoproximally to plantodistally (Fig. S11 D). The plantar face is narrow and rough (Fig. S11 C). The proximoplantar part of the bone is fragmented.

The cuboid facet is concave and ovoid, located dorsoproximally to the dorsal face (Fig. S11 B, D, E). The metatarsal IV facet is sigmoidal and distally contiguous with the cuboid facet, which is separated by a transversal crest. The metatarsal IV facet is slightly concave and inclined distoplantarly in the proximal portion, as well as flat in the distal portion (Fig. S11 B, D, E). Distal to this facet there is a crest that is the dorsal edge of the bone axis.

The bone is slightly flat and rough on the plantar face. Distally, the bone is narrow and flat, forming a medially-directed curve. The distal end of this metatarsal is partially fragmented at the mediodistal part (Fig. S11 F).

Proximal phalanx of digit 2. This phalanx is plantomedially-dorsolaterally flattened and is co-ossified with mesocuneiform. A sulcus present in the dorsomedial region, probably correspond to the boundary of these bones (Fig. S12 B).

In the proximal region (mesocuneiform), it is located the two navicular facets (Fig. S12 A-C). The proximal region is separated from the distal region by a deep plantar groove, lateral groove, and dorsal sulcus.

Three tuberosities are located on the lateral margin of the bone. Lateral in the lateral face, is located the circular metatarsal III facet (Fig. S12 A, B, E). Distomedial is the middle phalanx facet (Fig. S12 B-F), and medial to this facet on the dorsal face is located a large tuberosity (Fig. S12 B, D, F).

On the plantomedial view the distal region there is a groove, that is separated from the groove of the proximal region (mesocuneiform) by a lateroplantar crest (Fig. S12 C). In the medial margin of the distal groove is located a tuberosity.

Middle phalanx of digit 2. This phalanx has the proximal portion larger than the distal portion. In the proximal face is located the facet for the proximal phalanx, which is concave (Fig. S13 A). Dorsal and plantar on the lateral edge of the proximal region there are tubercles, with the proximodorsal region two times larger than the proximoplantar one.

A distal process is extended distally and shows an acute tip. On the distal face is located the distal phalanx facet. This facet is composed of two crests separated by a groove and is “reel-shaped” (Fig. S13 D).

On the plantar face of this facet, there is a rough distoplantar tuberosity (Fig. S13 C-F). On the dorsal face, there is a rough distodorsal tuberosity that covers almost the entire medial part of the distal phalanx facet (Fig. S13 A-D). On the proximal region of this tuberosity, there

is a rough depression limited proximally by a rough crest that borders the groove of the medial face. Lateral to this crest there is a rough depression extended laterally.

The lateral face of the distal process has a depression between the distal phalanx facet and the proximal region. A fovea is present in the distal face on the middle of the proximal part.

Proximal phalanx of digit 3. This phalanx is quadrangular and compressed proximodistally. On the metatarsal III facet (Fig. S14 A, C, D), the proximal region has a deep fossa by the fitting to the acute crest of metatarsal III and a flat facet separated by a low crest of the referred fossa. The medioplantar edge of the fossa is bifurcated. The plantar edge of the facet for the metatarsal III is prominent.

On the dorsal view, the bone is rough, with tubercles at the distomedial part. A crest oriented distomedially to proximolaterally is located in the medial part of the dorsal face. On the lateral portion, there is a dorsolateral tuberosity (Fig. S14 A, B, F). On the lateral region, this tuberosity is limited proximally by two depressions (Fig. S14 E).

The dorsolateral tuberosity is the edge of the middle phalanx facet, that is located distally (Fig. S14 F). There is a depression mediolaterally oriented. Following this orientation, the fossa has a line of foveas set.

On the plantar face, there is a plantolateral tuberosity and a plantomedial tuberosity, separated by a depression (Fig. S14 C). The plantomedial tuberosity is larger than the plantolateral tuberosity. On the plantar margin of these tuberosities, it is located the sesamoid facet.

Middle phalanx of digit 3. The proximal portion is larger than the distal portion and is extended lateromedially into two tuberosities with the ends directed proximally. The proximal face is concave and shows the proximal phalanx facet. On this facet, there is a low crest with a fovea located in the middle that separates the dorsal and plantar depressions (Fig. S15 A). The general shape of the proximal phalanx facet is triangular with the *tuberositas flexoria* on the lateral region (Fig. S15 B-D).

The dorsal face of the bone is inclined distoplantarly. The distal region of the distal face is bifurcated in two condyles, forming a structure like a reel, which is the distal phalanx facet (Fig. S15 B-F). The dorsal condyle has a laterodorsal tuberosity (Fig. S15 B), and the plantar condyle shows a lateroplantar tuberosity (Fig. S15 C, D). On the dorsal and plantar regions, there are depressions in the center of the condyles.

Distal phalanx of digit 3. This phalanx has two parallel concavities divided by a crest on the middle phalanx facet (Fig. S16 A). The edges of this facet are rough and extended proximally. The lateral edge is the extensor process.

On the medial face, the flexor tubercle sustains the claw (Fig. S16 B, C, E). This structure has three foramina located parallel to the edge of the middle phalanx facet on the proximal region. Distal there are two solar foramina (Fig. S16 E), which are located dorsally and plantarly. Between these two foramina on the proximal face, there is a rough tuberosity, and distally to this, there is a proximodistal crest that divides two depressions (Fig. S16 E). The claw is conical. The flexor tubercle is located in the medial region (Fig. S16 B-D).

On the lateral view, the claw is slightly narrow in the direction to the distal end, corresponding to the dorsal border (Fig. S16 D). However, the claw widens distally because the two extensions are directed proximomedially to distolaterally in the dorsal and plantar faces. This slight narrowness is almost imperceptible.

In both dorsal and plantar faces of the, there is a ramified sulcus originated in the dorsal and plantar foramina of the flexor tubercle, respectively (Fig. S16 B, C). Both sulci (dorsal and plantar) are ramified and mediolaterally oriented. The ramification is subdivided into five parts in the dorsal face and into four parts in the plantar.

Proximal phalanx of digit 4. It is compressed proximodistally and is “U-shaped”. The metatarsal IV facet is a wide depression, bordered dorsally by an elongated fossa and plantarly by a set of rough tuberosities (Fig. S17 A-D). These tuberosities are the proximal limit of the striated and concave region. Laterodistal to this region there is a distally directed crest-edge. This crest is limited by a curved fossa in the distal face.

The middle phalanx facet is divided into a more elevated part and depression (Fig. S17 B-F). The most elevated section shows the most curved plantar region, and the dorsal region is flat. On the dorsal and plantar face of the bone, there is a large tuberosity (Fig. S17 B-F). Laterally to the plantar tuberosity, there is another tuberosity.

Middle phalanx of digit 4. This bone has one plantomedial tip, one lateral tip and one distomedial tip (Fig. S18 A-C). The proximal phalanx facet is concave on the plantar region and flat on the dorsal one (Fig. S18 A). In the ventral region, there is a medially projected small facet.

On the plantar view, the bone surface is rough, with a process that is centrally limited by the plantar edge of the proximal phalanx facet (Fig. S18 A). On the lateral end, there is a

rough process medially limited by a tenuous semicircular fossa. Distal to this fossa, there is a tubercle medioproximally extended, forming the plantomedial tip. Distal to this tubercle there is another tubercle, but smaller, that originates the distomedial tip.

On the medial view of the bone, there is a deep depression divided the plantomedial and the distomedial tips. Dorsoproximal there is a flat process. It is the base for the edge of the proximal phalanx facet.

The lateral face is rough and proximoplantarly shows a tubercle that forms the lateral tip. This tubercle is distoplantarly narrow and forms a plantar tubercle limited by the semicircular fossa of the plantar face. Dorsal to this tubercle, there is a proximodistally extended depression.

The dorsal face shows the flat part of the proximal phalanx facet in the proximal region. Distal to this facet, there is a rough tubercle extended through the axis of the distomedial tip. On the dorsal view, the distomedial tip is curved medially.

Phalanx of digit 5. This bone is “dome-shaped” and rough. The facet for the metatarsal V is concave and bordered by a rough surface. This bone has several foveas. At the distal end, it has a deep depression with internal foveas. This depression is limited by one dorsal tuberosity and by one plantar tuberosity connected by a “bridge” (Fig. S19).

Discussion

Morphological and taxonomic remarks

The cheek teeth morphology of UFSM 11535 resembles those mentioned by Gervais (1855) for *Lestodon armatus*, showing an ML2 with flat lingual surface; ml2, and ml3 with oval outlines; and ml4 with the shape of an “elongated eight”, unlike *Thinobadistes*, which has a straight part between the lobes (Webb 1989). The presence of lingual and labial longitudinal grooves on the ml4 differs from *Paramylodon*, which has two grooves on the labial surface and one on the lingual surface (Owen 1842). Also different from *Glossotherium*, whose labial groove of ml4 is not parallel to the lingual groove (Pitana 2011), UFSM 11535 shows the two grooves in parallel. *Myiodon* shows the lobes of ml4 with equal size, differing from UFSM 11535. *Scelidotherium* has an unequal eight on lobes of ml4, differing from the specimen studied herein (Miño-Boilini 2012). *Thinobadistes* shows the grooves of the ml4 mesiodistally wider (Webb 1989) than UFSM 11535, which presents narrow grooves.

The stylohyal of UFSM 11535 is medially compressed, resembling that of *Glossotherium* and *Scelidothorium*, mainly at the proximal region (Pérez et al. 2010). It is gracile and has a small articular surface like in *Scelidothorium* when compared to *Glossotherium* and *Paramylodon* (Stock 1925; Pérez et al. 2010). The stylohyal of UFSM 11535 differs from that attributed to a juvenile *L. armatus* (Tambusso et al. 2015), and resembles the specimen SGO.PV.2 assigned to *Glossotherium*, figured by Püschel et al. (2017), because it has a convex edge on the proximal end and a curvature in the axis bone, but differing in its larger size. Therefore, the stylohyal of UFSM 11535 could represent an individual or ontogenetic variation of *Lestodon*.

In the atlas of UFSM 11535, the process that forms the atlas wing originates caudally to the face of the occipital condyle, distinctly from *Myiodon darwini*, in which these processes form as a continuation of the occipital condyle facets, like the specimen FMNH P14288, figured by McAfee (2016). In ventral view, the apertures in the wing that are limited with the vertebral body are located cranially, while in *M. darwini* these apertures are located in the middle of the vertebral body, also in the limit with the wings (McAfee 2016).

The axis facets of UFSM 11535 are more rounded in comparison to *M. darwini*, which resembles *Glossotherium* (McAfee 2016) and *Thinobadistes* (Webb 1989). However, the presence of a protrusion in the medial edge of the axis facets in the atlas of UFSM 11535 is different from *Glossotherium* and *Paramylodon* and similar to *Myiodon* (McAfee 2016). In *Thinobadistes*, the vertebroarterial canal passes in the medial part of the occipital condylar edge and opens in the lateral of the axis facet (Webb 1989), and in UFSM 11535 the vertebroarterial canal goes through the mediodorsally part of the occipital condylar facet and opens laterodorsally to the axis facet.

The main postcranial features that identify UFSM 11535 as *Lestodon armatus* are present in the hindlimb elements. In the Mylodontidae femur, the condyle facets are contiguous to the patellar facet (McDonald and De Iuliis 2008). In UFSM 11535, the proximal edge of the patellar facet is straight, unlike what was represented by Owen (1842) in the drawings of *Glossotherium*, which are curved. A slightly accentuated curve in the proximal edge of the patellar facet is present in *Thinobadistes* (Webb 1989). However, the patellar facet of UFSM 11535 resembles *L. cordorensis*, even as the size and position of the medial condyle in relation to the lateral (Linares 2004), although UFSM 11535 has the medial condyle more robust and is located more distally than in *L. cordorensis*.

The femur of UFSM 11535 resembles Kraglievich's (1934) *M. darwini*, and Webb's (1989) *Thinobadistes*, in which the patellar facet is connected with the lateral condyle, and the

medial condyle is bulkier and located more cranially than the lateral condyle. However, the femur of this study is distinct from the others by not having a “strong longitudinal crest that descends of great trochanter parallel to the external edge” (Kraglievich 1928, p. 283). It also does not have a deep fossa proximal to the patellar facet. In comparison with the illustrations of *Thinobadistes* by Webb (1989), the distal end of the femur of UFSM 11535 is similar to that taxon, although the medial edge is straighter. The curvature of the patellar facet of UFSM 11535 has a smaller curve than Owen’s figure (1842) for *Glossotherium*. The condyle plan is oblique (medial condyle projected more distally than the lateral) in UFSM 11535, unlike *Thinobadistes*, in which the condyle plan is parallel (both condyles at the same level) (Webb 1989).

The tibia of UFSM 11535 has the medial condyle larger than the lateral condyle, which is flat. The proximal end of this bone resembles *Glossotherium*, in which the medial condyle occupies most of the bone, and the lateral condyle is shallow (Owen 1842; Pitana 2011), both separated by the intercondylar eminence as *Thinobadistes* (Webb 1989). These features also resemble *Myiodon*, even as the general form and curvature of the tibia and the roughness close to the fibula (Kraglievich 1934). However, in UFSM 11535, the medial condyle is circular, and the lateral condyle is quadrangular, unlike *Glossotherium*, in which the medial condyle is elliptical (Owen 1842; Pitana 2011).

On the astragalar facet of UFSM 11535 there is a crest, not present in *Glossotherium robustum* (MCN-PV 2388) (Pitana 2011). Nevertheless, the union of the two astragalar facets of the tibia is rounded, such as in *Glossotherium*, *Lestodon*, and *Paramyiodon*, differently from *Myiodon* (Kraglievich 1934). Therefore, the angle between the two astragalar facets of UFSM 11535 is around 90°, which is more than Kraglievich’s angle (1928), mentioned for the three above mentioned genus and differing from the obtuse angle of *Myiodon*. In *Thinobadistes*, there is no marked separation between the two astragalar facets (Webb 1989), with no crest as other taxa.

The fibular facet of astragalus in UFSM 11535 it is oval, like MNHN 1854, MNHN 2117, and MNHN 2127; but elongated-shape in MNHN 1173, MNHN 1174 MNHN 1752, MNHN 1892, and MNHN 1939, and an almost quadrangular-shape in MCN-PV 2514.

The fibula of UFSM 11535 fused with the tibia at the proximal end and almost fuses at the distal end, which differs from previous descriptions of *Lestodon armatus* (Gervais 1873). This pattern is also present in Megatheriidae, i.e. *Megatherium* (De Iuliis 1996), and Scelidotheriinae, i.e. *Valgipes bucklandi* (Cartelle et al. 2009). Regarding the comparative sample, the Brazilian specimens MCTFM 0914 and EPM-PV 0127 from the Chuí Creek assigned to *L. armatus* also show the tibio-fibular fusion. On the other hand, in six analyzed

Uruguayan specimens (MNHN 1?, MNHN 17, MNHN 151, MNHN 191, MNHN, 1665 and MNHN 1719) this fusion is not present. Therefore, this fusion can be related to the intraspecific variation instead of an autapomorphic trait of the species (temporal or geographic variety).

The cuboid facet of the astragalus of UFSM 11535 is convex, unlike *Scelidotheriinae*, which is concave (Miño-Boilini et al. 2014). The cuboid facet is separated from the navicular facet by a curvilinear arris, as mentioned by Gervais (1873) for *Lestodon* and *Myiodon*.

The ectal and sustentacular facets of the astragalus of UFSM 11535 are separated by the *sulcus tali*, different from *Glossotherium* (Owen 1842; Pitana 2011; Püschel et al. 2017), *Paramyiodon* (Stock 1917, 1925), *Myiodon*, and *Scelidothorium* (Kraglievich 1928, 1934), but it resembles *Lestodon* (Kraglievich 1934), *Megalonyx* (Gervais 1873), and *Thinobadistes* (Webb 1989). Unlike the specimen of this study, *Megalonyx* does not have pedolateral condition (McDonald 2012), and the odontoid process of *Thinobadistes* is not “pulley-shaped” (Webb 1989). However, the separation of these two facets is also present in Megatheriidae. The fibular facet is entirely extended in the dorsoplantar direction in UFSM 11535, as mentioned by McDonald (2012) for *Lestodon* and *Paramyiodon*.

The calcaneus of UFSM 11535 is similar to *Lestodon*, in which the *sulcus calcanei* is divided into two astragalar facets. The smallest one is contiguous with the cuboid facet (Gervais 1873).

The second cuneiform (mesocuneiform) of UFSM 11535 has the function of the metatarsal II, as mentioned by Gervais (1873) for *Lestodon*. This feature (also present in *Thinobadistes*; Webb 1989) distinguishes *Lestodon* from *Paramyiodon* (Stock 1917, 1925) and *Glossotherium* (Owen 1842).

UFSM 11535 has the proximal and middle phalanx of the digit III, differently from megatheriids of similar size, such as *Pyramiodontherium* (Brandoni et al. 2004), *Megatherium* (Owen, 1859; De Iuliis 1996), and *Eremotherium* (De Iuliis 1996), which have these two phalanges fused. The fusion of these bones is also reported by *Scelidothorium* (Stock, 1917, 1925). Also, the metatarsal III has the same morphology described by Gervais (1873) for *Lestodon*, unlike *Scelidothorium*, *Myiodon*, and *Megatherium* (Gervais, 1873).

The record of sesamoid bones in the digits of Mylodontidae have been reported for the manus of *Glossotherium*, *Myiodon*, *Paramyiodon* (McAfee 2016) and *Valgipes* (Cartelle et al. 2009), and the metatarsal IV of the *P. harlani* (Stock 1925). Here we report the presence of sesamoid bones in the metatarsal of *Lestodon armatus*, contributing to the knowledge of the pes anatomy of this taxon.

Conclusion

Herein, we report a new finding (UFSM 11535) of a mylodontid from southern Brazil. It was assigned to *Lestodon armatus* based on the presence of: i) bilobated teeth; ii) fusion of proximal and middle phalanx from the thirty digit of pes; iii) separation of the sustentacular and ectal facets in the astragalus and calcaneus; iv) metatarsal II acting as mesocuneiform; v) and larger size than other mylodontids. For the first time, the sesamoid of metatarsal III, the fusion of the tibia and fibula, and the stylohyoid from an adult specimen are described.

For a better understanding of the age of deposition of the fossiliferous layers exposed in Arroio do Seival and “Arroio do *Lestodon*”, absolute ages and stratigraphic studies are necessary.

Acknowledgments: Leopoldo Witeck Neto, who found the specimen and guided the team during the fieldwork. Jean Fernando Nunes for help during the preparation and assistance during the fieldwork; Ane E. Branco Pavanato and Ana Carolina B. Brust for the collaboration in the fieldwork; Guilherme Chiarello for assistance in the identification of the anatomic structures; Ana Maria Ribeiro, who permitted the access to the collection of the Fundação Zoobotânica do Rio Grande do Sul; Jamil Pereira, who permitted the access to the collection of the Museu Coronel Tancredo Fernandes de Mello; Andrés Rinderknecht, who permitted the access to the collection of the Museo Nacional de Historia Natural of Uruguay. Universidade Federal de Santa Maria (Edital PRPGP/UFSM 025/2018) for the English grammar review and the Sistema de Concessão de Diárias e Passagens PCDP 003861/18 for the assistance in the travels. LK is supported by Fundação de Amparo à Pesquisa do Estado do Rio Grande do Sul (FAPERGS 17/2551-0000816-2) and Conselho Nacional de Desenvolvimento Científico e Tecnológico (CNPq 422568/2018-0). This study was financed in part by the Coordenação de Aperfeiçoamento de Pessoal de Nível Superior – Brasil (CAPES) – Finance Code 001.

References

Amson E, Argot C, McDonald HG, Muizon C. 2014. Osteology and functional morphology of the hind limb of the marine sloth *Thalassocnus* (Mammalia, Tardigrada). *Journal of the Mammalian Evolution*. 22(3):355–419.

Asher R, Bennet N, Lehmann T. 2009. The new framework for understanding placental mammal evolution. *BioEssays*. 31(8):853–864.

Bargo MS, Menegaz AN, Prado JL, Salemme MC, Tambussi CP, Tonni EP. 1986. Mamíferos y Bioestratigrafía. Una nueva fauna local de la Unidad Mamífero Lujanense (Pleistoceno Tardío) de la Provincia de Buenos Aires. [Mammals and Biostratigraphy. A new local fauna of the Lujanian Mammal Unit (Late Pleistocene) of the Province of Buenos Aires]. *Ameghiniana*. 23(3-4):229–232.

Bargo MS, De Iuliis G, Vizcaíno SF. 2006. Hypsodonty in Pleistocene ground sloths. *Acta Palaeontologica Polonica*. 51(1):53–61.

Brandoni D, Carlini AA, Pujos F, Scillato-Yané GJ. 2004. The pes of *Pyramiodontherium bergi* (Moreno & Mercerat, 1891) (Mammalia, Xenarthra, Phyllophaga): the most complete pes of a Tertiary Megatheriinae. *Geodiversitas*. 26(4):643–659.

Cartelle C, De Iuliis G, Ferreira RL. 2009. Systematic revision of tropical Brazilian Scelidotheriinae sloths (Xenarthra, Milodontoidea). *Journal of Vertebrate Paleontology*. 29(2):555–566.

Carvalho AMV. 1952. Ocorrências de *Lestodon trigonidens* na mamalofauna de Álvares Machado. [Occurrences of *Lestodon trigonidens* on the mammal fauna of Álvares Machado]. Faculdade de Filosofia, Ciências e Letras da Universidade de São Paulo. 134(7):43–55.

Cione AL, Tonni EP. 1995. Chronostratigraphy and ‘Land mammal-ages’: the Uquían problem. *Journal of Paleontology*. 69(1):135–159.

Cione AL, Tonni EP. 2005. Bioestratigrafía basada en mamíferos del Cenozoico Superior de la Provincia de Buenos Aires, Argentina. [Biostratigraphy based on mammals of the Upper Cenozoic of the Province of Buenos Aires, Argentina]. In: Barrio RE, Etcheverry RO, Caballé MF, Llambias E, editors. *Geología y Recursos Minerales de la Provincia de Buenos Aires: Relatorio del XVI Congreso Geológico Argentino*. [Geology and Mineral Resources of the Province of Buenos Aires: Report of the XVI Argentine Geological Congress]. La Plata: Asociación Geológica Argentina; p. 183 – 200.

Cione AL, Gasparini GM, Soibelzon E, Soibelzon LH, Tonni EP. 2015. The Great American Biotic Interchange: A South American Perspective. New York (US): SpringerBriefs in Earth System Sciences.

Coltorti M, Abbazzi L, Ferretti MP, Iacumin P, Paredes-Rios F, Pellegrini M, Pieruccini P, Rustioni M, Tito G, Rook L. 2007. Last glacial mammals in South America: a new scenario from the Tarija basin (Bolivia). *Naturwissenschaften*. 94:288–299.

Czerwonogora A, Fariña RA, Tonni EP. 2011. Diet and isotopes of Late Pleistocene ground sloths: first results for *Lestodon* and *Glossotherium* (Xenarthra, Tardigrada). *Neues Jahrbuch für Geologie und Paläontologie*. 262(3):257–266.

Czerwonogora A, Fariña RA. 2012. How many Pleistocene species of *Lestodon* (Mammalia, Xenarthra, Tardigrada)? *Journal of Systematic Palaeontology*. 11(2):1–13.

De Iuliis G. 1994. Relationships of the Megatheriinae, Nothrotheriinae and Planopsinae: some skeletal characteristics and their importance for phylogeny. *Journal of Vertebrate Paleontology*. 14(4):577–591.

De Iuliis G. 1996. A systematic review of Megatheriinae (Mammalia: Xenarthra: Megatheriidae). [Dissertation]. Toronto: University of Toronto

Deschamps CM, Borromei AM. 1992. La fauna de vertebrados pleistocénicos del bajo San José (Provincia de Buenos Aires, Argentina). Aspectos paleoambientales. [The fauna of Pleistocene vertebrates of the lower San José (Province of Buenos Aires, Argentina). Paleoenvironmental aspects]. *Ameghiniana*. 29(2):177–183.

Deschamps CM, Esteban GI, Bargo MS. 2001. El registro más antiguo del género *Lestodon* Gervais, 1855 (Xenarthra, Tardigrada, Mylodontidae) (Montehermosense, Plioceno temprano). [The oldest record of the genus *Lestodon* Gervais, 1855 (Xenarthra, Tardigrada, Mylodontidae) (Montehermosian, early Pliocene)]. *Ameghiniana*. 38(2):151–156.

Deschamps CM. 2005. Late Cenozoic mammal bio-chronostratigraphy in southwestern Buenos Aires Province, Argentina. *Ameghiniana*. 42(4):733–750.

Fariña RA, Tambusso PS, Varela L, Czerwonogora A, Giacomo MD, Musso M, Bracco R, Gasque A. 2013. Arroyo del Vizcaíno, Uruguay: a fossil-rich 30-ka-old megafaunal locality with cut-marked bones. *Proc. R. Soc. B.* [accessed 2018 august 8]:[7 p.]. <http://dx.doi.org/10.1098/rspb.2013.2211>.

Gallo V, Avilla LS, Pereira RCL, Absolon BA. 2013. Distributional patterns of herbivore megamammals during the Late Pleistocene of South America. *Anais da Academia Brasileira de Ciências.* 85(2):533–546.

Gaudin TJ. 2004. Phylogenetic relationships among sloths (Mammalia, Xenarthra, Tardigrada): the craniodontal evidence. *Zoological Journal of the Linnean Society.* 140:255–305.

Gaudin TJ, McDonald HG. 2008. Morphology-based investigations of the phylogenetic relationships among extant and fossil xenarthrans. In: Vizcaíno SF, Loughry HJ, editors. *The Biology of Xenarthra*. Gainesville: University Press of Florida; p. 24 – 36.

Gervais P. 1855. *Mammifères fossiles de l'Amérique Meridionale*. [Mammal fossil of the Meridional Americ]. Paris: Chez P. Bertrand libraire-editeur.

Gervais P. 1873. *Mémoire sur plusieurs espèces de mammifères fossiles propres a l'Amérique Meridionale*. [Memory on several species of fossil mammals unique to South America]. *Mémoires de la Société Géologique de France.* 24:1–44.

Ghilardi AM, Fernandes MA, Bichuette ME. 2011. Megafauna from the Late Pleistocene-Holocene deposits of the Upper Ribeira karst area, southeast Brazil. *Quaternary International.* 245(2):369–378.

Hoffstetter R. 1978. *Une faune de mamifères au Paraguay*. [A mammal fauna in Paraguay]. *C. R. Som. Soc. Géol. France.* 1:32–33.

Kraglievich L. 1928. “*Mylodon darwini*” Owen, es la especie genotipo del “*Mylodon*” Owen. Rectificación de la nomenclatura genérica de los milodontos. [“*Mylodon darwini*” Owen, is the

genotype species of the "*Mylodon*" Owen. Rectification of the generic nomenclature of the milodonts]. *Physis*. 9(33):169–185.

Kraglievich L. 1934. Contribución al conocimiento de *Mylodon darwini* Owen y especies afines. [Contribution to the knowledge of *Mylodon darwini* Owen and related species]. *Revista del Museo de La Plata*. 35:255–292.

Linares OJ. 2004. Nuevos restos del género *Lestodon* Gervais, 1855 (Xenarthra, Tardigrada, Mylodontidae), del Mioceno Tardío y Plioceno Temprano de Urumaco (Venezuela), con descripción de nuevas especies. [New remains of the genus *Lestodon* Gervais, 1855 (Xenarthra, Tardigrada, Mylodontidae), Late Miocene and Early Pliocene of Urumaco (Venezuela), with description of new species]. *Paleobiología Neotropical*. 2:1–14.

Lopes RP, Buchmann FSC, Caron F, Itusarry ME. 2001. Tafonomia dos fósseis de vertebrados (megafauna extinta) encontrados nas barrancas do arroio Chuí e linha de costa, Rio Grande do Sul, Brasil. [Tafonomy of vertebrate fossils (extinct megafauna) found in the ravines of the Chuí stream and coastline, Rio Grande do Sul, Brazil]. *Pesquisas em Geociências*. 28(2):67–73.

Marshall LG. 1988. Land mammals and the Great American Interchange. *American Scientist*. 76(4):380–388.

Marshall LG, Sempere T. 1991. The Eocene to Pleistocene vertebrates of Bolivia and their stratigraphic context: a review. *Fósiles y Facies de Bolivia: Vertebrados*. 12(3-4):631–652.

Martínez S, Ubilla M. 2004. El Cuaternario del Uruguay. [The Quaternary of Uruguay]. In: Veroslavsky G, Ubilla M, Martínez S, editors. *Cuencas sedimentarias de Uruguay: Geología, Paleontología y recursos naturales*. [Uruguay sedimentary basins: Geology, Paleontology and natural resources]. Montevideo: D.I.R.A.C.; p. 195–228.

McAfee RK. 2016. Description of new postcranial elements of *Mylodon darwini* Owen 1839 (Mammalia: Pilosa: Mylodontinae), and functional morphology of the forelimb. *Ameghiniana*. 53(4):418–443.

McDonald HG. 2012. Evolution of the pedolateral foot in ground sloths: patterns of change in the astragalus. *Journal of Mammalian Evolution*. 19:209–215.

McDonald HG, De Iuliis G. 2008. Fossil history of sloths. In: Vizcaíno SF; Loughry WJ. *The biology of Xenarthra*. Gainesville: University Press of Florida; p. 39 – 55.

Miño-Boilini AR. 2012. Sistemática y evolución de los Scelidotheriinae (Xenarthra, Mylodontidae) cuaternarios de la Argentina. Importancia estratigráfica, paleobiogeográfica y paleoambiental. [Systematics and evolution of the Scelidotheriinae (Xenarthra, Mylodontidae) quaternaries of Argentina. Stratigraphic, paleobiogeographical and paleoenvironmental importance] [dissertation]. La Plata: Universidad Nacional de La Plata.

Miño-Boilini AR, Carlini AA, Scillato-Yané GJ. 2014. Revisión sistemática y taxonómica del género *Scelidotherium* Owen, 1839 (Xenarthra, Phyllophaga, Mylodontidae). [Systematic and taxonomic review of the genus *Scelidotherium* Owen, 1839 (Xenarthra, Phyllophaga, Mylodontidae)]. *Revista Brasileira de Paleontologia*. 17(1):43–58.

Murphy WJ, Eizirik E, O’Brien SJ, Madsen O, Scally M, Douady CJ, Teeling E, Ryder OA, Stanhope MJ, De Jong WW, Springer MS. 2001a. Resolution of the early placental mammal radiation using Bayesian phylogenetics. *Science*. 294(5550):2348–2351.

Murphy WJ, Johnson WE, Zhang YP, Ryderk OA, O’Brienn SJ. 2001b. Molecular phylogenetics and the origins of placental mammals. *Nature*. 409:614–618.

O’Leary MA, Bloch JI, Flynn JJ, Gaudin TJ, Giallombardo A, Giannini NP, Goldberg SL, Kraatz BP, Luo ZX, Meng J, et al. 2013. The placental mammal ancestor and the Post-K-Pg radiation of placentals. *Science*. 339(662):662–667.

Oliveira EV. 1996. Mamíferos Xenarthra (Edentata) do Quaternário do Estado do Rio Grande do Sul, Brasil. [Xenarthra (Edentata) Mammals of the Quaternary of the state of Rio Grande do Sul, Brazil]. *Ameghiniana*. 33(1):65–75.

Oliveira EV, Dutra TL, Zeltzer F. 2002. Megaterídeos (Mammalia, Xenarthra) do Quaternário de Caçapava do Sul, com considerações sobre a flora associada. [Megateriids (Mammalia,

Xenarthra) of the Quaternary of Caçapava do Sul, with considerations on the associated flora]. *Geología Colombiana*. 27:77–86.

Owen R. 1842. Description of the skeleton of an extinct giant sloth, *Myiodon robustus*, Owen, with observations of the osteology, natural affinities, and probable habits the megatherioid quadrupeds in general. London: R. & J. E. Taylor.

Owen R. 1859. On the *Megatherium* (*Megatherium americanum*, Cuvier and Blumenbach). Part V – Bones of posterior extremities. *Philosophical Transactions*. 149:809–829.

Paula Couto C. 1944. Sobre a presença dos gêneros *Hippidion* e *Toxodon* Owen, no Pleistoceno do Rio Grande do Sul. [On the presence of the genera *Hippidion* and *Toxodon* Owen, in the Pleistocene of Rio Grande do Sul]. *Boletim do Museu Nacional*. 2:1–12.

Paula Couto C. 1973. Edentados fósseis de São Paulo. [Edentates fóssil of São Paulo]. *Anais da Academia Brasileira de Ciências*. 45(2):261–275.

Paula Couto C. 1979. *Tratado de Paleomastozoologia*. [Paleomastozoology Treaty]. Rio de Janeiro: Academia Brasileira de Ciências.

Pérez LM, Toledo N, De Iuliis G, Bargo SM, Viscaíno SF. 2010. Morphology and function of the hyoid apparatus of fóssil xenarthrans (Mammalia). *Journal of Morphology*. 271:1119–1133.

Pitana VG. 2011. Estudo do gênero *Glossotherium* Owen, 1840 (Xenarthra, Tardigrada, Mylodontidae), Pleistoceno do estado do Rio Grande do Sul, Brasil. [Study of the genus *Glossotherium* Owen, 1840 (Xenarthra, Tardigrada, Mylodontidae), Pleistocene of the Rio Grande do Sul state, Brazil] [master's thesis]. Porto Alegre: Universidade Federal do Rio Grande do Sul.

Pujos F, Gaudin TJ, De Iuliis G, Cartelle C. 2012. Recent advances on variability, morpho-functional adaptations, dental terminology, and evolution of sloths. *Journal of Mammalian Evolution*. 19:159–169.

- Püschel HP, Püschel TA, Rubilar-Rogers D. 2017. Taxonomic comments of a *Glossotherium* specimen from the Pleistocene of Central Chile. *Boletín del Museo Nacional de Historia Natural, Chile*. 66(2):223–262.
- Ribeiro AM, Scherer CS. 2009. Mamíferos do Pleistoceno do Rio Grande do Sul, Brasil. [Pleistocene mammals of the Rio Grande do Sul, Brazil]. In: Ribeiro AM, Bauermann SG, Scherer CS, editors. *Quaternário do Rio Grande do Sul: integrando conhecimentos*. [Quaternary of the Rio Grande do Sul: integrating knowledge]. Porto Alegre: Monografias da Sociedade Brasileira de Paleontologia; p. 171 – 191.
- Salas R, Pujos F, Muizon C. 2005. Ossified meniscus and cyamo-fabella in some fossil sloths: a morpho-functional interpretation. *Geobios*. 38:389–934.
- Schaller O. 2007. *Illustrated Veterinary Anatomical Nomenclature*. Stuttgart: Enke.
- Stock C. 1917. Structure of the pes in *Mylodon harnali*. *Bulletin of the Department of Geology*. 10 (16):267–286.
- Stock C. 1925. Cenozoic gravigrade edentates of Western North America. *Carnegie Institution of Washington Publications*. 331:1–206.
- Tambusso PS, McDonald HG, Fariña RA. 2015. Description of the stylohyal bone of a giant sloth (*Lestodon armatus*). *Palaeontologia Electronica*. 18.1.19A:1–10.
- Tonni EP, Soibelzon E, Cione AL, Carlini AA, Scillato-Yané GJ, Zurita AE, Ríos FP. 2009. Preliminary correlation of the Pleistocene sequences of the Tarija valley (Bolivia) with the Pampean chronological standard. *Quaternary International*. 210:57–65.
- Ubilla M. 2004. Mammalian biostratigraphy of Pleistocene fluvial deposits in northern Uruguay, South America. *Proceedings of the Geologists Association*. 115:347–357.
- Ubilla M, Perea D, Aguilar CG, Lorenzo N. 2004. Late Pleistocene vertebrates from northern Uruguay: tools for biostratigraphic, climatic and environmental reconstruction. *Quaternary International*. 114:129–142.

Webb SD. 1989. Osteology and relationships of *Thinobadistes segnis*, the first mylodont in North America. In: Redford KH, Eisenberg JF, editors. *Advances in Neotropical Mammalogy*. Gainesville: Sandhill Crane Press; p. 469 – 532.

Woodburne MO. 2010. The Great American Biotic Interchange: dispersals, tectonics, climate, sea level and holding pens. *Journal of Mammalian Evolution*. 17(4):245–264.

Varela L, Fariña RA. 2016. Co-occurrence of mylodontid sloths and insights on their potential distributions during the late Pleistocene. *Quaternary Research*. 85:66–74.

Supplementary Data (SD)

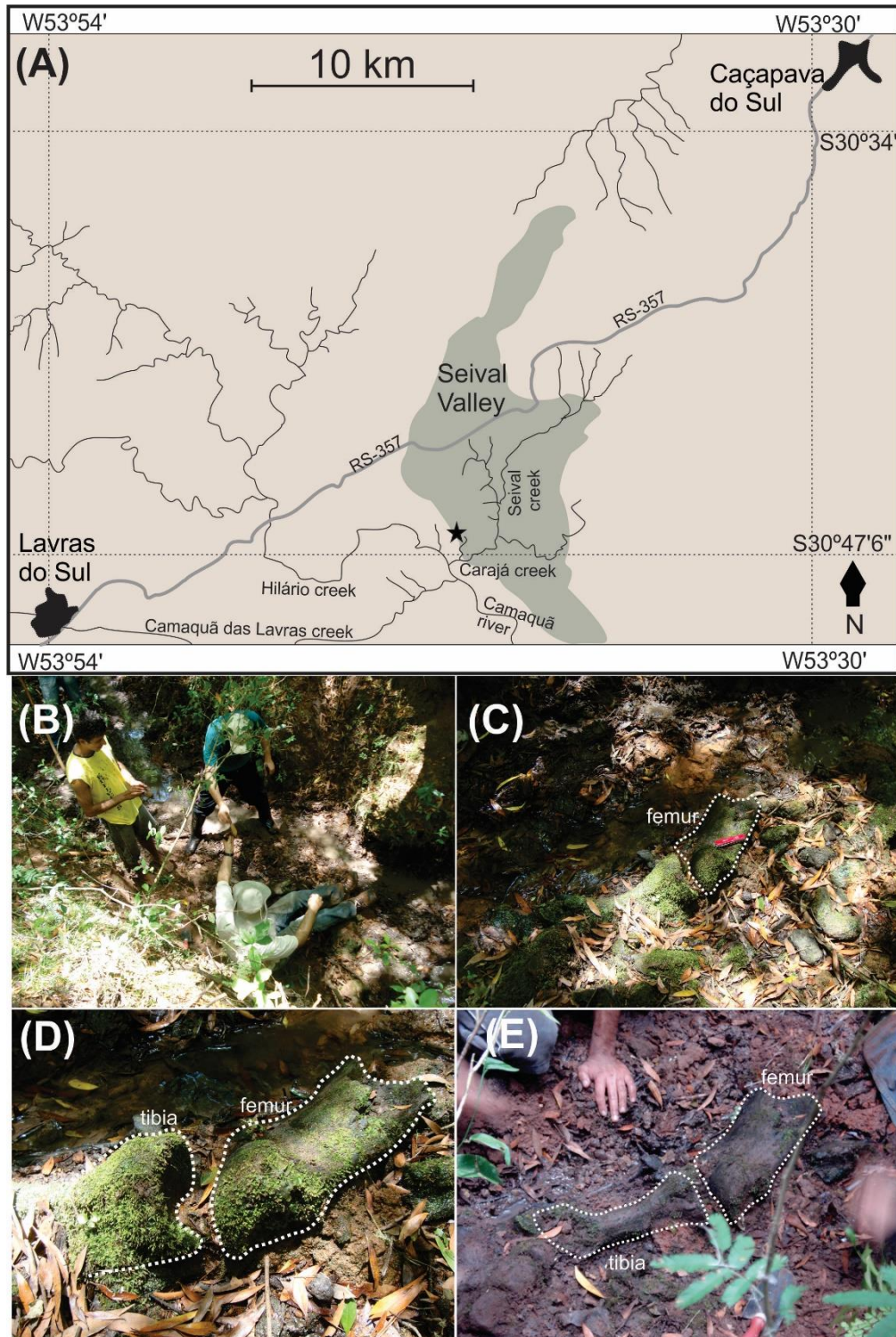


Figure S1. Collecting of UFSM 11535 at “Arroio do *Lestodon*” locality. (A) Seival locality and “Arroio do *Lestodon*” fossiliferous site, (C)-(D) fossil *in situ*.

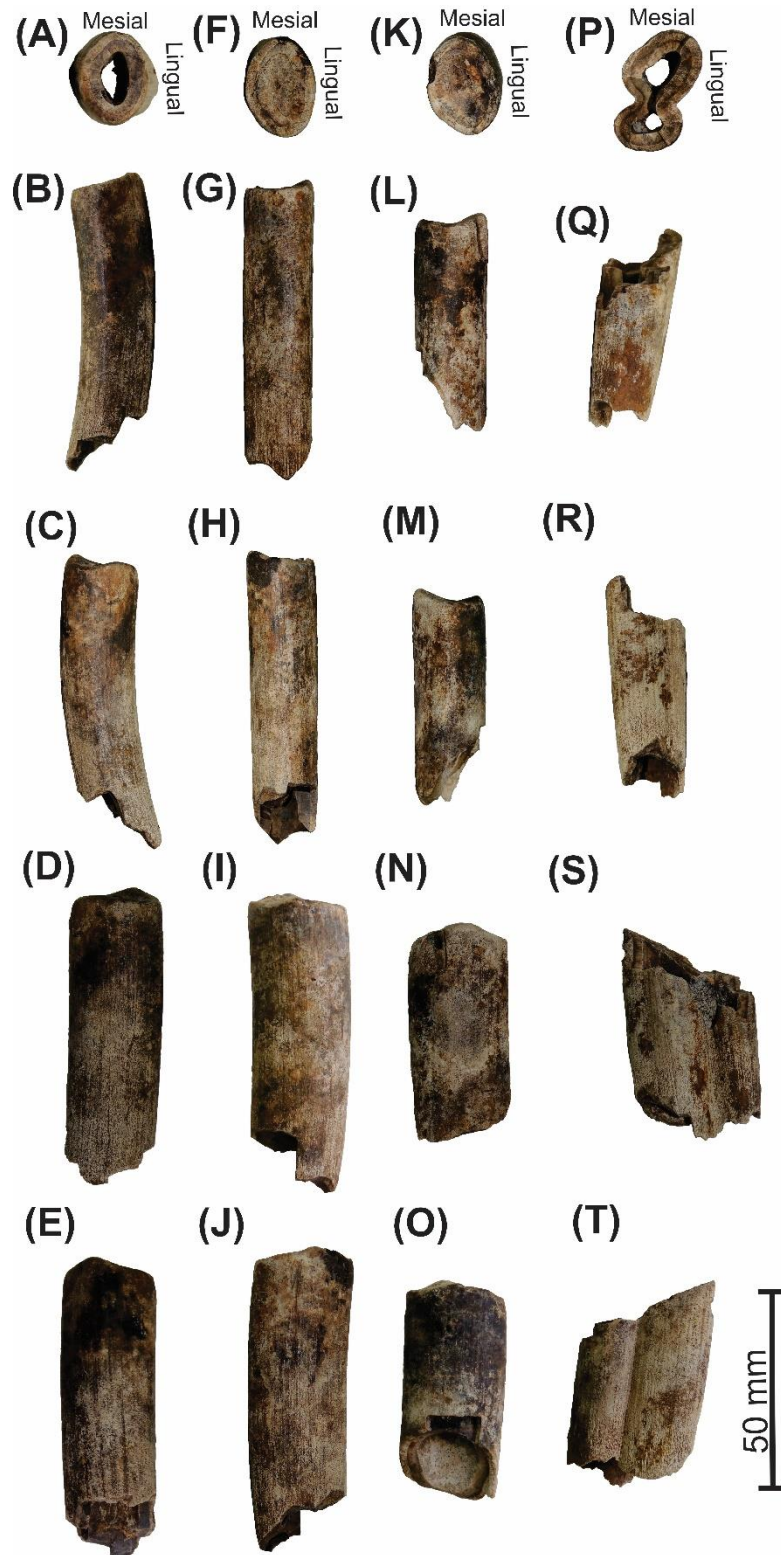


Figure S2. Teeth of *Lestodon armatus* (UFSM 11535). (A-E) upper molariform 2, (F-J) lower molariform 2, (K-O) lower molariform 3, (P-T) lower molariform 4 in (A, F, K, P) occlusal, (B, G, L, Q) mesial, (C, H, M, R) distal, (D, I, N, S) lingual and (E, J, O, T) labial views. Scale: 50 mm.

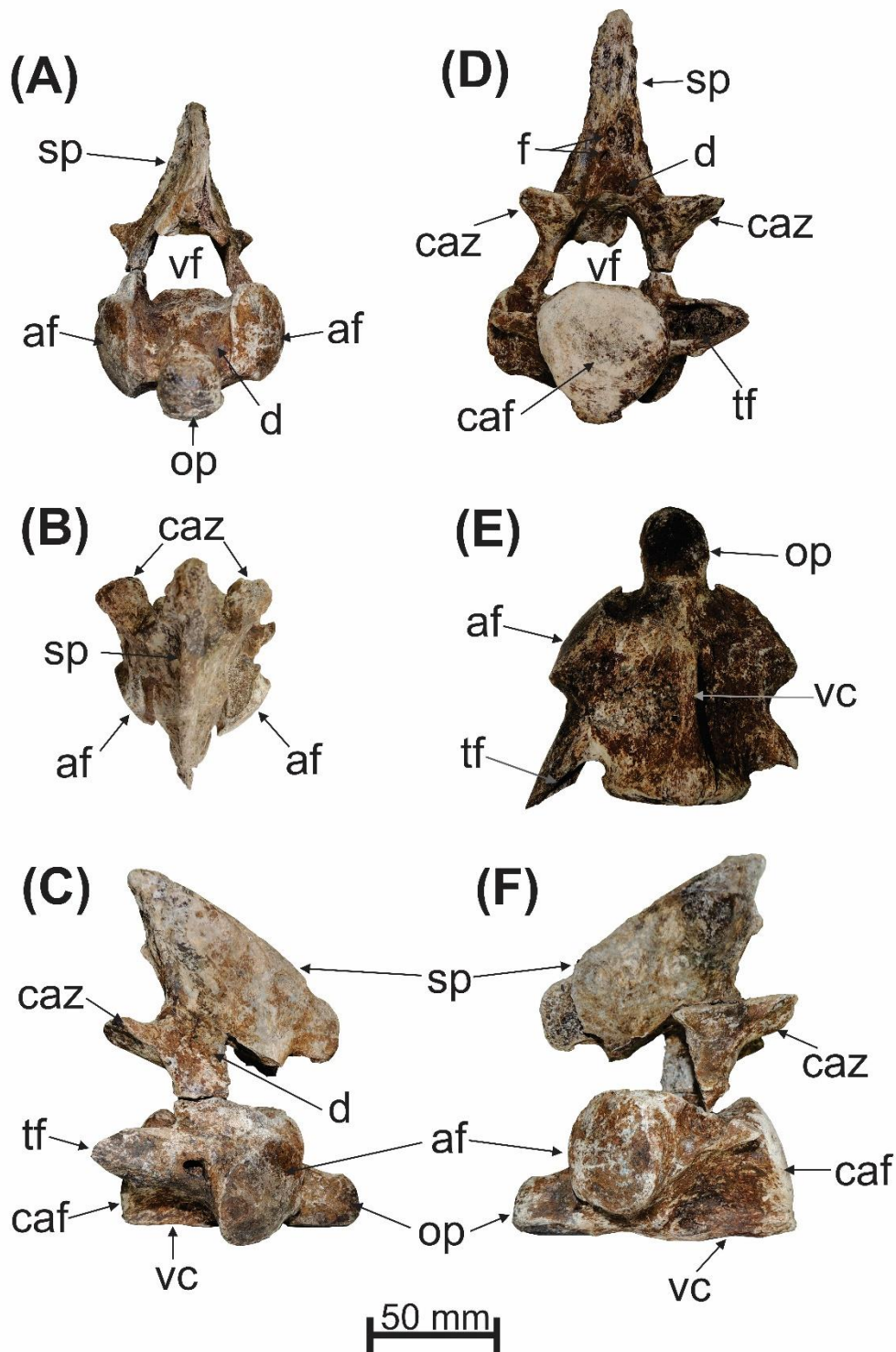


Figure S3. Axis of *Lestodon armatus* (UFSM 11535). (A) cranial, (B) dorsal, (C) right lateral, (D) caudal, (E) ventral and (F) lateral left views. Abbreviations: af, atlas facet; caf, caudal facet; caz, caudal zygapophysis; d, depression; f, fovea; op, odontoid process; sp, spinous process; tf, transverse foramen; vc, ventral crest; vf, vertebral foramen. Scale: 50 mm.

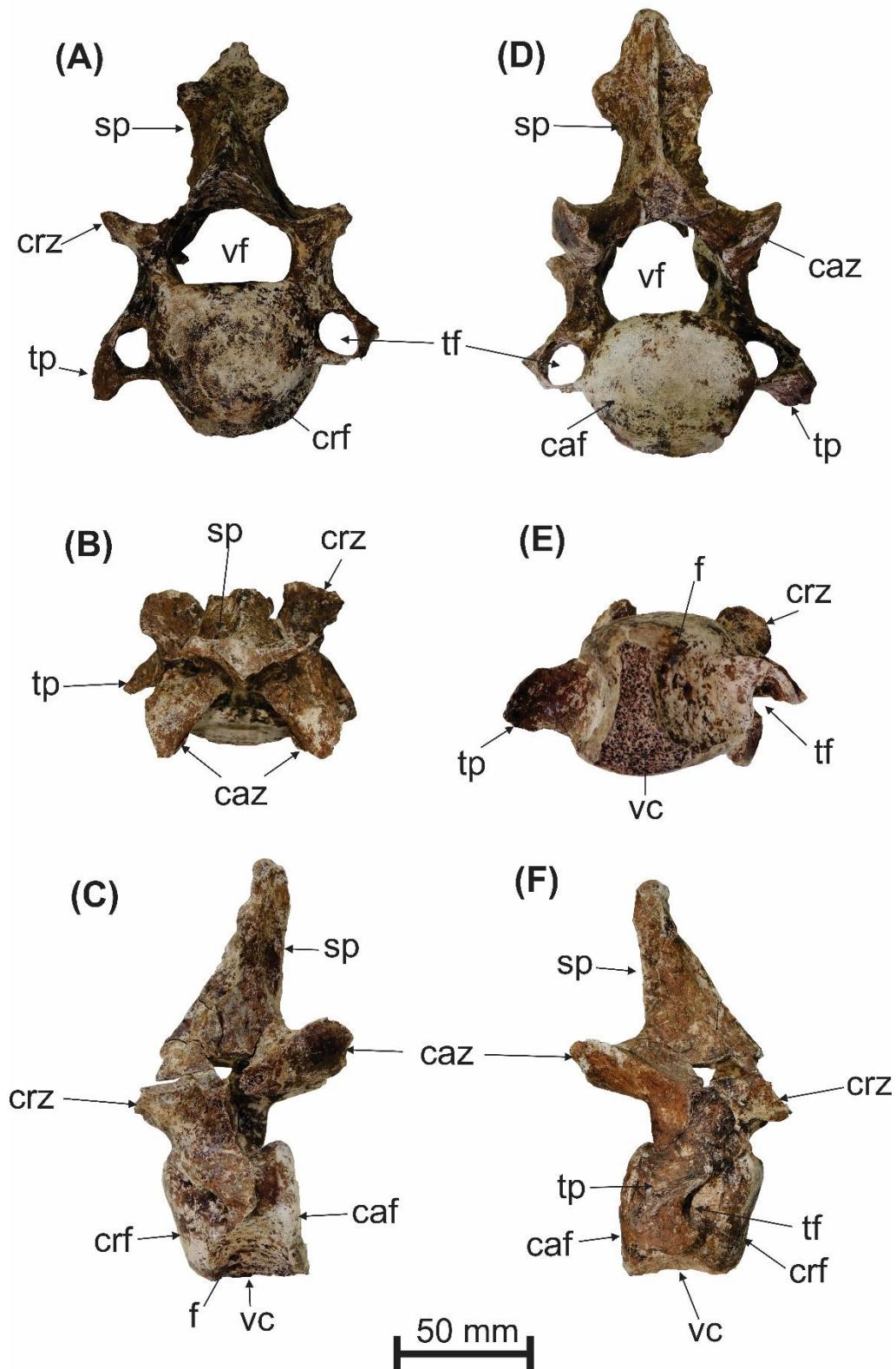


Figure S4. Third cervical vertebrae of *Lestodon armatus* (UFSM 11535). (A) cranial, (B) dorsal, (C) left lateral, (D) caudal, (E) ventral and (F) lateral right views. Abbreviations: caf, caudal facet; caz, caudal zygapophysis; crz, cranial zygapophysis; crf, cranial facet; f, fovea; sp, spinous process; tf, transverse foramen; tp, transverse process; vc, ventral crest; vf, vertebral foramen. Scale: 50 mm.

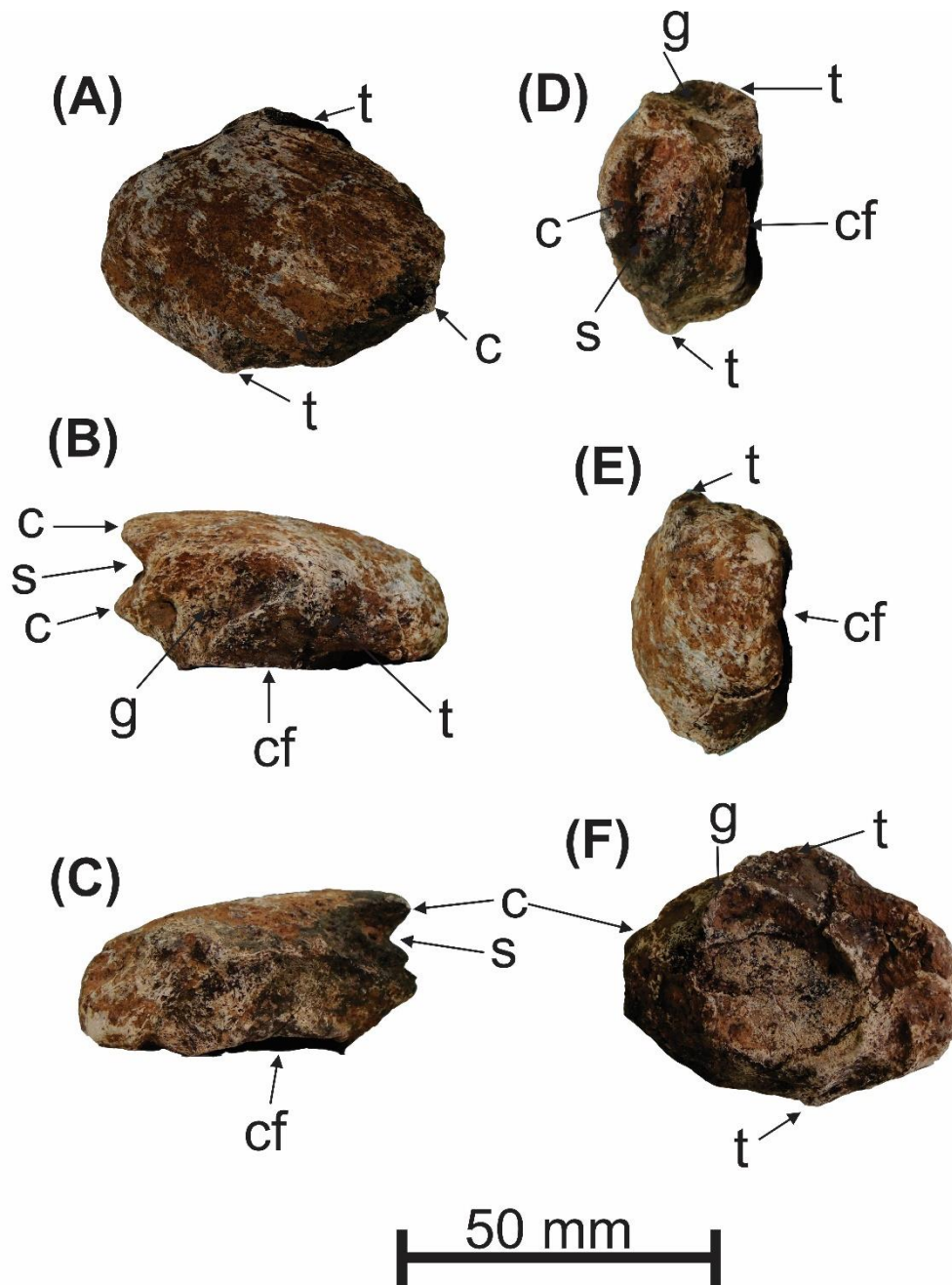


Figure S5. Cyamo-fabella of *Lestodon armatus* (UFSM 11535). (A) caudal, (B) dorsal, (C) ventral, (D) medial, (E) lateral and (F) cranial views. Abbreviations: c, crest; cf, cranial facet; g, groove; s, sulcus; t, tuberosity.

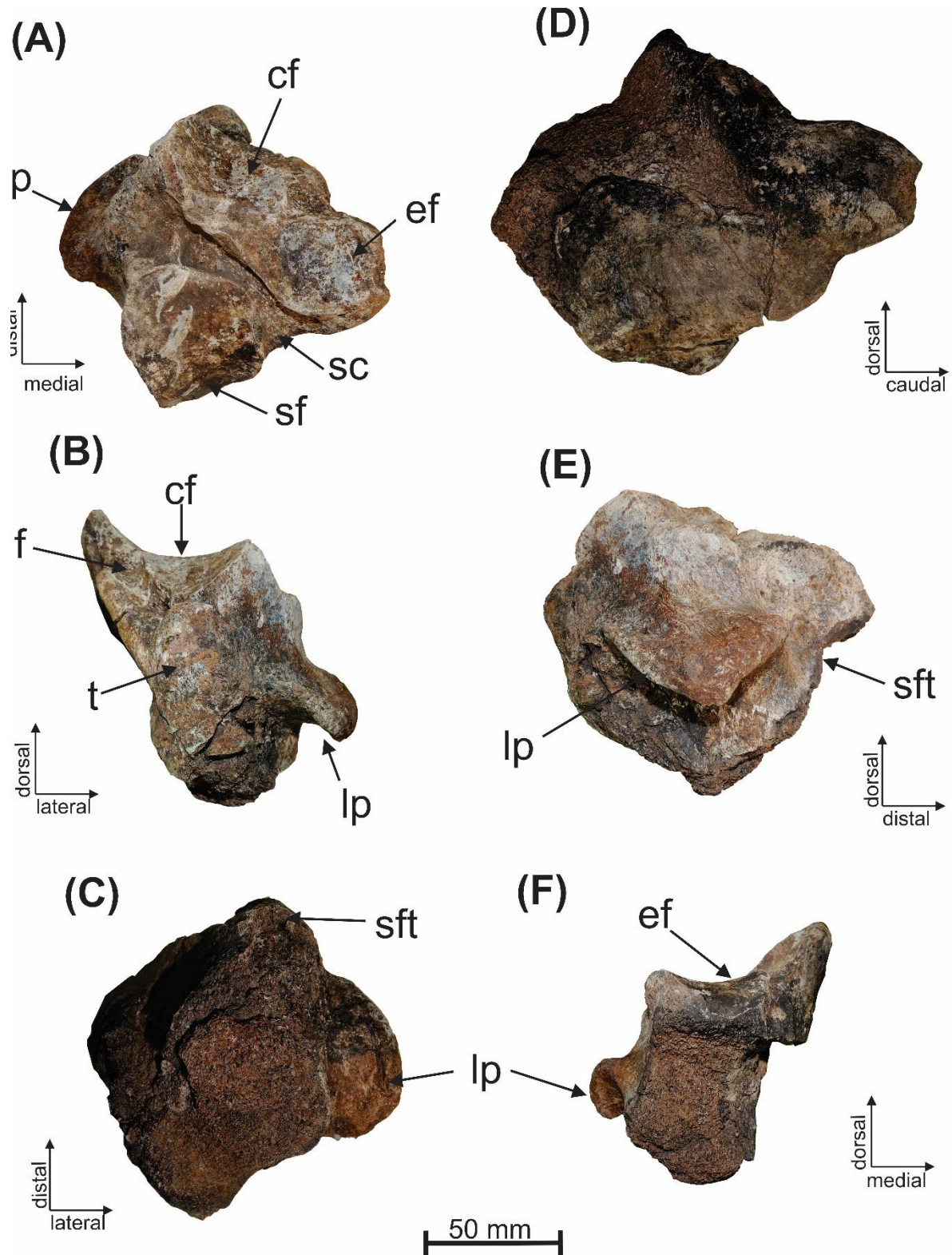


Figure S6. Left calcaneus of *Lestodon armatus* (UFSM 11535). (A) dorsal, (B) cranial, (C) plantar, (D) medial, (E) lateral and (F) distal views. Abbreviations: cf, cuboid facet; ef, ectal facet; f, fossa; lp, lateroproximal process; sc, sulcus calcanei; sf, sustentacular facet; sft, sustentacular facet tuberosity; t, tuberosity. Scale: 50 mm.

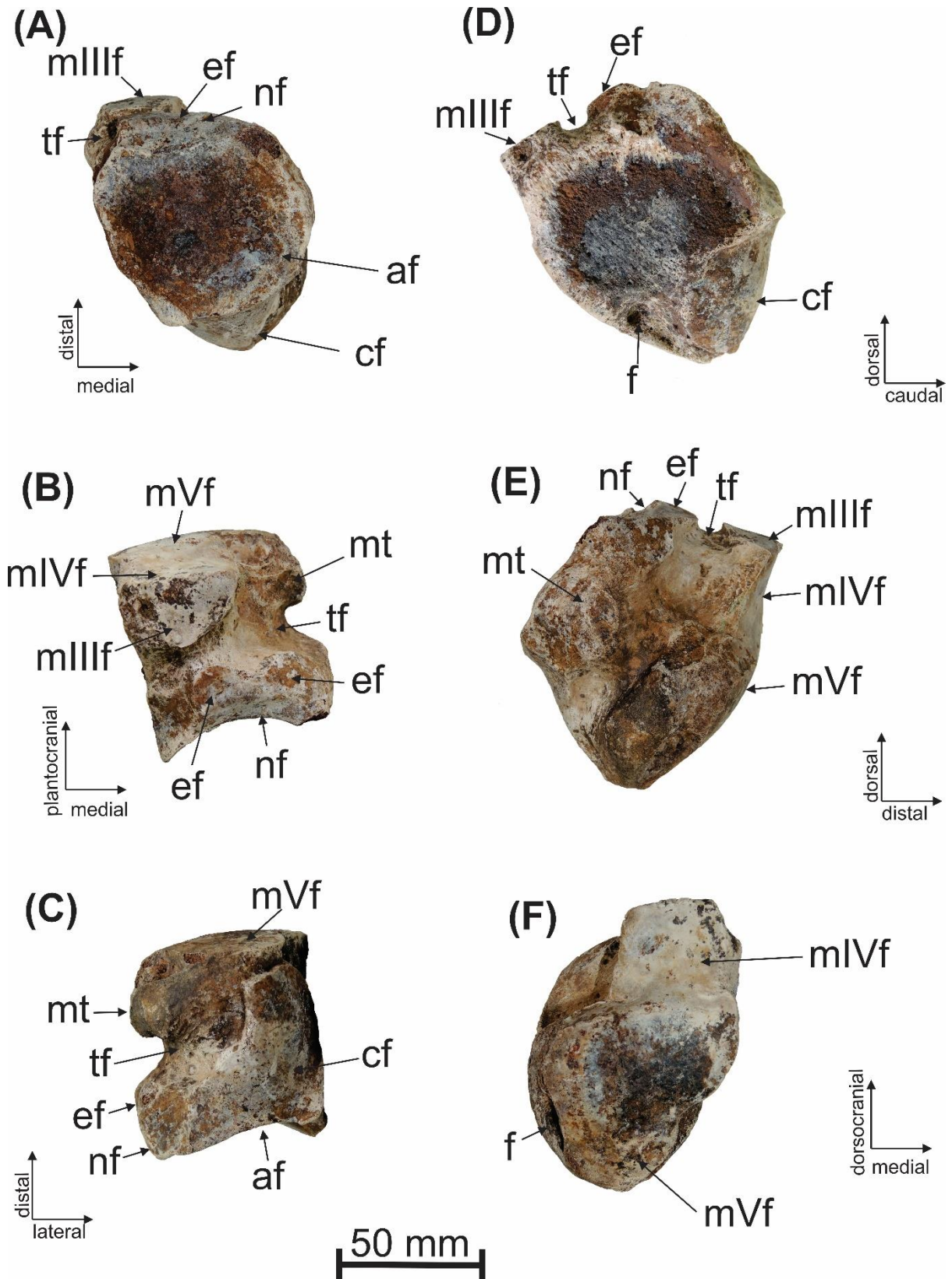


Figure S7. Left cuboid of *Lestodon armatus* (UFSM 11535). (A) dorsoproximal, (B) dorsocranial, (C) plantolateral, (D) lateral, (E) medial and (F) plantocaudal views. Abbreviations: af, astragalar facet; cf, calcaneus facet; ef, ectocuneiform facet; f, fovea; mIII f, metatarsal III facet; mIV f, metatarsal IV facet; mt, medioplantar tuberosity; mVf, metatarsal V facet; nf, navicular facet; tf, transversal fossa. Scale: 50 mm.

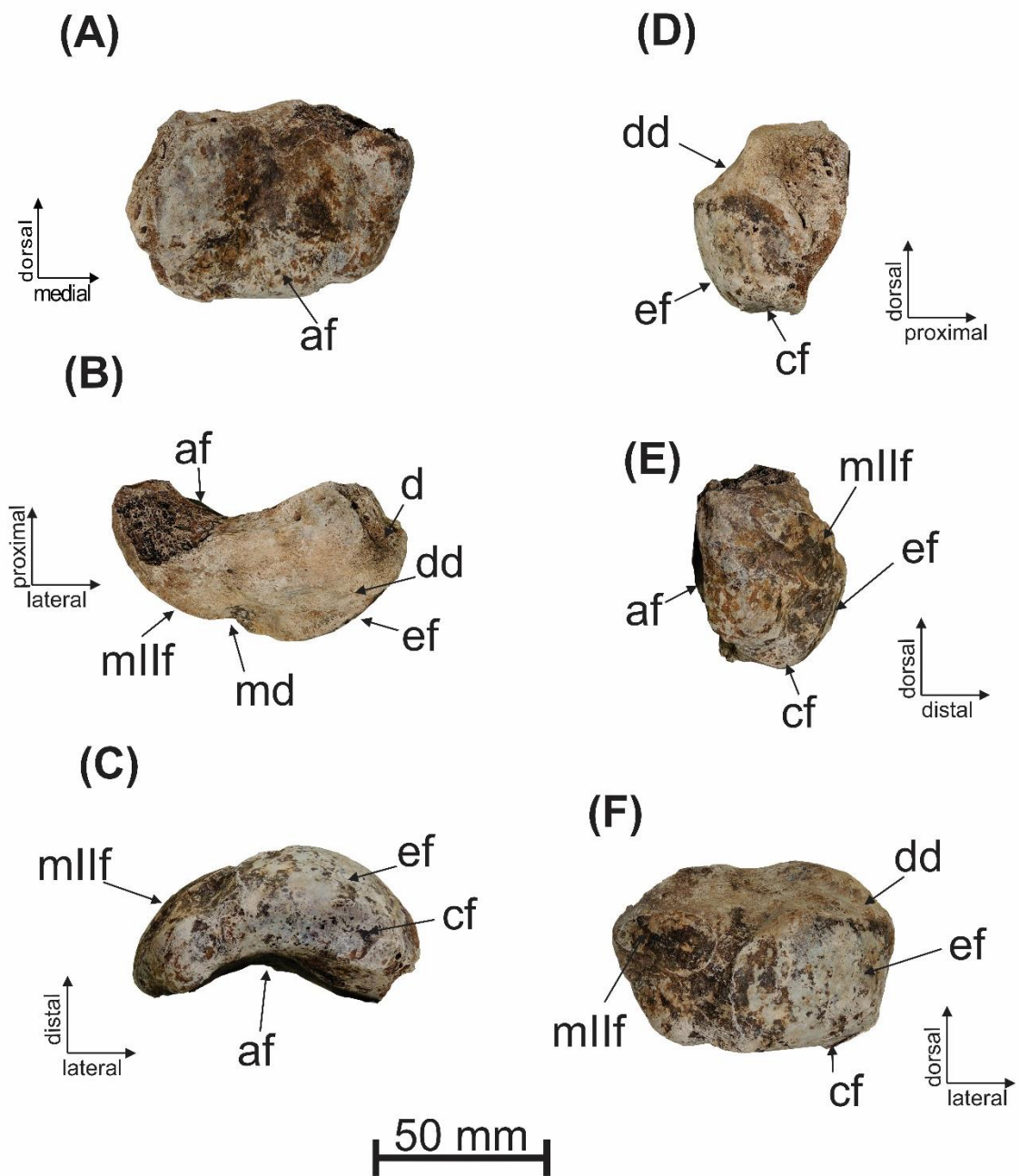


Figure S8. Left navicular of *Lestodon armatus* (UFSM 11535). (A) proximal, (B) dorsal, (C) plantar, (D) medial, (E) lateral and (F) distal views. Abbreviations: af, astragalar facet; cf, cuboid facet; dd, dorsal depression; ef, ectocuneiform facet; mllf, metatarsal II facet. Scale: 50 mm.

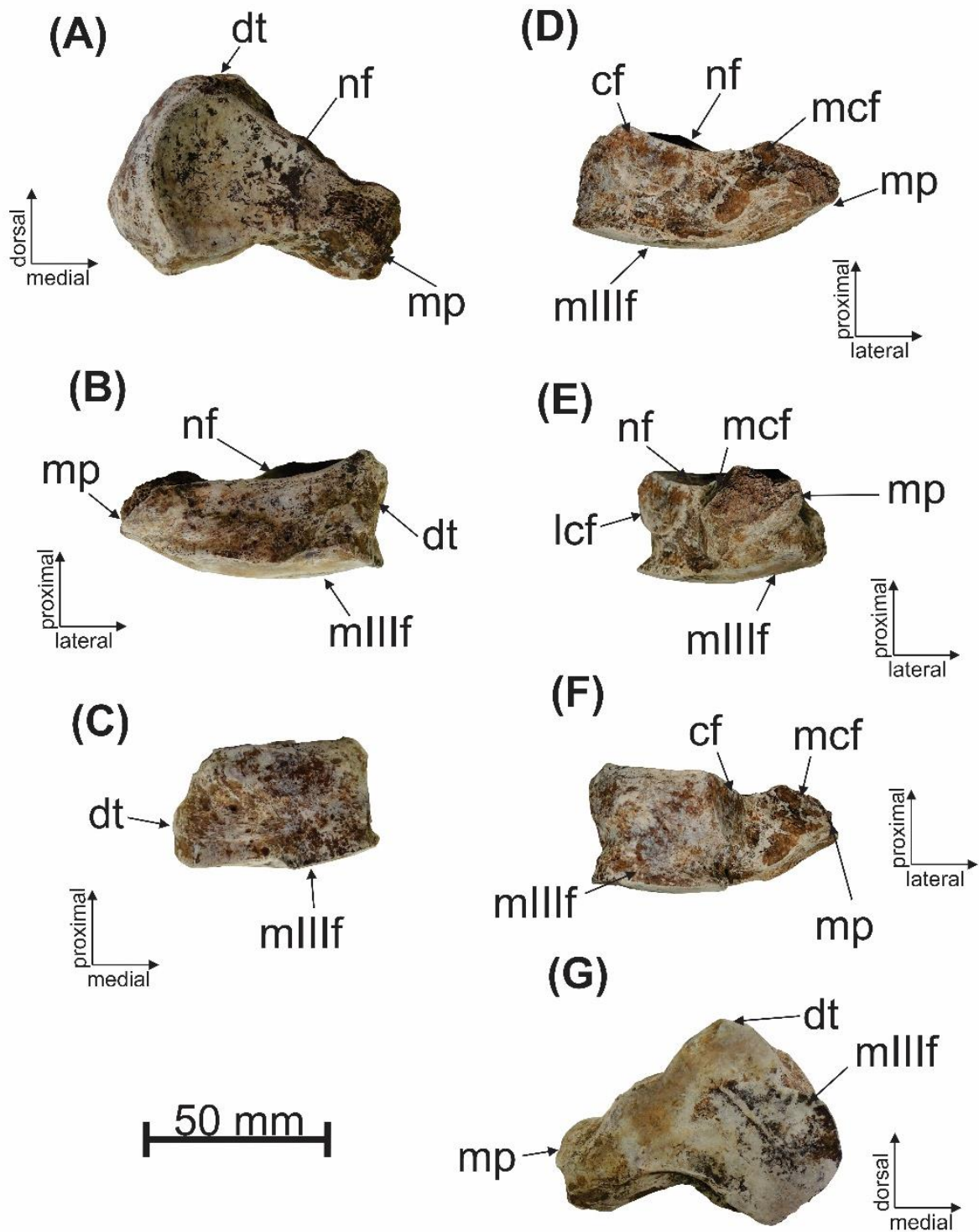


Figure S9. Left ectocuneiform of *Lestodon armatus* (UFSM 11535). (A) proximal, (B) dorsomedial, (C) dorsolateral, (D) plantar, (E) plantomedial, (F) plantolateral and (G) distal views. Abbreviations: dt, dorsal tubercle; f, fovea; lcf, lateral cuboid facet; mIII f, metatarsal III facet; mcf, medial cuboid facet; mp, medioplantar process; nf, navicular facet. Scale: 50 mm.

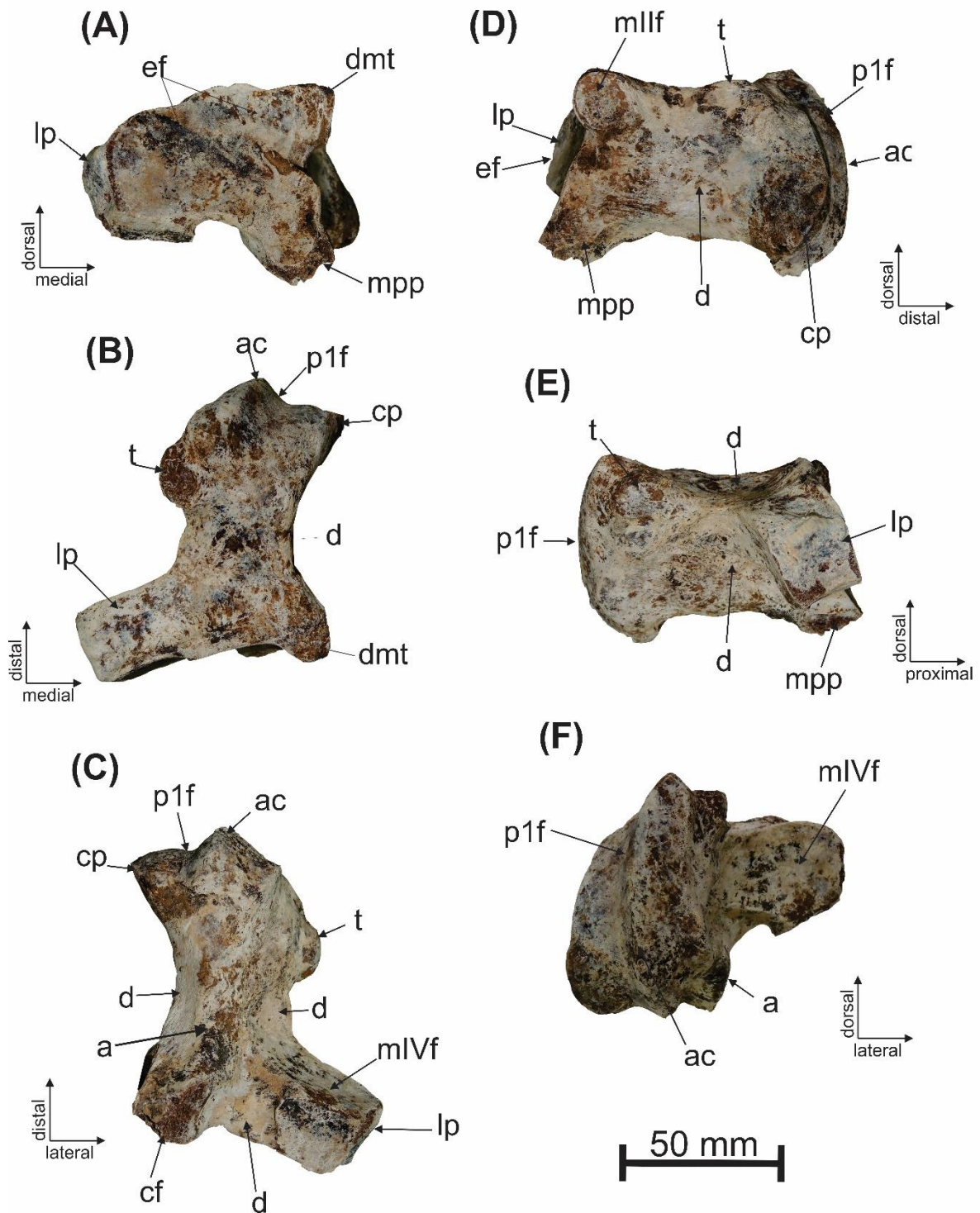


Figure S10. Left metatarsal III of *Lestodon armatus* (UFSM 11535). (A) proximal, (B) dorsal, (C) plantar, (D) medial, (E) lateral and (F) distal views. Abbreviations: ac, acute crest; cf, cuboid facet; dmt, dorsomedial tubercle; ef, ectocuneiform facet; lp, lateral process; mIIIf, metatarsal II facet; mIVf, metatarsal IV facet; mpp, medioplantar process; p1f, proximal phalanx facet. Scale: 50 mm.

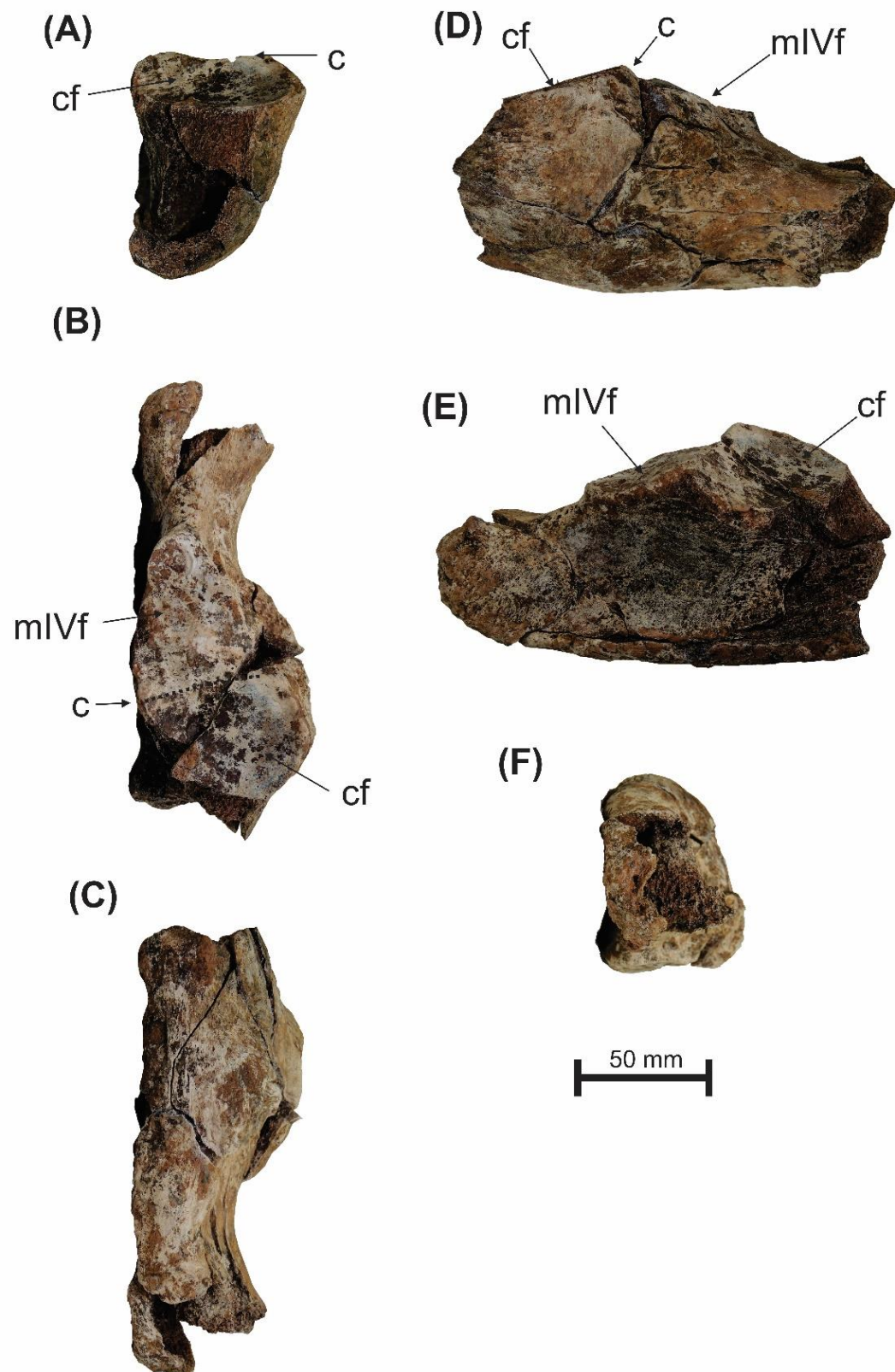


Figure S11. Left metatarsal V of *Lestodon armatus* (UFMSM 11535). (A) proximal, (B) dorsal, (C) plantar, (D) medial, (E) lateral and (F) distal views. Abbreviations: c, crest; cf, cuboid facet; mIVf, metatarsal IV facet. Scale: 50 mm.

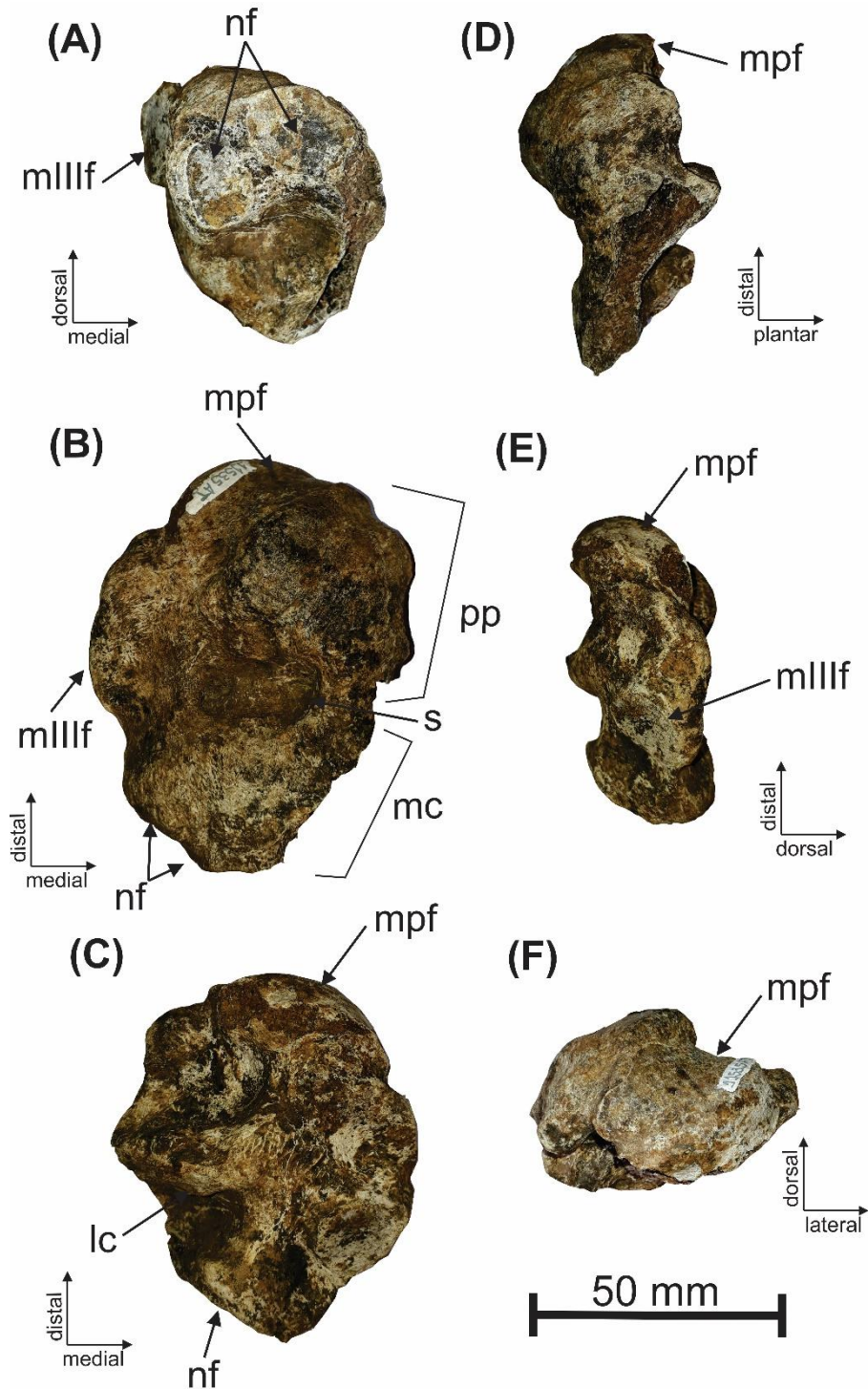


Figure S12. Left proximal phalanx of digit 2 of *Lestodon armatus* (UFSM 11535). (A) Proximal, (B) dorsal, (C) plantar, (D) medial, (E) lateral and (F) distal views. Abbreviations: lc, lateroplantar crest; mc, mesocuneiform; mIIIIf, metatarsal III facet; mpf, medial phalanx facet; nf, navicular facet; pp, proximal phalanx; s, sulcus. Scale: 50 mm.

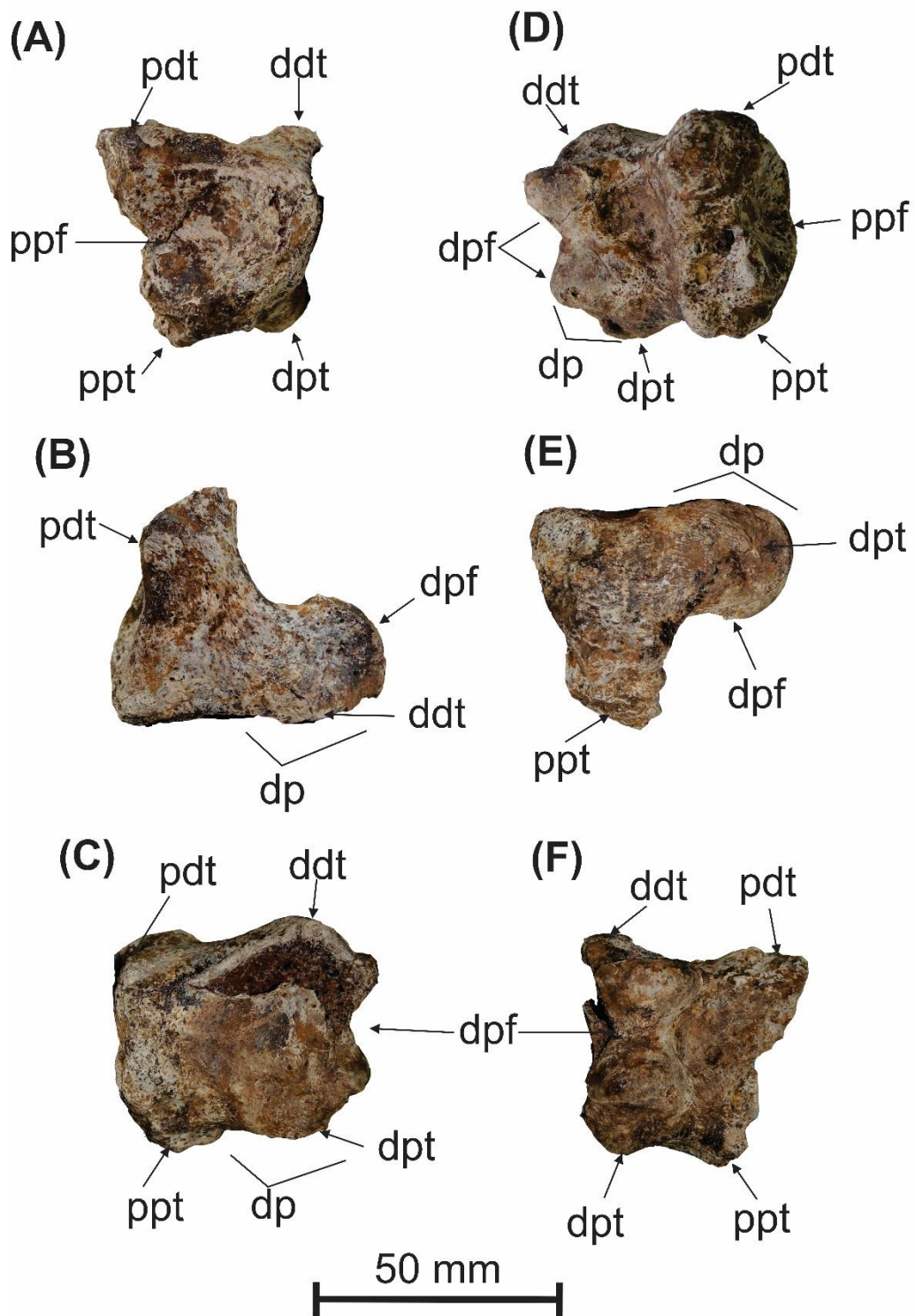


Figure S13. Left medial phalanx of digit 2 of *Lestodon armatus* (UFSM 11535). (A) proximal, (B) dorsal, (C) medial, (D) lateral, (E) plantar and (F) distal views. Abbreviations: ddt, distodorsal tuberosity; dp, distal process; dpf, distal phalanx facet; dpt, distoplantar tuberosity; pdt, proximodorsal tuberosity; ppf, proximal phalanx facet; ppt, proximoplantar tuberosity. Scale: 50 mm.

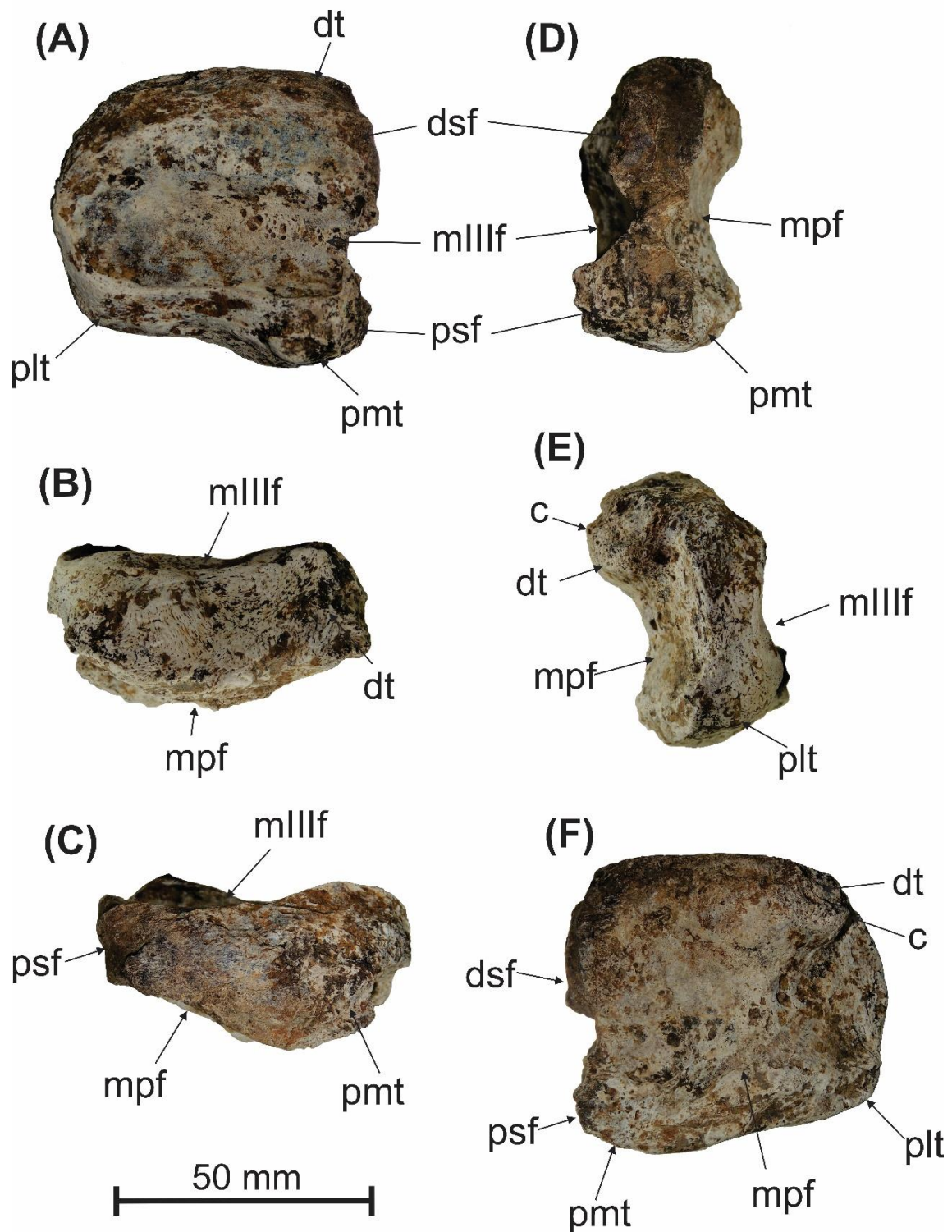


Figure S14. Left proximal phalanx of digit 3 of *Lestodon armatus* (UFSM 11535). (A) proximal, (B) dorsal, (C) plantar, (D) medial, (E) lateral and (F) distal views. Abbreviations: c, crest; dsf, dorsal sesamoid facet; dt, dorsolateral tuberosity; mIII f, metatarsal III facet; mpf, medial phalanx facet; plt, plantolateral tuberosity; pmt, plantomedial tuberosity; psf, plantar sesamoid facet. Scale: 50 mm.

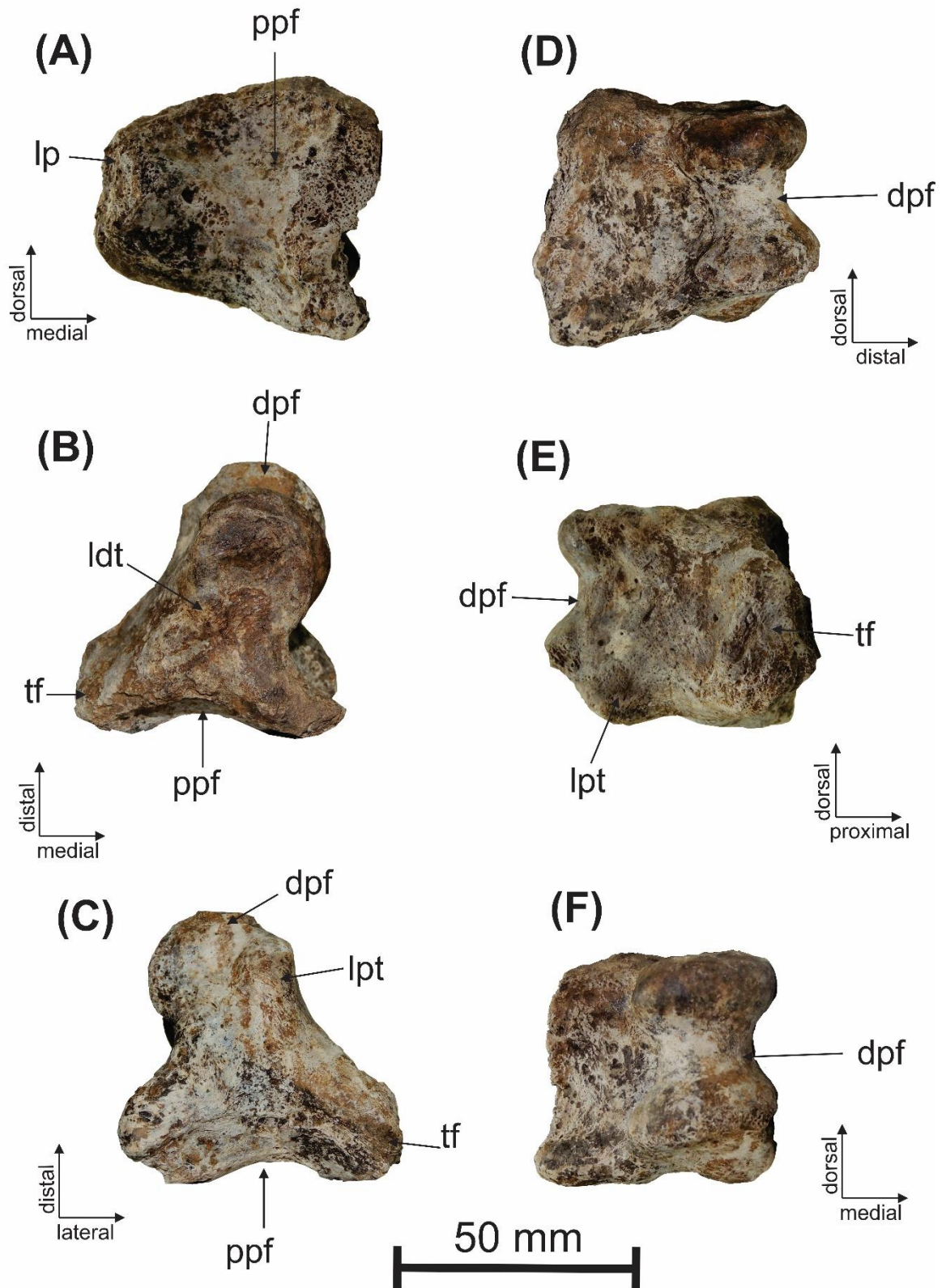


Figure S15. Left medial phalanx of digit 3 of *Lestodon armatus* (UFSM 11535). (A) proximal, (B) dorsal, (C) plantar, (D) medial, (E) lateral and (F) distal views. Abbreviations: dpf, distal phalanx facet; ldt, laterodorsal tuberosity; lpt, lateroplantar tuberosity; ppf, proximal phalanx facet; tf, tuberitas flexoria. Scale: 50 mm.

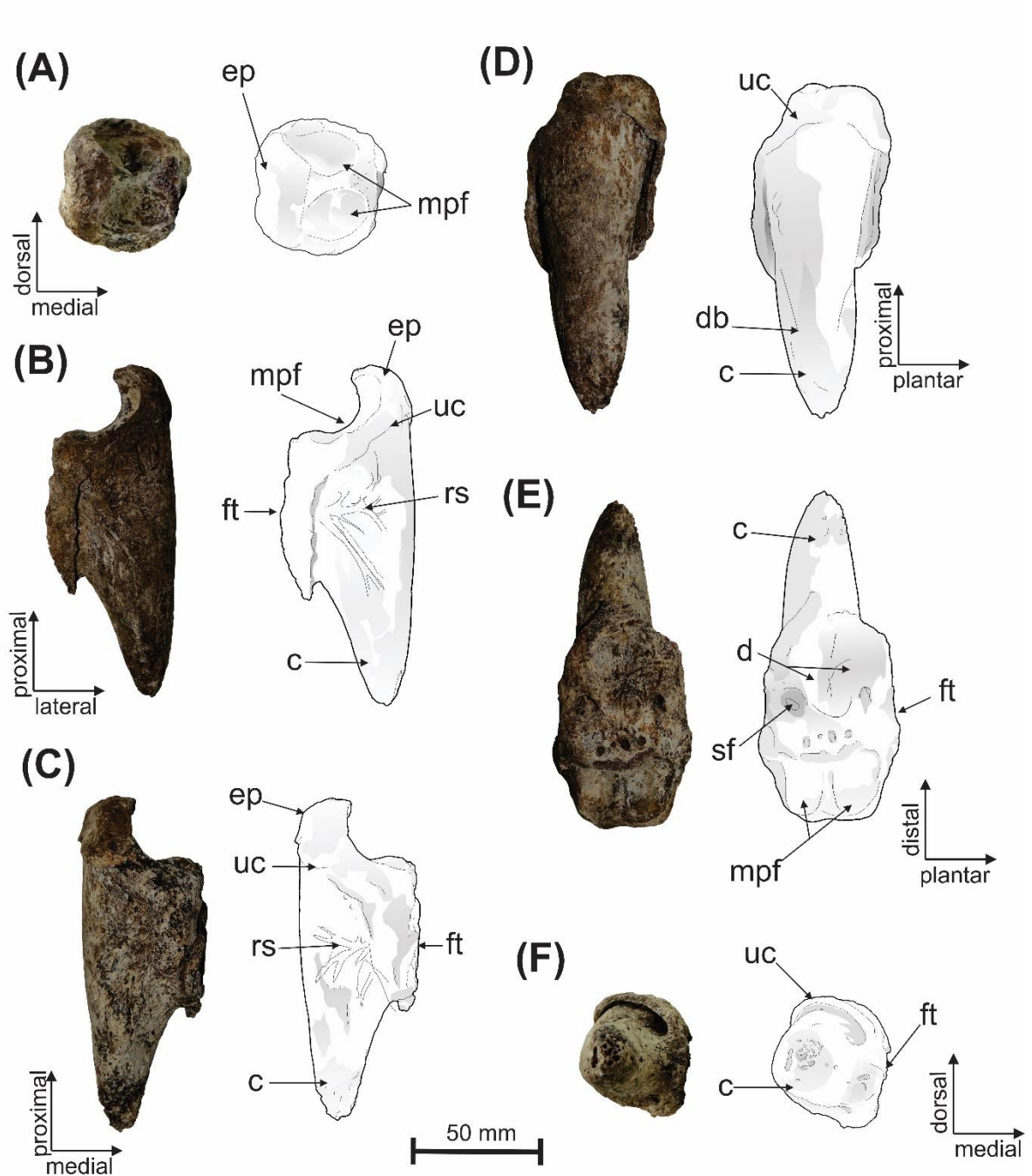


Figure S16. Left distal phalanx of the digit 3 of *Lestodon armatus* (UFSM 11535). (A) proximal, (B) dorsal, (C) plantar, (D) lateral, (E) medial (F) distal views. Abbreviations: c, claw; d, depression; db, dorsal boarder; ep, extensor process; ft, flexor tubercle; mpf, medial phalanx facet; rs, ramified sulcus; sf, solar foramina; uc, unguicular crest. Scale: 50 mm.

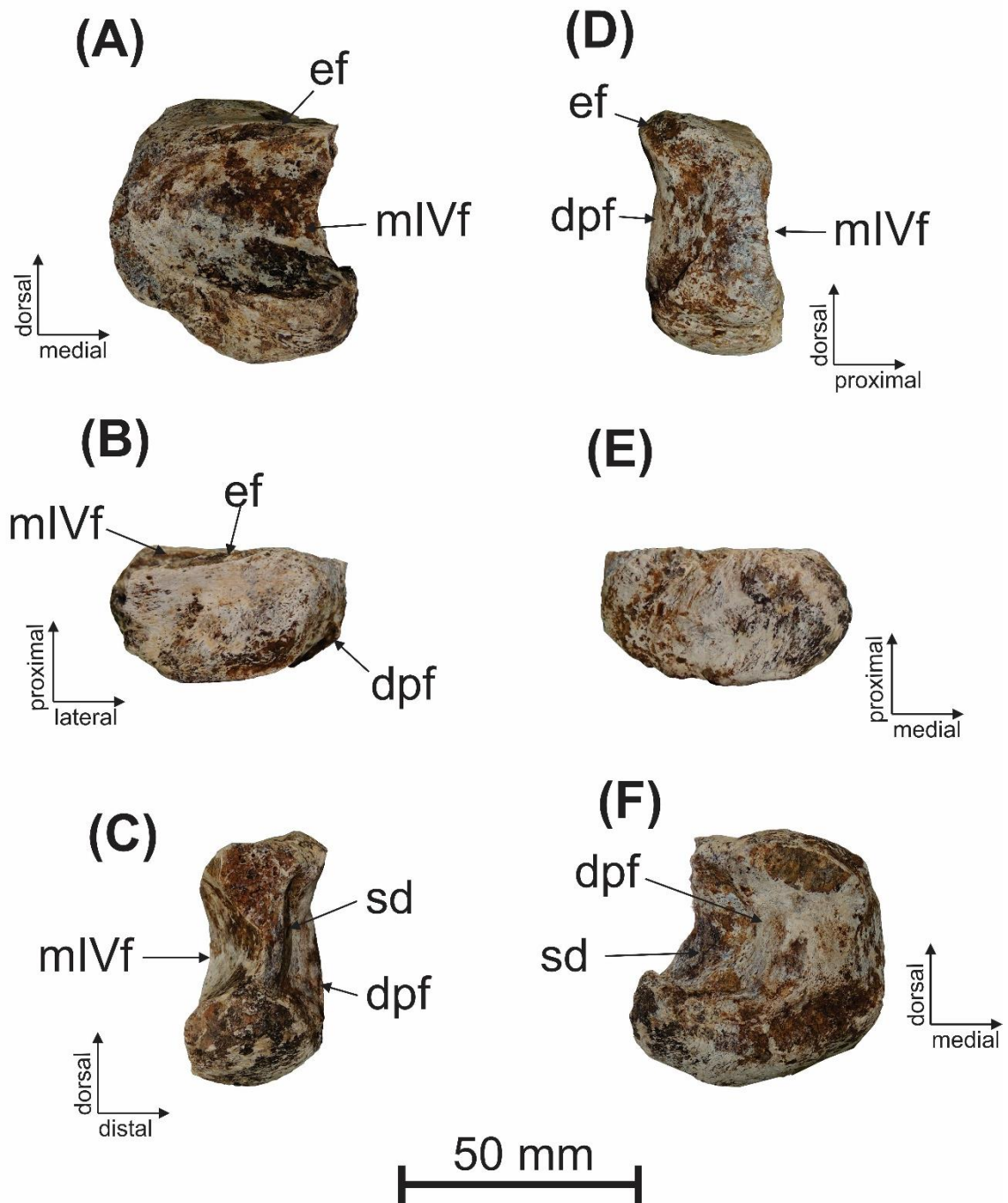


Figure S17. Left proximal phalanx of digit 4 of *Lestodon armatus* (UFSM 11535). (A) proximal, (B) dorsal, (C) medial, (D) lateral, (E) plantar and (F) distal views. Abbreviations: dpf, distal phalanx facet; ef, elongated fossa; mIVf, metatarsal IV facet; sd, semicircular depression. Scale: 50 mm.

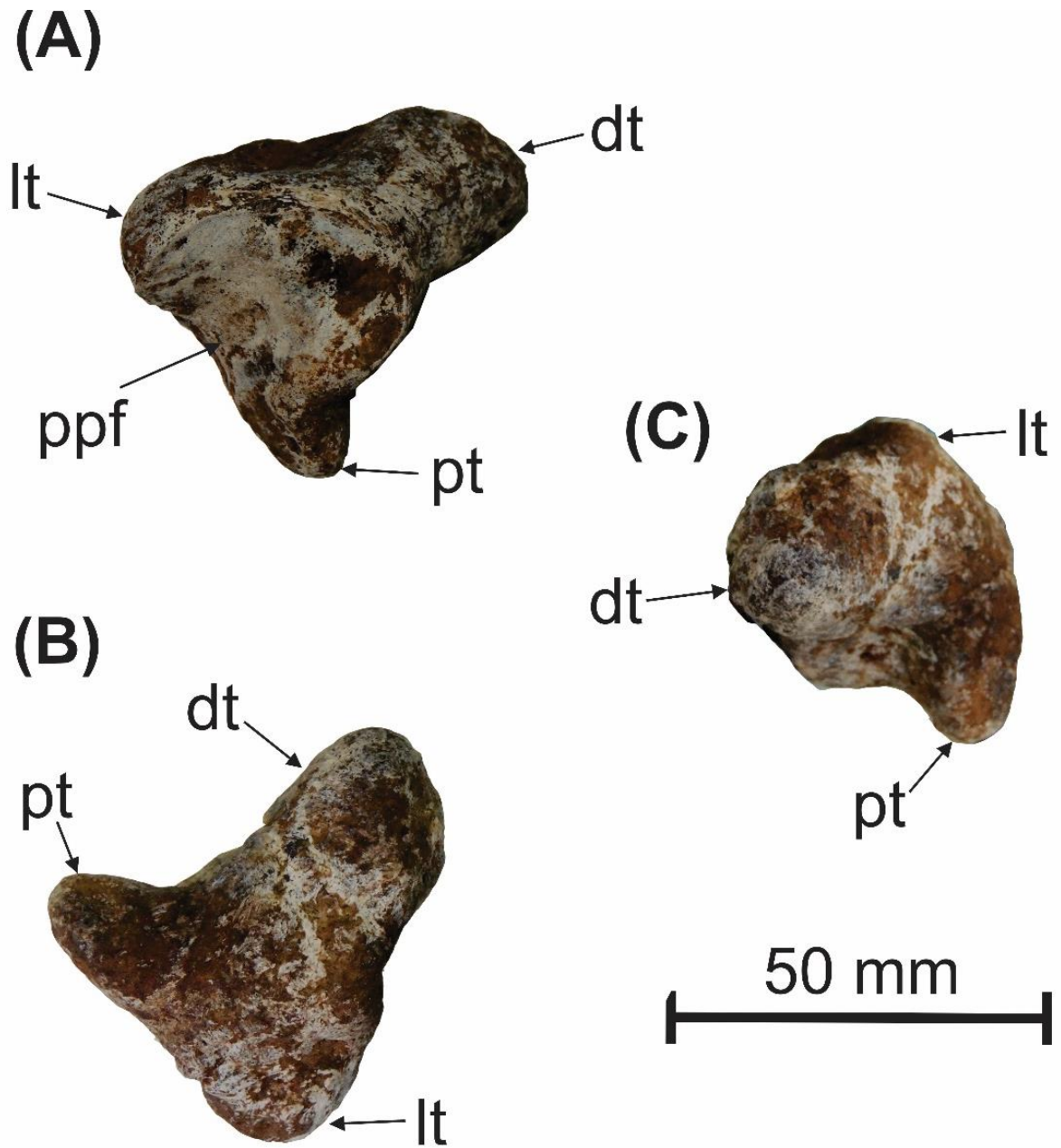


Figure S18. Left distal phalanx of digit 4 of *Lestodon armatus* (UFSM 11535). (A) dorsoproximal, (B) plantar and (C) distal views. Abbreviations: dt, distomedial tip; lt, lateral tip; ppf, proximal phalanx facet; pt, plantomedial tip. Scale: 50 mm.

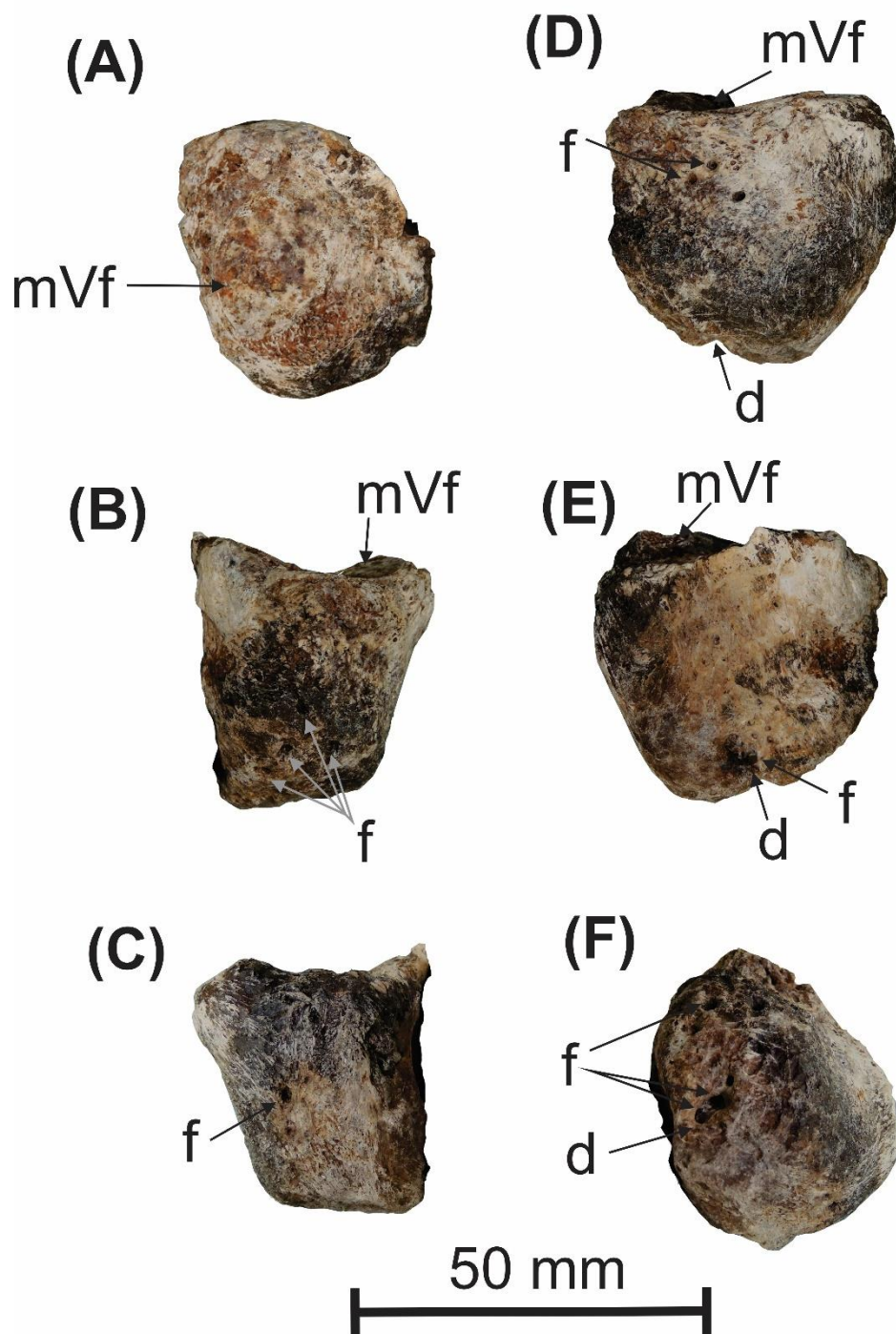


Figure S19. Left phalanx of digit 5 of *Lestodon armatus* (UFSM 11535). (A) proximal, (B) dorsal, (C) medial, (D) lateral, (E) plantar and (F) distal views. Abbreviations: d, depression; f, fovea; mVf, metatarsal V facet. Scale: 50 mm.

Table S1. Measures of the stylohyal compared with *Lestodon armatus* UFSM 11535 (bold).

Specimen/taxa	Stylohyal lenght	Widht of the proximal region
UFSM 11535	155.75	71.66
<i>Glossotherium robustus</i> SGO.PV.2 (Püschel et al. 2017)	127.3	57
<i>Lestodon armatus</i> CAV 476 (Tambusso et al. 2015)	105	38
<i>Paramylodon harlani</i> (average) (Stock 1925)	129.3	47.6

Table S2. Measures of the atlas compared with *Lestodon armatus* UFSM 11535 (bold).

Specimen/taxa	Body length	Width through the cranial condyle	Width across the caudal condyle	Width between the cranial condylons	Cranaiocaudal wing length
UFSM 11535	55.39	161.27	164.34	65.98	126.37
<i>Lestodon armatus</i> EPM-PV 014 (average)	115	195	115	81	
<i>L. armatus</i> EPM-PV 288 (average)	125	190	160	75	
<i>L. armatus</i> MCTFM-PV 976 (average)	113	172	152	73	
<i>L. armatus</i> MNHN 2921 (average)	129	176	119	71	132
<i>Myiodon darwini</i> FMNH P14288 (McAfee 2016)	29.3	141.3	87.8	60.4	72.2
<i>Paramylodon harlani</i> (average)(McAfee 2016)	38.5	129.7	97.4	55.1	79.2

Table S3. Measures of the femur compared with *Lestodon armatus* UFSM 11535 (bold).

Specimen/taxa	Larger width of medial condyle	Width of the infercondylar fossa	Width of the condyles
UFSM 11535	145.39	52.91	228.31
<i>Glossotherium</i> aff. <i>G. robustum</i> MCN PV-1424 (Pitana 2011)	73.49	36.87	175.41
<i>Glossotherium intertropical</i> MCL 4105 (Pitana 2011)	68.0	41	191.0
<i>Glossotherium intertropical</i> MCL 4292 (Pitana 2011)	84.0	31	206.0
<i>Glossotherium robustum</i> (Owen 1842)		52.91	182.0
<i>Glossotherium</i> sp. MHD-P 489 (Pitana 2011)	72.46	34	208.50
<i>Lestodon armatus</i> (Gervais 1873)			230
<i>Paramylodon harlani</i> (average) (Stock 1925)	88.7	47	188.5

Table S4. Measures of the tibia and fibula compared with *Lestodon armatus* UFSM 11535 (bold).

Speciemen/taxa	Tibial length (intercondylar eminence to distal tubercle)	Fibular length	Greater width of the distal end of the tibia	Craniocaudal diameter of medial condyle of tibia
UFSM 11535	355.76	357.97	150.48	117.21
<i>E. laurillardi</i> MCL 9570 (De Iuliis 1996)	457			
<i>Eremotherium laurillardi</i> UCMP V4201-36885 (De Iuliis 1996)	665			
<i>G. intertropical</i> MCL 4304/09 (Pitana 2011)	220.15		117.61	73.4
<i>G. robustum</i> MHD-P 114 (Pitana 2011)	245.58		122.97	106.07
<i>G. robustum</i> MLP (Kraglievich 1934)	225		125	
<i>Glossotherium aff. robustum</i> MCN-PV 1482 (Pitana 2011)	228.96		139.98	83.4
<i>Glossotherium aff. robustum</i> MCN-PV 2388 (Pitana 2011)	250.1		124.54	94.41
<i>Glossotherium intertropical</i> MCL 4304/08 (Pitana 2011)	227.77		117.38	72.13
<i>Glossotherium sp.</i> MHD-P 182 (Pitana 2011)	248.61		127.7	89.27

<i>Glossotherium</i> sp. MHD-P 349 (Pitana 2011)	240.51		127.22	95.19
<i>Glossotherium</i> sp. MHD-P 480 (Pitana 2011)	248.55		125.67	84.29
<i>Glossotherium</i> sp. MNHN 914 (Pitana 2011)	204.56		126.89	78.8
<i>Lestodon armatus</i> (Gervais 1873)	360	380	170	
<i>L. armatus</i> EPM-PV 025	310		115	91
<i>L. armatus</i> EPM-PV 127 (average)	370		152	122
<i>L. armatus</i> EPM-PV 261 (average)	372		151	108
<i>L. armatus</i> EPM-PV 321 (average)				125
<i>L. armatus</i> EPM-PV 329				117
<i>L. armatus</i> EPM-PV 334				107
<i>L. armatus</i> MCTFM 656	365		129	113
<i>L. armatus</i> MCTFM 914	311	317	122	118
<i>L. armatus</i> MNHN 1? (average)	360		155	118
<i>L. armatus</i> MNHN 17 (average)	335		143	113
<i>L. armatus</i> MNHN 151 (average)	339		142	115
<i>L. armatus</i> MNHN 191 (average)	325		156	116
<i>L. armatus</i> MNHN 1665 (average)	315		143	114
<i>L. armatus</i> MNHN 1719 (average)	350		123	115.5
<i>Megatherium americanum</i> BMNH 19953u (De Iuliis 1996)	425			

<i>M. americanum</i> MACN 54 (De Iuliis 1996)	594			
<i>Paramylodon harlani</i> (average) (Stock 1925)	247.3	263	142.5	

Table S5. Measures of the astragalus compared with *Lestodon armatus* UFSM 11535 (bold).

Specimen/taxa	Craniocaudal length	Craniocaudal length of discoid facet	Craniocaudal length of odontoid process	Astragalar height (included odontoid process)
UFSM 11535	146.72	146.25	63.34	60.25
<i>Eremotherium laurillardi</i> (mean) (De Iuliis 1996)	208			209
<i>G. intertropical</i> MCL 4115/29 (Pitana 2011)				118.65
<i>G. intertropical</i> MCL 4307/33 (Pitana 2011)	108.98	101.58		100.78
<i>Glossotherium aff. robustum</i> MCN-PV 5617 (Pitana 2011)	111.36	97.34		92.53
<i>Glossotherium intertropical</i> MCL 4310 (Pitana 2011)	107.46	112.68		109.37

<i>Glossotherium robustum</i> (SGO.PV.2) (Püschel et al. 2017)	130	101.3		
<i>Glossotherium sp.</i> MHDP-113 (Pitana 2011)	101.38	94.3		97.03
<i>Glossotherium sp.</i> MHDP-187 (Pitana 2011)	102.91	101.80		107.24
<i>Glossotherium sp.</i> MNHN 914 (Pitana 2011)		105.39		91.65
<i>Lestodon armatus</i> (Gervais 1873)	200			
<i>L. armatus</i> EPM-PV 012 (average)	150	126	56	124
<i>L. armatus</i> EPM-PV 260 (average)	152	140	60	144
<i>Lestodon sp.</i> MCN-PV 1809	227.8	155.76	60.63	150.42
<i>Lestodon sp.</i> MCN-PV 2514	158.59	145.77	69.49	136.08
<i>Lestodon sp.</i> MCN-PV 3224	193.21	141.94	62.83	156.86
<i>Lestodon sp.</i> MCN-PV 5715	131.79	116.35	49.86	111.10
<i>Lestodon sp.</i> MCN-PV 5719	163.64	128.05	54.71	117.35
<i>Lestodon sp.</i> MCN-PV 5720	158.62	141.95	60.56	131.99
<i>Lestodon sp.</i> MCN-PV 5722	189.39	147.65	59.86	142.89
<i>Lestodon sp.</i> MCN-PV 6899	137.86	115.84	48.61	110.60
<i>Lestodon sp.</i> MCN-PV 8653	186.1	147.23	58.80	135.01

<i>Lestodon</i> sp. MCN-PV 9652	155.76	135.79	58.91	130.30
<i>Lestodon</i> sp. MCN-PV 9655	153.93	124.91	56.67	133.01
<i>Lestodon</i> sp. MCN-PV 9656	153.38	138.12	60.48	129.93
<i>Lestodon</i> sp. MCN-PV 9657	155.80	132.65	56.16	138.45
<i>L. armatus</i> MNHN 978	160	134.2	57	
<i>L. armatus</i> MNHN 1058	170	143	61	135
<i>L. armatus</i> MNHN 1139	169	148		
<i>L. armatus</i> MNHN 1172 (average)	171	138.5	66	142.5
<i>L. armatus</i> MNHN 1173 (average)	156	136	66.50	129
<i>L. armatus</i> MNHN 1174	158	135	62	143
<i>L. armatus</i> MNHN1183	156.5	130.5	69	139
<i>L. armatus</i> MNHN 1741	160	138	61	126
<i>L. armatus</i> MNHN 1752		145	62	141
<i>L. armatus</i> MNHN 1795	156	134	55	134
<i>L. armatus</i> MNHN 1854	155	139	55	144
<i>L. armatus</i> MNHN 1864	163	136	59	116
<i>L. armatus</i> MNHN 1868 (average)	174	142	63.5	143
<i>L. armatus</i> MNHN 1892 (average)	158	142	64	135

<i>L. armatus</i> MNHN 1900 (average)	150	123	61.5	117
<i>L. armatus</i> MNHN 1914	155	133.5	63	125
<i>L. armatus</i> MNHN 1915 (average)	171	141	62	138
<i>L. armatus</i> MNHN 1916	163	142	60	139
<i>L. armatus</i> MNHN 1939 (average)	150.5	135	58.5	122
<i>L. armatus</i> MNHN 2107 (average)	176	143	63	
<i>L. armatus</i> MNHN 2110	165	150	68.5	140
<i>L. armatus</i> MNHN 2111 (average)	156	124	51	131.5
<i>L. armatus</i> MNHN 2113 (average)	156	136	54.5	129
<i>L. armatus</i> MNHN 2114 (average)	145	120	54.5	120
<i>L. armatus</i> MNHN 2116	163	141	51	131
<i>L. armatus</i> MNHN 2123 (average)	155.5	127.5	58	141
<i>L. armatus</i> MNHN 2124 (average)	157	130	51	131
<i>L. armatus</i> MNHN 2125 (average)	149	129	56	120

<i>L. armatus</i> MNHN 2126 (average)	158	135	60	127
<i>L. armatus</i> MNHN 2127 (average)	158	129	60	120
<i>L. armatus</i> MNHN 2128 (average)	180	141	61	136
<i>L. armatus</i> MNHN 2130	179	140.5	61.5	143.5
<i>L. armatus</i> MNHN 2131	158	125	57	
<i>L. armatus</i> MNHN 2133 (average)	155	134	62	
<i>L. armatus</i> MNHN 3202 (average)	175	133.5	65	129
<i>Megatherium americanum</i> (mean) (De Iuliis 1996)	204			214
<i>Paramylodon harlani</i> (average) (Stock 1925)	140.2	121.4	49.1	129

3 CONCLUSÕES

Neste trabalho, reportou-se pela primeira vez a presença de fósseis em uma nova localidade informalmente denominada como “Arroio do *Lestodon*” dentro do Vale do Seival, município de Caçapava do Sul. Ali foram coletados os fósseis aqui estudados (UFSM 11535), além de um osteodermo bastante fragmentário atribuído a um Glyptodontidae. Para a melhor compreensão sobre a deposição sedimentar dos níveis portadores de vertebrados são necessários estudos estratigráficos, bem como datações absolutas para conhecer a idade dos fósseis ali encontrados.

O espécime UFSM 11535, o fóssil mais completo ali coletado, foi atribuído a *Lestodon armatus* por comparação com outras preguiças terrícolas. UFSM 11535 é identificado com um Mylodontidae devido à presença de dentes ovais e bilobados, falanges 1 e 2 não fusionadas no dígito III do pé e a presença da união das facetas dos côndilos com a faceta patelar no fêmur.

A atribuição a *L. armatus* se dá devido ao compartilhamento de caracteres com este táxon, como: I) separação das facetas ectal e sustentacular no astrágalo, o que difere de *Glossotherium*, *Myloodon* e *Paramyloodon*; II) a função do ectocuneiforme como metatarsal II pela fusão dos dois ossos; III) pelo processo odontóide do astrágalo em forma de polia com cerca de 90° em relação à faceta discoide; IV) a separação por uma crista das facetas astragalianas na tíbia, e V) o côndilo medial do fêmur maior que o côndilo lateral. Sendo assim, UFSM 11535 é atribuído a *L. armatus*, única válida para o Pleistoceno segundo Czerwonogora e Fariña (2012).

Em relação aos principais aportes anatômicos da presente dissertação, observou-se que UFSM 11535 possui peculiaridades que indicam a presença de caracteres que são individualmente variáveis. Entre tais características, ressalta-se o formato do estilóide, o qual é semelhante a *Scelidotherium* (embora muito maior) quanto ao comprimento e curvatura de seu eixo em relação à parte proximal do osso, e o fusionamento parcial da tíbia com a fíbula, até então não descrita para a espécie. Além disso, estão relatados pela primeira vez a presença de sesamóides no metatarsal III.

Análises mais abrangentes da morfologia pós-craniana dos Mylodontidae, bem como de outros pilosos, são necessárias para verificar a presença de variações anatômicas individuais, bem como testar a relevância filogenética dos caracteres presentes nesta região do esqueleto.

4 REFERÊNCIAS

AMSON, E.; ARGOT, C.; MCDONALD, H. G.; MUIZON, C. Osteology and functional morphology of the hind limb of the marine sloth *Thalassocnus* (Mammalia, Tardigrada). **Journal of Mammalian Evolution**, v. 22, n. 3, p. 355-419, 2015a.

AMSON, E.; ARGOT, C.; MCDONALD, H. G.; MUIZON, C. Osteology and functional morphology of the axial postcranium of the marine sloth *Thalassocnus* (Mammalia, Tardigrada) with paleobiological implications. **Journal of Mammalian Evolution**, v. 22, n. 4, p. 473-518, 2015b.

BROOK, B. W.; BOWMAN, D. M. J. S. The uncertain blitzkrieg of Pleistocene megafauna. **Journal of Biogeography**, v. 31, p. 517-523, 2004.

CARTELLE, C. (1999). Pleistocene mammals of the Cerrado and Caatinga of Brazil. In: **Mammals of Neotropics: the central tropics**. Chicago/London: University of Chicago. Vol. 3, 1999, p. 27-46.

CARTELLE, C.; DE IULLIS, G.; FERREIRA, R. L. Systematic revision of tropical Brazilian scelidotheriine sloths (Xenarthra, Mylodontoidea). **Journal of Vertebrate Paleontology**, v. 29, n. 2, p. 555-566, 2009.

CARVALHO, A. M. V. Ocorrências de *Lestodon trigonidens* na mamalofauna de Álvares Machado. **Faculdade de Filosofia, Ciências e Letras da Universidade de São Paulo**, v. 134, n. 7, p. 43-55, 1952.

CIONE, A. L.; TONNI, E. P.; SOIBELZON, L. The Broken Zig-Zag: Late Cenozoic large mammal and tortoise extinction in South America. **Revista del Museo Argentino de Ciencias Naturales**, v. 5, n. 1, p. 1-19, 2003.

CIONE, A. L.; GASPARINI, G. M., SOIBELZON, E., SOIBELZON, L. H., TONNI, E. P. The Great American Biotic Interchange: A South American Perspective. New York: Springer Briefs in Earth System Sciences, 2015, 97 p.

COLTORTI, M.; ABBAZZI, L.; FERRETTI, M. P.; IACUMIN, P.; PAREDES-RIOS, F.; PELLEGRINI, M.; PIERUCCINI, P.; RUSTIONI, M.; TITO, G.; ROOK, L. Last glacial mammals in South America: a new scenario from the Tarija basin (Bolivia). **Naturwissenschaften**, v. 94, p. 288-299, 2007.

CZERWONOGORA, A.; FARIÑA, R. A. (2012). How many Pleistocene species of *Lestodon* (Mammalia, Xenarthra, Tardigrada)? **Journal of Systematic Palaeontology**, v. 11, n. 2, p. 1-13, 2012.

DELSUC, F.; VIZCAÍNO, S. F.; DOUZERY, E. J. P. 2004. Influence of Tertiary paleoenvironmental changes on the diversification of South America mammals: a relaxed molecular clock study within xenarthrans. **BMC Evolutionary Biology**, v. 4, n. 11, p. 1-13.

DESCHAMPS, C. M.; BORROMEI, A. M. La fauna de vertebrados pleistocénicos del bajo San José (Provincia de Buenos Aires, Argentina). Aspectos paleoambientales. **Ameghiniana**, v. 29, n. 2, p. 177-183, 1992.

DESCHAMPS, C. M. Late Cenozoic mammal bio-chronostratigraphy in southwestern Buenos Aires Province, Argentina. **Ameghiniana**, v. 42, n. 4, p. 733-750, 2005.

FARIÑA, R. A.; TAMBUSO, P. S.; VARELA, L.; CZERWONOGORA, A.; GIACOMO, M. D.; MUSSO, M.; BRACCO, R.; GASCUE, A. Arroyo del Vizcaíno, Uruguay: a fossil-rich 30-ka-old megafaunal locality with cut-marked bones. **Proceedings of the Royal Society B**, v. 281, n. 20132211, p. 1-6, 2013.

FERIGOLO, J. Late Pleistocene South-American land-mammal extinction: the infection hypothesis. **Quaternary of South America and Antarctic Peninsula**, v. 12, p. 279-310, 1999.

GALLO, V.; AVILLA, L. S.; PEREIRA, R. C. L.; ABSOLON, B. A. Distributional patterns of herbivore megamammals during the Late Pleistocene of South America. **Anais da Academia Brasileira de Ciências**, v. 85, n. 2, p. 533-546, 2013.

GAUDIN, T. J. The ear region of Edentates and phylogeny of the Tardigrada (Mammalia, Xenarthra). **Journal of Vertebrate Paleontology**, v. 15, n. 3, p. 672-705, 1995.

GAUDIN, T. J. Phylogenetic relationships among sloths (Mammalia, Xenarthra, Tardigrada): the craniodental evidence. **Zoological Journal of the Linnean Society**, v. 140, p. 255-305, 2004.

GAUDIN, T. J.; MCDONALD, H. G. Morphology-based investigations of the phylogenetic relationships among extant and fossil xenarthrans. In: **The Biology of Xenarthra**. Gainesvill: University Press of Florida, 2008, p. 24-36.

GERVAIS, P. Mémoire sur plusieurs espèces de mammifères fossiles propres a l'Amérique Meridionale. **Mémoires de la Société Géologique de France**, v. 24, p. 1-44, 1873.

GHILARDI, A. M.; FERNANDES, M. A.; BICHUETTE, M. E. Megafauna from the Late Pleistocene-Holocene deposits of the Upper Ribeira karst area, southeast Brazil. **Quaternary International**, v. 245, n. 2, p. 369-378, 2011.

HOFFSTETTER, R. Une faune de mamifères au Paraguay. **C. R. Som. Soc. Géol. France**, n. 1, p. 32-33, 1978.

HSIOU, A. S. A new Teiidae species (Squamata, Scincomorpha) from the Late Pleistocene of Rio Grande do Sul state, Brazil. **Revista Brasileira de Paleontologia**, v. 10, n. 3, p. 181-194, 2007.

KERBER, L.; OLIVEIRA, E. V. Fósseis de vertebrados da Formação Touro Passo (Pleistoceno Superior), Rio Grande do Sul, Brasil: atualização dos dados e novas contribuições. **Journal of Geoscience**, v. 4, n. 2, p. 49-64, 2008a.

KERBER, L.; OLIVEIRA, E. V. Sobre a presença de *Tapirus* (Tapiridae, Perissodactyla) na Formação Touro Passo (Pleistoceno Superior), oeste do Rio Grande do Sul. **Biodiversidade Pampeana**, v. 6, n. 1, p. 9-14, 2008b.

KERBER, L.; OLIVEIRA, E. V. Novos fósseis de vertebrados para a Sanga da Cruz (Pleistoceno Superior), Alegrete, RS, Brasil. **Pesquisas em Geociências**, v. 35, n. 2, p. 39-45, 2008c.

KERBER, L.; LOPES, R. P.; VUCETICH, M. G.; RIBEIRO, A. M.; PEREIRA, J. Chinchillidae and Dolichotinae rodents (Rodentia: Hystricognathi: Caviomorpha) from de Late Pleistocene of Southern Brazil. **Revista Brasileira de Paleontologia**, v. 14, n. 3, p. 229-238, 2011.

KERBER, L.; PITANA, V. G.; RIBEIRO, A. M.; HSIU, A. S.; OLIVEIRA É. V. Late Pleistocene vertebrates from Touro Passo Creek (Touro Passo Formation), Southern Brazil: a review. **Revista Mexicana de Ciencias Geológicas**, v. 31, p. 248-259, 2014.

KRAGLIEVICH, L. "Myloodon darwini" Owen, es la especie genotipo del "Myloodon" Owen. Rectificación de la nomenclatura genérica de los milodontos. **Physis**, v. 9, n. 33, p. 169-185, 1928.

KRAGLIEVICH, L. Contribución al conocimiento de *Myloodon darwini* Owen y especies afines. **Revista del Museo de La Plata**, n. 35, p. 255-292, 1934.

LINARES, O. J. Nuevos restos del género *Lestodon* Gervais, 1855 (Xenarthra, Tardigrada, Myloodontidae), del Mioceno Tardío y Plioceno Temprano de Urumaco (Venezuela), con descripción de nuevas especies. **Paleobiologia Neotropical**, n. 2, p. 1-14, 2004.

LOPES, R. P.; BUCHMANN, F. S. C.; CARON, F.; ITUSARRY, M. E. Tafonomia dos fósseis de vertebrados (megafauna extinta) encontrados nas barrancas do arroio Chuí e linha de costa, Rio Grande do Sul, Brasil. **Pesquisas em Geociências**, v. 28, n. 2, p. 67-73, 2001.

MARSHALL, L. G. Land mammals and the Great American Interchange. **American Scientist**, v. 76, n. 4, p. 380-388, 1988.

MARSHALL, L. G.; SEMPERE, T. The Eocene to Pleistocene vertebrates of Bolivia and their stratigraphic contexto: a review. **Fósiles y Facies de Bolivia: Vertebrados**, v. 12, n. 3-4, p. 631-652, 1991.

MARTÍNEZ, S.; UBILLA, M. El Cuaternario del Uruguay. In: **Cuencas sedimentarias de Uruguay: Geología, Paleontología y recursos naturales**. Montevideo: D.I.R.A.C., 2004, p. 195-228.

MCAFEE, R. K. Description of new postcranial elements of *Myiodon darwini* Owen 1839 (Mammalia: Pilosa: Mylodontinae), and functional morphology of the forelimb. **Ameghiniana**, v. 53, n. 4, p. 418-443, 2016.

MCDONALD, H. G. Evolution of the pedolateral foot in ground sloths: patterns of change in the astragalus. **Journal of Mammalian Evolution**, n. 19, p. 209-215, 2012.

MCDONALD, H. G.; DE IULIIS, G. Fossil history of sloths. In: **The biology of Xenarthra**. Gainesville: University Press of Florida, 2008, p. 39-55.

MCKENNA, M. C.; WYSS, A. S.; FLYNN, J. J. Paleogene Pseudoglyptodon xenarthrans from Central Chile and Argentine Patagonia. **American Museum Novitates**, n. 3536, p. 1-18, 2006.

MIÑO-BOILINI, A. R. **Sistemática y evolución de los Scelidotheriinae (Xenarthra, Mylodontidae) cuaternarios de la Argentina**: Importancia estratigráfica, paleobiogeográfica y paleoambiental. Monografía (Tese), 2012. Universidad Nacional de La Plata, La Plata, 2012.

MIÑO-BOILINI, A. R.; CARLINI, A. A.; SCILLATO-YANÉ, G. J. Revisión sistemática y taxonómica del género *Scelidotherium* Owen, 1839 (Xenarthra, Phyllophaga, Mylodontidae). **Revista Brasileira de Paleontologia**, v. 17, n. 1, p. 43-58, 2014.

MOTHÉ, D.; ÁVILLA, L. S.; COZZUOL, M.; WINCK, G. R. Taxonomic revision of the Quaternary gomphotheres (Mammalia: Proboscidea: Gomphotheriidae) from the South America lowlands. **Quaternary International**, v. 276/277, p. 2-7, 2012.

OLIVEIRA, E. V. Mamíferos Xenarthra (Edentata) do Quaternário do estado do Rio Grande do Sul, Brasil. **Ameghiniana**, v. 33, n. 1, p. 65-75, 1996.

OLIVEIRA, E. V.; DUTRA, T. L.; ZELTZER, F. Megaterídeos (Mammalia, Xenarthra) do Quaternário de Caçapava do Sul, Rio Grande do Sul, com considerações sobre a flora associada. **Geologia Colombiana**, n. 27, p. 77-86, 2002.

OWEN, R. Description of the skeleton of an extinct giant sloth, *Myiodon robustus*, Owen, with observations of the osteology, natural affinities, and probable habits the megatherioid quadrupeds in general. Londres: R. & J. E. Taylor, 1842, 176 p.

OWEN, R. Memoir on the *Megatherium* or Giant Ground-Sloth of America (*Megatherium americanum*, Cuvier). Londres, Edinburg: Willians and Norgate, 1861, 177p.

PAULA COUTO, C. Sôbre a presença dos gêneros *Hippidion* e *Toxodon* Owen, no Pleistoceno do Rio Grande do Sul. **Boletim do Museu Nacional**, n. 2, p. 1- 12, 1944.

PAULA COUTO, C. Edentados fósseis de São Paulo. **Anais da Academia Brasileira de Ciências**, v. 45, n. 2, p. 261-275, 1973.

PAULA COUTO, C. **Tratado de Paleomastozoologia**. Rio de Janeiro: Academia Brasileira de Ciências, 1979. 590 p.

PITANA, V. G. (2011). **Estudo do gênero *Glossotherium* Owen, 1840 (Xenarthra, Tardigrada, Mylodontidae), Pleistoceno do estado do Rio Grande do Sul, Brasil**. Monografia (Dissertação), 2011. Universidade Federal do Rio Grande do Sul, Porto Alegre, 2011.

PUJOS, F.; GAUDIN, T. J.; DE IULIIS, G.; CARTELLE, C. Recent advances on variability, morpho-functional adaptations, dental terminology, and evolution of sloths. **Journal of Mammalian Evolution**, n. 19, p. 159-169, 2012.

QUATTROCCHIO, M. E.; BORROMEI, A. M.; DESCHAMPS, C. M.; GRILL, S. C.; ZAVALA, C. A. Landscape evolution and climate changes in the Late Pleistocene-Holocene, southern Pampa (Argentina): evidence palynology, mammals and sedimentology. **Quaternary International**, v. 181, p. 123-138, 2008.

RIBEIRO, A. M.; DA-ROSA, Á. A. S.; SCHERER, C. S.; HSIU, A. S.; PITANA, V. G. Sítio Cerro da Tapera, uma nova localidade fossilífera para o Pleistoceno do Rio Grande do Sul, Brasil. **Paleontologia em Destaque** (Edição Especial), p. 164-165, 2008.

SCHERER, C. S.; PITANA, V. G.; RIBEIRO, A. M. Protherootheriidae and Macraucheniidae (Litopterna, Mammalia) from the Pleistocene of Rio Grande do Sul state, Brazil. **Revista Brasileira de Paleontologia**, v. 12, n. 3, p. 231-246, 2009.

STOCK, C. Structure of the pes in *Myiodon harnali*. **Bulletin of the Department of Geology**, v. 10, n. 16, p. 267-286, 1917.

STOCK, C. Cenozoic gravigrade edentates of Western North America. **Carnegie Institution of Washington Publications**, n. 331, p. 1-206, 1925.

UBILLA, M. Mammalian biostratigraphy of Pleistocene fluvial deposits in northern Uruguay, South America. **Proceedings of the Geologists Association**, n. 115, p. 347-357, 2004.

UBILLA, M.; PEREA, D.; AGUILAR, C. G.; LORENZO, N. Late Pleistocene vertebrates from northern Uruguay: tools for biostratigraphic, climatic and environmental reconstruction. **Quaternary International**, n. 114, p. 129-142, 2004.

WEBB, S. D. Faunal interchange between North and South America. **Acta Zoologica Fennica**, v. 170, p. 177-178, 1985.

WEBB, S. D. Osteology and relationships of *Thinobadistes segnis*, the first mylodont in North America In: **Advances in Neotropical Mammalogy**. Florida: Sandhill Crane Press, 1989, p. 469-532.

WOODBURNE, M. O. The Great American Biotic Interchange: dispersals, tectonics, climate, sea level and holding pens. **Journal of Mammalian Evolution**, v. 17, n. 4, p. 245-264, 2010.

VARELA, L.; FARIÑA, R. A. Co-occurrence of mylodontid sloths and insights on their potential distributions during the late Pleistocene. **Quaternary Research**, n. 85, p. 66-74, 2016.